5-2010

Characterization and Physicochemical Modifications of Polymer Hollow Fiber Membranes for Biomedical and Bioprocessing Applications

Benjamin R. Madsen
Utah State University

CHARACTERIZATION AND PHYSICOCHEMICAL MODIFICATIONS OF POLYMER HOLLOW FIBER MEMBRANES FOR BIOMEDICAL AND BIOPROCESSING APPLICATIONS

by

Benjamin R. Madsen

A dissertation submitted in partial fulfillment
of the requirements for the degree

of

DOCTOR OF PHILOSOPHY

in

Biological Engineering

Approved:

_____	_____
David W. Britt Committee Chairman	Chih-Hu Ho Committee Member
_____	_____
Timothy A. Taylor Committee Member	Anne J. Anderson Committee Member
_____	_____
Soonjo Kwon Committee Member	Byron R. Burnham Dean of Graduate Studies

UTAH STATE UNIVERSITY
Logan, Utah

2010

ABSTRACT

CHARACTERIZATION AND PHYSICOCHEMICAL MODIFICATIONS OF POLYMER HOLLOW FIBER MEMBRANES FOR BIOMEDICAL AND BIOPROCESSING APPLICATIONS

by

Benjamin R. Madsen, Doctor of Philosophy

Utah State University, 2010

Major Professor: Dr. David W. Britt
Department: Biological and Irrigational Engineering

Hollow fiber membranes (HFMs) formed through phase inversion methods exhibit specific physicochemical characteristics and generally favorable surface and mechanical properties, supporting their use in diverse applications including ultrafiltration, dialysis, cell culture, bioreactors, and tissue engineering. Characterization of, and modifications to, such membranes are important steps in achieving desired characteristics for specific applications.

HFMs subject to gas, irradiation, and chemical sterilization techniques were characterized based on several analytical techniques. It was revealed that these common sterilization techniques can cause inadvertent changes to HFM properties. While these changes may cause detrimental effects to HFMs used in filtration, the methods of sterilization are also presented as a facile means of tuning properties toward specific applications.

Modifications to HFM surface chemistries were also sought as a method of adsorbing bacterial lipopolysaccharide (LPS) from solutions used in hemodialysis treatments and bioprocessing applications. It was found that additives such as polyvinylpyrrolidone (PVP), polyethyleneglycol (PEG), and poly-L-lysine (PLL) can facilitate adsorption capacities of HFMs toward LPS. Additionally, chemical changes are presented as a means of preferentially adsorbing LPS to specific locations on the HFM surface.

(161 Pages)

To

Mom and Dad

And

Christy

ACKNOWLEDGMENTS

I would like to express gratitude to my professor and advisor, Dr. David W. Britt, for guiding me into the path of research where I have been able to reach out with the arms of my imagination. His continual guidance, support, and insights were a blessing as I worked toward the end goal of receiving my Ph.D. I would also like to thank the other professors on my committee, including Dr. Chih-Hu Ho, Dr. Tim Taylor, Dr. Anne Anderson, and Dr. Soonjo Kwon, for the enjoyment I was able to have in their classes and their varied inputs that proved valuable in guiding the directions of the research.

I am deeply indebted to Fresenius Medical Care North America for their continued funding, support, and guidance. Dr. Ho, Eric Stroup, Mike Henrie, and Cheryl Ford have all been integral contributors to the research.

I would like to thank all of my friends and colleagues in Dr. Britt's lab who helped push forward with new discoveries and insights into this project. Specifically, Floyd Griffiths, Elise McKenna, Christel Olsen, Landon Stoker, Ben Draper, and Myles Thomas were instrumental in executing numerous experiments.

Lastly I would like to thank my family, friends, and especially my loving wife, Christy, for their unwavering support and encouragement over these past several years. My parents have always provided me with the means of expanding my mind. My incredible friends not only provided me with insightful guidance but kept me sane and entertained during my education years. My wife has been an amazing blessing to me. She was always supportive of me as deadlines came and went, always lends a listening ear, and helps me find joy in life every day.

Benjamin Madsen

CONTENTS

Page

ABSTRACT iii

DEDICATION v

ACKNOWLEDGMENTS vi

LIST OF TABLES xi

LIST OF FIGURES xii

CHAPTER

1 INTRODUCTION 1

ESRD AND DIALYSIS 1
BIOPROCESSING 5
BACTERIA 8

Endotoxin 8
Bacteria in solutions 11

RESEARCH OBJECTIVES 13
REFERENCES 14

2 LITERATURE REVIEW 19

HOLLOW FIBER MEMBRANE (HFM) MATERIALS 19
CHARACTERIZATION OF HFMS 21
CLEANING OF HFMS 23

Sterilization techniques 24
Reprocessing techniques 26

REMOVAL OF LPS FROM SOLUTIONS 27

Removal of LPS from dialysate and water solutions 27
Removal of LPS from biological solutions 29

REFERENCES 32

3 EFFECT OF STERILIZATION TECHNIQUES ON PHYSICOCHEMICAL PROPERTIES OF POLYSULFONE HOLLOW FIBERS 40

ABSTRACT....40
INTRODUCTION 41
MATERIALS AND METHODS....42

Membrane preparation....42
Water contact angle measurement 44
AFM morphology 44
Water evaporation rate....45

RESULTS 45

Surface hydrophilicity by CAM....45
AFM morphology 47
Water evaporation rate....51

DISCUSSION....51
CONCLUSION....56
REFERENCES 57

4 HEMODIALYSIS MEMBRANE SURFACE CHEMISTRY AS A BARRIER TO ENDOTOXIN TRANSFER....61

ABSTRACT....61
INTRODUCTION 62
MATERIALS AND METHODS....64

Membranes....64
Dialysate with bacterial culture filtrates 65
In vitro dialysis circuit 65
Fluorescent imaging....67
Surface characterization by water contact angle....68
SEM imaging 69

RESULTS 69

Dialysis simulations using bacterial culture filtrates as challenge material 69
Surface hydrophobicity by contact angle analysis....71
Imaging of dialysis membranes 72

DISCUSSION....76

CONCLUSION....82
REFERENCES....83

5 POLY-L-LYSINE AS SCAVENGER OF BACTERIAL ENDOTOXIN: CHARACTRIZATION OF SOLUTIONS AND APPLICATION....88

ABSTRACT....88
INTRODUCTION....89
MATERIALS AND METHODS....90

Solutions....90
Surface tension measurement....91
Particle size with dynamic light scattering....91
Atomic force microscopy of solutions on mica and OTS-modified glass....91
Fluorescence studies....92

RESULTS....94

Surface tension of solutions....94
Particle sizes from DLS measurements....96
AFM of LPS and PLL solutions on mica and OTS-modified glass....97
Fluorescence studies....99

DISCUSSION....102
CONCLUSION....106
REFERENCES....107

6 CONCLUSIONS AND FUTURE WORK....111

KEY FINDINGS....111
FUTURE DIRECTIONS....113

Chemical modifications to filtration membranes in other geometries....113
Selective removal of LPS from protein solutions....113
Adsorption of LPS to outer surface of hollow fiber membranes....114
Localization of LPS on HFM surfaces....117

REFERENCES....118

APPENDICES....120

A....121

B.....123

C.....130

D.....131

E.....132

F.....134

CURRICULUM VITAE.....143

LIST OF TABLES

Table Page

3.1. Experimental results for water evaporation rate 50

B.1. RMS roughness values for lumen side and outside of membranes (mean ± s.d., n = 5). Lumen side imaged at 2 x 2 μm^2 and outside imaged at 10 x 10 μm^2. 129

LIST OF FIGURES

Figure Page

1.1. Diagram of hemodialysis procedure. (A) Blood is removed from a patient and filtered through a dialyzer, then returned to the body. (B) Blood is passed through the inside of a hollow fiber membrane while dialysate flows countercurrent on the outside. 4

1.2. Diagram representing the outer cell wall of gram-negative bacteria. LPS molecules in the outer membrane are represented with lipid A anchored in the phopholipid bilayer and core and oligosaccharide chains extending into the extracellular space. 8

1.3. Schematic view of the chemical structure of endotoxin from E. coli O111:B4 (26). Hep, L-glycero-D-manno-heptose; Gal, galactose; Glc, Glucose; KDO, 2-keto-3-deoxyoctonic acid; NGa, N-acetyl-galactosamine; NGc, N-acetyl-glucosamine. This research was originally published in the Journal of Biological Chemistry. Ohno N, Morrison DC. Lipopolysaccharide interaction with lysozyme. *J Biol Chem*. 1989; 264:4434-41. © the American Society for Biochemistry and Molecular Biology. 9

1.4. Structures of LPS aggregates in aqueous solutions. An LPS monomer is depicted on the left with lipid A (black rod), phosphate groups (black circles), and saccharide group (white rod). Bivalent cations (white circles) facilitate formation of micelles and vesicles. (Reprinted from Journal of Biotechnology, 76, Petsch D, Anspach FB, Endotoxin removal from protein solutions, 97-119, Copyright (2000), with permission from Elsevier (35). 11

3.1. SEM of PS-PVP asymmetric dialysis hollow fiber [19]. 44

3.2. CAM of hollow fibers, both lumen (dark) and outside (light). Mean ± s.d., n = 8. PS and e-beam sterilized fibers show higher and lower contact angles, respectively, than the ETO sterilized and bleach treated fibers ($p < 0.05$). The 2-minute bleach treated fiber had identical contact angle to the ETO fiber. Fibers bleached for 1 hour showed contact angles approaching those of PS fibers (data not shown). 46

3.3. AFM images of the ETO sterilized hollow fiber, lumen (A) and outside (B). The asymmetrical membrane shows nodule aggregates on lumen and porous structure on outside. 47

3.4. AFM images of e-beam sterilized hollow fiber, lumen (A) and outside (B). Nodule aggregates for this membrane are significantly smaller than those on the ETO sterilized membrane. Pores on the outside are also larger than those on the ETO sterilized membrane. 47

3.5. AFM images of bleach treated hollow fiber, lumen (A) and outside (B). The membrane is structurally very similar to e-beam sterilized hollow fibers on both lumen and outside. 48

3.6. AFM images of PS hollow fiber, lumen (A) and outside (B). Membrane is structurally different, especially on the outside, than other fibers due to chemical differences of PS polymer versus PS-PVP polymer blend. 48

3.7. RMS roughness of hollow fibers, both lumen (dark) and outside (light). Mean ± s.d., n = 5. No significant difference among lumen RMS values is reported ($p < 0.05$). Bleach treated and e-beam sterilized fibers show significantly higher RMS values than ETO sterilized and PS fibers. 49

3.8. Averaged evaporation profiles of hollow fibers measured by tensiometer, with mass of absorbed water in the hollow fiber versus time (n = 9). Sensitivity of the tensiometer probe allows for highly accurate measurements (< 0.1 μg). Error bars have been removed for clarity. 50

4.1. Experimental dialysis simulation setups for the LPS challenge tests. The diffusive setup is first run for 60 minutes, after which the system is changed to the convective setup and run for an additional 60 minutes. 66

4.2. Mini-module used for fluorescence imaging, showing polycarbonate housing and T's, with UV curable epoxy for potting material. Approximately 30 fibers, 15 cm in length, provide the mini-module with about 15 cm^2 of surface area. 68

4.3. Semi-log plot of LPS concentrations in the DC (closed circle) and BC (open circle) for Optiflux (control) membrane (mean ± s.d., n = 3). 70

4.4. Semi-log plot of LPS concentration in BC and DC of high-PVP and low-PVP membranes (mean ± s.d., n = 3). 70

4.5. Semi-log plot of LPS concentration in BC and DC of bleached and PS-PEG copolymer membranes (mean ± s.d., n = 3). 71

4.6. Contact angle measurements of both inner lumen and outside of fiber membranes (mean ± s.d., n = 8). Statistical analysis revealed significant difference ($p < 0.05$) among all samples. Significant difference between the outside and lumen side contact angle was found only in the copolymer and high-PVP membranes. 72

4.7. Optiflux membrane: Fluorescence image (A), SEM images of the cross section (B), near the lumen (C), and near the outer wall (D), and fluorescence intensity profile (E). Fluorescent-labeled LPS conjugate is distributed throughout the entire membrane cross-section, accumulating near the inner lumen surface. The intensity profile shows the distribution of LPS adsorption from lumen (left) to outside (right). The arrow in Panel C indicates the boundary of the lumen wall.....73

4.8. Bleached fiber membrane: Fluorescence image (A), SEM images of the cross-section (B), near the lumen (C), and near the outer wall (D), and fluorescence intensity profile (E). Fluorescence distribution and surface structure were similar to the Optiflux membrane. The different structure in the bottom left of the fluorescence image is due to cryostat cutting artifact. 74

4.9. High-PVP membrane: Fluorescence image (A), SEM images of the cross-section (B), near the lumen (C), and near the outer wall (D), and fluorescence intensity profile (E). Fluorescence intensity for the matrix portion of the membrane is much lower for this sample compared to the other samples indicating less adsorption of LPS. 75

4.10. Low-PVP fiber membrane: Fluorescence image (A), SEM images of the cross-section (B), near the lumen (C), and near the outer wall (D), and fluorescence intensity profile (E). Distribution of LPS for this membrane is similar to the Optiflux membrane. However, intensity is much stronger here indicating a higher affinity of the LPS to the membrane. 76

4.11. PS-PEG Copolymer fiber membrane: Fluorescence image (A), SEM images of the cross-section (B), near the lumen (C), and near the outer wall (D), and fluorescence intensity profile (E). In contrast to the other fiber types, a distinct transition in the porosity of the spongy matrix is observed and LPS is restricted to the outer surface. 77

5.1. Mini-module showing polycarbonate housing and T's, with UV curable epoxy for potting material. Approximately 30 fibers, 15 cm in length, provide the mini-module with about 15 cm^2 of surface area. 93

5.2. Experimental setup for PLL coatings and LPS challenge tests. Fibers were first coated for 60 minutes with PLL, dried overnight in an oven, and then challenged with LPS for 60 minutes. 93

5.3. Semi-log plot of LPS surface tension of LPS in PBS (mean ± s.d., n = 3), including best curve fits for upper (below 10 μg/ml LPS) and lower (above 1000 μg/ml LPS) plateaus and logarithmic drop (between 10 and 1000 μg/ml LPS). 95

5.4. Semi-log plot of surface tensions (mean ± s.d., n = 9) and hydrodynamic diameters (mean ± s.d., n = 3) of solutions containing PLL in 47.5 μg/ml LPS. Surface tension and particle size both showed a transition point between 5 and 50 μg/ml PLL in LPS. Solutions containing PLL only did not alter surface tension from that of PBS (data not shown). Also, solutions containing PLL only did not produce meaningful particle sizes up to 1 mg/ml (data not shown). 96

5.5. AFM images of LPS on mica from solutions containing (A) 1 μg/ml, (B) 10 μg/ml, (C) 50 μg/ml, and (D) 100 μg/ml LPS in PBS. Solutions containing more than 10 μg/ml LPS led to images containing small "islands," presumably LPS deposits on the mica surface. 98

5.6. AFM images of LPS and PLL on OTS-modified glass from solutions containing 47.5 μg/ml LPS and (A) 0.5 μg/ml PLL, (B) 5 μg/ml PLL, and (C) 50 μg/ml PLL. OTS "anchors" allowed for LPS and PLL to form organized strands on surface. Increasing PLL concentration led to larger surface features. 99

5.7. Fluorescence images of polymer hollow fibers modified with PLL and challenged with fluorescent-labeled LPS. (A) Native-unchallenged hollow fiber used to show background fluorescence of polymer membrane. Polymer hollow fibers coated with PLL using (B) 0.1 μg/ml, (C) 1 μg/ml, and (D) 1000 μg/ml PLL. Polymer hollow fibers coated with PLL and cross-linked using GA at PLL concentrations of (E) 0.1 μg/ml, (F) 1 μg/ml, and (G) 1000 μg/ml. Fig. D.1. (Appendix D) contains images of all samples tested. 100

5.8. Relative fluorescence intensities of cross-sectional images of hollow fiber membranes (mean ± s.d., n ≥ 3). Background fluorescence due to the membrane has been subtracted from the presented values. Statistical analysis reveals significant difference between the 1 μg/ml PLL only sample and all other PLL samples. Among the cross-linked samples, 10, 100, and 1000 μg/ml PLL were all significantly brighter than lower PLL concentrations. 101

5.9. Fluorescence images of polymer hollow fibers modified using a solution containing 1 μg/ml PLL and challenged with solutions containing 100 ng/ml of fluorescent-labeled LPS and (A) 0 ng/ml, (B) 10 ng/ml, (C) 100 ng/ml, and (D) 1000 ng/ml PLL. 102

6.1. Schematic of cross section of hollow fiber membrane modified using positively-charged PLL as a negatively-charged LPS adsorbent. 116

6.2. Schematic of methods for imaging LPS with AFM. Method 1 involves tapping mode AFM to view LPS aggregates. Method 2 employs a gold

labeled anti-LPS antibody. Method 3 employs an anti-LPS antibody and a labeled anti-antibody antibody. Method 4 involves coating the AFM tip with anti-LPS antibody for use with tapping mode AFM. 116

A.1. Water contact angles of flat-sheet geometry PS-PVP membranes subjected to 0.57% bleach for varying amounts of time. "Lumen" represents the top side of the membrane, equivalent to the lumen side of a hollow fiber membrane. "Backside" represents the bottom side of the membrane, equivalent to the outside surface of a hollow fiber membrane. 122

B.1. AFM and SEM images of control (Optiflux®) membrane. (A) AFM of lumen at 2 x 2 μm^2 x 50 nm. (B) AFM of outside at 10 x 10 μm^2 x 500 nm. (C) SEM of lumen at 20000X. (D) SEM of outside at 5000X. AFM and SEM images reveals nodule aggregates as described in Chapter 3 as well as porous outer membrane. 124

B.2. AFM images of bleached membrane. (A) AFM of lumen at 2 x 2 μm^2 x 50 nm. (B) AFM of outside at 10 x 10 μm^2 x 500 nm. (C) SEM of lumen at 20000X. (D) SEM of outside at 5000X. Nodule aggregates are smaller than those from the control membrane, while pores on the outside are significantly larger than those of the control membrane. 125

B.3. AFM images of high PVP membrane. (A) AFM of lumen at 2 x 2 μm^2 x 50 nm. (B) AFM of outside at 10 x 10 μm^2 x 500 nm. (C) SEM of lumen at 20000X. (D) SEM of outside at 5000X. Membrane is very similar to the bleached membrane on the outside, but the lumen exhibits a rougher surface comprised of small nodule aggregates. 126

B.4. AFM images of low PVP membrane. (A) AFM of lumen at 2 x 2 μm^2 x 50 nm. (B) AFM of outside at 10 x 10 μm^2 x 500 nm. (C) SEM of lumen at 20000X. (D) SEM of outside at 5000X. Membrane is similar to bleached and high PVP membrane on both lumen and outside surfaces. 127

B.5. AFM images of PS-PEG copolymer membrane. (A) AFM of lumen at 2 x 2 μm^2 x 50 nm. (B) AFM of outside at 10 x 10 μm^2 x 500 nm. (C) SEM of lumen at 20000X. (D) SEM of outside at 5000X. Lumen surface is similar to PS-PVP membranes with small nodule aggregates, but the outside surface is more similar to the control membrane, containing smaller pores. 128

C.1. Sieving coefficients of polymer hollow fibers. All hollow fibers effectively limit molecular weight transfer below approximately 5% at 60 kDa, except the copolymer membrane. This membrane may have undergone a physical breach allowing transfer of higher molecular weight species. 130

D.1. Fluorescence images of polymer hollow fiber modified with PLL at various concentrations and challenged with 0.1 μg/ml fluorescent-labeled LPS. Images (A)-(F) represent fibers modified with PLL using no cross-linking agent, whereas images (G)-(L) represent fibers modified with PLL and cross-linked using GA.....131

E.1. AFM images of LPS and PLL on mica from solutions containing 47.5 μg/ml LPS and (A) 0.5 μg/ml PLL, (B) 5 μg/ml PLL, and (C) 50 μg/ml PLL. A film layer of LPS and PLL formed on the mica starting at a concentration of 50 μg/ml PLL.....132

E.2. AFM images of LPS on mica from solutions containing (A) 1 μg/ml, (B) 10 μg/ml, (C) 50 μg/ml, and (D) 100 μg/ml LPS in PBS, and subsequently profile cuts using Nanoscope III Imaging Software. Solutions containing more than 10 μg/ml LPS led to images containing small “islands”, presumably LPS deposits on the mica surface.....133

CHAPTER 1

INTRODUCTION

ESRD AND DIALYSIS

Chronic renal failure (end stage renal disease, ESRD) is the final pathway of several kidney diseases. The choices for a patient that has reached the point where renal function is no longer sufficient to sustain life are 1) chronic dialysis treatment (hemodialysis, peritoneal dialysis), 2) renal transplantation, or 3) death. In 2006, more than 506,000 people in the United States suffered from ESRD, while 327,000 patients were receiving chronic hemodialysis. The costs of Medicare spending on ESRD in 2006 were $23 billion (6.4% of total Medicare budget), while $17 billion was spent on dialysis alone (1). ESRD research, then, is of great importance to both the economy and society in general.

ESRD is the final stage of chronic kidney disease (CKD). CKD is defined as either kidney damage or decreased kidney function for 3 or more months (2). There are several factors that either cause susceptibility to or direct initiation of CKD. Susceptibility factors include age, family history, reduction in kidney mass, low birth weight, racial or ethnic minority status, and low income status (3). Initiation factors include diabetes, high blood pressure, autoimmune diseases, systemic infections, urinary tract infections, and urinary stones (3).

There are several markers currently used to diagnose reduced kidney function including persistent proteinuria, abnormalities in urine sediment, blood and urine chemistry measurements, abnormal findings on imaging studies, and decreased

glomerular filtration rate (GFR) (2, 4). Of these, GFR is considered the most accurate method of determining kidney function (5). Kidney failure, or stage 5 CKD, occurs when the GFR of the kidney is less than 15 ml/min per 1.73 m^2 (3). Normal GFR for a young adult is approximately 120-130 ml/min per 1.73 m^2, however, GFR levels are largely dependent on age, sex, and body size (5-6).

While kidneys are generally known as the filters of the body, they have many other functions such as regulating the circulation of blood volume through hormonal control of red blood cell mass, directly controlling salt and water excretion, regulating bone mineralization through calcium and phosphorus excretion and Vitamin D synthesis, and controlling the acid-base balance in the body, plasma tonicity, potassium levels, and blood pressure (7-8). Dialysis, which filters blood by transport of toxins through a membrane, is very limited in its ability to mimic the kidney. Thus, the ideal solution to kidney failure is kidney transplantation, with dialysis serving as a short-term bridge to transplantation.

The 2008 Renal Data System annual report (1) showed that in 2006 there were over 68,000 people in the United States waiting for a kidney or kidney-pancreas transplant, while only 18,052 transplants were performed. The median wait time for kidney transplantation was 2.84 years in 2003, with wait time varying by race from 2.3 years for whites, 3.8 years for blacks, and 4.0 years for other races. Four percent of patients in their first year of waiting for a transplant die, while 28% die who are in their fifth year of waiting. Therefore, improvements in technology and procedures for those undergoing dialysis is of vital importance to kidney failure patients.

Once kidney function decreases sufficiently to be classified as ESRD, there are two dialysis possibilities available to a patient: hemodialysis (HD) and peritoneal dialysis (PD). PD involves using the peritoneum (a membrane surrounding the abdominal cavity) to filter toxins from the blood by filling the peritoneal cavity with a dialysate solution. Because this method of dialysis can be self-administered it is a more attractive alternative than HD; however, only about 5% of patients in the U.S. were undergoing PD in 2006 (1). The reason for this can be attributed to the high dropout rate for PD due to technique-related problems. Only a limited number of patients stay on PD over a period of 5 years. Generally, technique failure is the main cause of either switching to HD or death, with peritonitis the leading complication (9). Improvements in materials, dialysate composition, and patient training are needed to covercome the main causes of PD failure including catheter infection, peritoneal sclerosis, and neoplasm of the gastrointestinal tract (10-11).

HD treatment is performed on approximately 65% of ESRD patients (the remaining 35% of those with ESRD are prevalent transplant patients or PD patients) (1). HD is the process by which blood is filtered extracorporeally by passing it through a semipermeable membrane, whereupon toxins in the blood are removed (Fig. 1.1). Thousands of hollow fibers are contained in a housing and together they comprise a dialyzer. A solution is passed on the outside of the fibers countercurrent to the blood, providing conditions necessary for cleaning the blood.

Dialysis is generally governed by three principles: diffusion, ultrafiltration, and convection (12). Diffusion refers to the movement of small molecular weight species, including electrolytes, across the dialyzer membrane. Ultrafiltration (UF) involves the

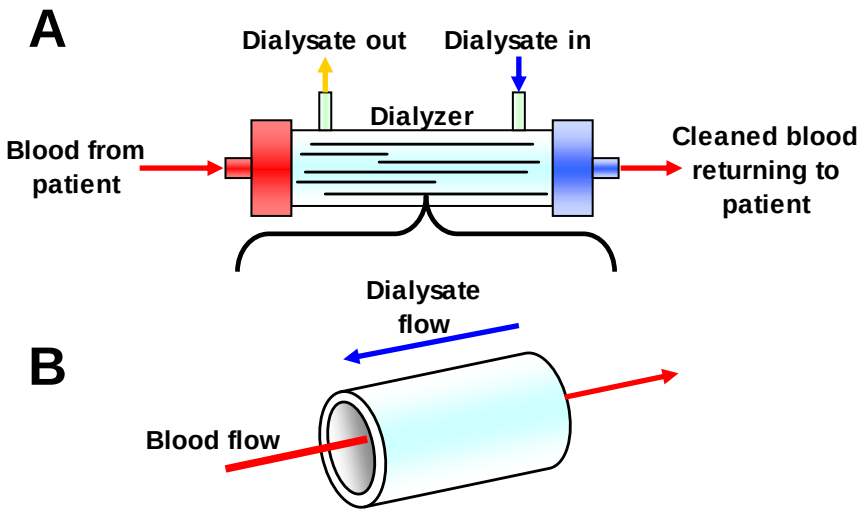

FIG. 1.1. Diagram of hemodialysis procedure. (A) Blood is removed from a patient and filtered through a dialyzer, then returned to the body. (B) Blood is passed through the inside of a hollow fiber membrane while dialysate flows countercurrent on the outside.

movement of water across the semipermeable membrane through the use of external pressure and is the primary method for water removal from the blood. With the movement of solvent molecules, larger molecules are transported by convection. Ideally, smaller molecules, such as sodium and potassium, can pass through the membrane easily due to diffusion. However, larger molecular weight species, such as human serum albumin (HSA), are limited based on the molecular weight cutoff of the dialyzer despite the convective forces.

Dialysate, the solution passed on the outside of the hollow fibers is a fluid composed of electrolytes, dextrose, and water with exact chemistries dependent on the needs of the dialysis patient (13). Recently there has been a trend toward using bicarbonate dialysate in conjunction with high-flux dialyzers (14). Bicarbonate dialysate has been shown to improve patient nutritional status accompanied by an increase in serum bicarbonate levels, which results in a decreased frequency of acidosis (15-16).

Credit for the first human dialysis treatment is generally ascribed to Georg Haas who treated an acute renal failure patient in 1924, but the process was further refined with more suitable conditions by Willem Kolff in the 1930's and 1940's (12). Further improvements in HD treatment sought to make the hollow fiber membrane more biocompatible, as well as improve the materials used in membrane manufacture. Cellulose membranes, because of their ease in manufacturing and excellent diffusivity and mechanical properties, were first used as dialysis membanes, but the introduction of synthetic membranes formed from polysulfone (PS) and polyacrylonitrile (PAN) caused a change in the dialysis community. PS membranes offered the ability to control molecular weight cutoff, improved biocompatibility, and the choice of steam-sterilization (17). Researchers today are focusing on improving the quality of life of patients, the cost-effectiveness of treatment, and the mortality rate of ESRD patients, which remains higher than that of the general population.

BIOPROCESSING

The ability to produce human proteins using genetic engineering rather than isolating them from tissue samples has become an important technology in therapeutic medicine. Since the first *E. coli* bacteria were infused with recombinant DNA to produce human insulin, over 100 other drug substances have been produced using recombinant technology. As this field expands, improvements in downstream processing to isolate a wider range of recombinant therapeutics from a wider range of cell types will be necessary.

Genetic engineering of cells involves the transplantation of a gene via a vector to a new host organism. The term transfection (transformation via infection) is often used to describe this process. This transfer of DNA is accomplished through one of several established techniques. Transfection by calcium phosphate involves precipitation of DNA, which is then added to the cells to be transfected. The complexed DNA is then taken up by the cells and incorporated in the genome (18). A method gaining in popularity is that of polymer-based gene delivery wherein plasmid DNA and cationic lipids or polymers such as polyethylenimine (PEI) or diethylaminoethylene-dextran (DEAE-dextran) form a complex which is then taken up by a cell. Uptake pathways are dependent on the polymer and cell type used (19). Incorporation of DNA fragments into liposomes has been shown to be very effective with mammalian cells (20).

Upon transfection, the host cell proliferates and produces the desired recombinant protein given the right conditions. While the first cell lines used to produce human proteins were often bacterial strains (most predominantly *E. coli*), transfection of eukaryotic cells was shown to be necessary in certain cases due to the need of glycosylation, wherein sugar moieties are added to the protein post-translational. Four eukaryotic cell lines are generally used: *S.* cerevisiea, Chinese hamster ovary (CHO), baby hamster (BHK), and human fibrosarcoma cells. It has been shown, however, that not all eukaryotic cells perform this step identically as yeast cells often yield different glycosylation patterns than mammalian cells. Metabolically engineered plant cells are also being investigated to produce human-like sugar moieties on proteins (21).

While glycosylation is necessary to produce some proteins, other proteins have been shown to be functional despite the lack of this step. *E. coli* cells are now capable of

producing functional therapeutic proteins such as interferon-α (IFN-α), IFN-β, IFN-γ, tissue necrosis factor-α (TNF-α), and interleukin-2. Yeast cells are often used to produce human insulin, glucagons, and several blood anticoagulant factors. It must be noted that some 'artificial proteins' have been shown to perform better than their 'natural protein' counterparts, as is the case with IFN-β-1b (21).

Production scale-up of protein production will not be discussed here. This is a very sensitive process wherein proper levels of nutrients and mixing conditions must be maintained to maximize production and minimize metabolic overload on cells.

Harvesting of proteins from cell cultures is also a complex subject which will be mentioned only briefly. Mammalian cells tend to secrete recombinant proteins, whereas bacteria usually sequester them (often in inclusion bodies) within the cell in a denatured state (21-22). Because the proteins are denatured, post-production modifications must take place to activate the protein. Downstream processing, specifically the removal of bacterial cell wall fragments, will be discussed in Chapter 2.

Mammalian cells represent the best option for producing viable human proteins. However, due to high costs of fermentation and high safety costs of working with mammalian cells, bacterial and yeast cell lines are more attractive. Continuing research is being done in the field of bioprocessing to lower overall costs and to produce other valuable proteins.

BACTERIA

Endotoxin

Of constant importance to both the dialysis and bioprocessing communities is the issue of bacterial endotoxin (lipopolysaccharide, LPS) that exists on the outer membrane of gram-negative bacteria. LPS is firmly anchored within and can constitute up to 75% of the cell outer membrane (Fig. 1.2) (23-24). It is responsible for organization and stability, although it is also important in interactions with other cells and proteins (24). Removing LPS from solution is necessary because there exist up to two million LPS molecules per bacterium (25).

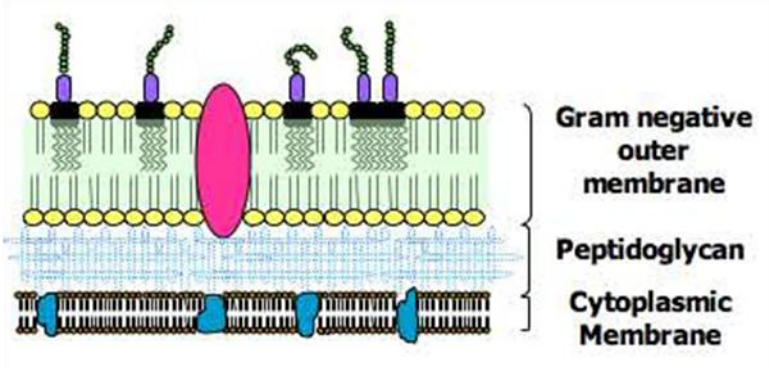

FIG. 1.2. Diagram representing the outer cell wall of gram-negative bacteria. LPS molecules in the outer membrane are represented with lipid A anchored in the phopholipid bilayer and core and oligosaccharide chains extending into the extracellular space.

LPS consists of three main parts: an outer-membrane-integrated lipid (Lipid A), a core oligosaccharide, and a long heteropolysaccharide chain (O-antigen) (25). The O-antigen, consisting of a chain of repeating oligosaccharide units (3-8 monosaccharides), varies among different bacterial strains and is the recognition site for blood-borne

antibodies. The lipid A portion is generally conserved among bacterial types and is responsible for eliciting pyrogenic reactions. A schematic view of a typical LPS monomer is depicted in Fig. 1.3.

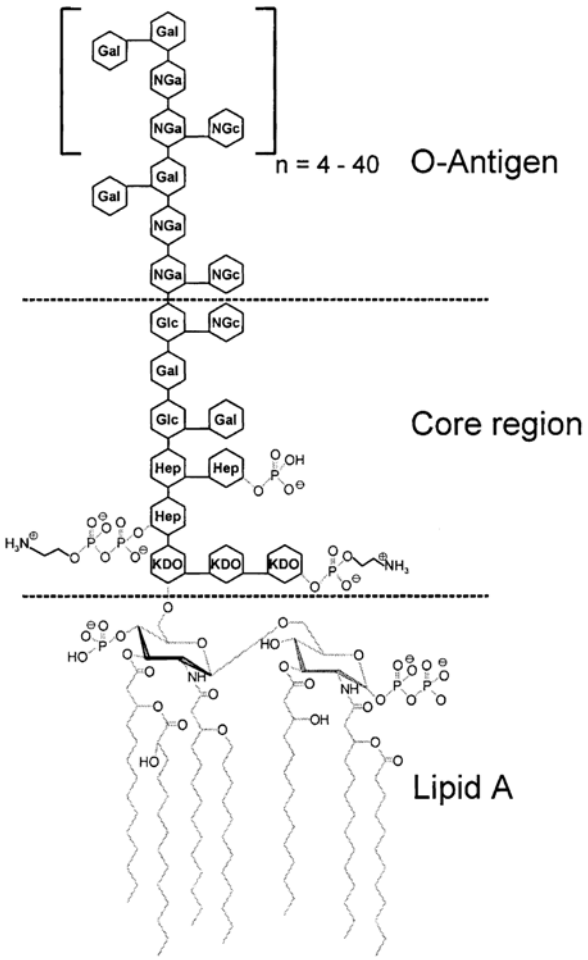

FIG. 1.3. Schematic view of the chemical structure of endotoxin from E. coli O111:B4 (26). Hep, L-glycero-D-manno-heptose; Gal, galactose; Glc, Glucose; KDO, 2-keto-3-deoxyoctonic acid; NGa, N-acetyl-galactosamine; NGc, N-acetyl-glucosamine. This research was originally published in the Journal of Biological Chemistry. Ohno N, Morrison DC. Lipopolysaccharide interaction with lysozyme. *J Biol Chem*. 1989; 264:4434-41. © the American Society for Biochemistry and Molecular Biology.

The lipid A consists of a phosphorylated *N*-acetyl-glucosamine (NAG) dimer, connected to typically 6 or 7 saturated fatty acid chains (26-27). The variability of the fatty acid chains plays an important role in determining toxic properties, resisting host antimicrobial factors, and avoiding recognition from specific components of the host immune system (28-30). The hydrophobic nature of lipid A allows attachment to hydrophobic surfaces (25). Also of importance are the phosphate groups on the lipid A and core saccharide regions, facilitating adsorption to surfaces through ionic interactions (25).

The size of LPS varies from monomers of 10 kDa, to micelles of 1000 kDa or larger (25, 31-32). The predominant form of LPS in solution is as aggregates in the form of micelles and vesicles. Several methods of analyzing LPS aggregates have been used including atomic force microscopy (AFM), steady-state fluorescence, dynamic light scattering, NMR diffusometry, and cryo-tunneling electron microscopy (TEM) (33-35). Aggregates has been reported to exist at concentrations from 10 μg/ml up to 300 μg/ml with an average micelle size of approximately 19 nm and larger aggregates up to 320 nm (33). The supramolecular structure has been described as in Fig. 1.4. These micelles and vesicles vary in size and stability depending on solution pH and concentration of any detergents or ions (25, 32, 35). It has also been described that LPS monomers can be released from micelles through the use of certain proteins (36).

LPS at concentrations as low as 4 ng/kg body weight are capable of eliciting a pyrogenic response in adults, however, critical concentrations depend on the virulence of the organism, the infection site, the host response, and some genetic factors (25, 37). Pyrogenic response can include fever, shivering, hypotension, adult respiratory distress

syndrome, disseminated intravascular coagulation, endotoxin shock, or death (25). Contrary to popular belief, endotoxin does not attack host cells directly but rather the pyrogenic response is a result of the host immune system reacting to the presence of LPS. LPS has been reported to activate the complement, coagulation, and kinin systems, although the exact method of recognition has only recently been discovered (25). Upon entrance into the blood stream LPS binds to LPS-binding protein (LBP). This complex then binds to a soluble receptor protein, CD14, which in turn binds to Toll-like receptor-4 (TLR-4), found on monocytes, inducing signal transduction. The monocytes then release pro-inflammatory cytokines such as interleukin-1 (IL-1), IL-6, and (TNF-α).

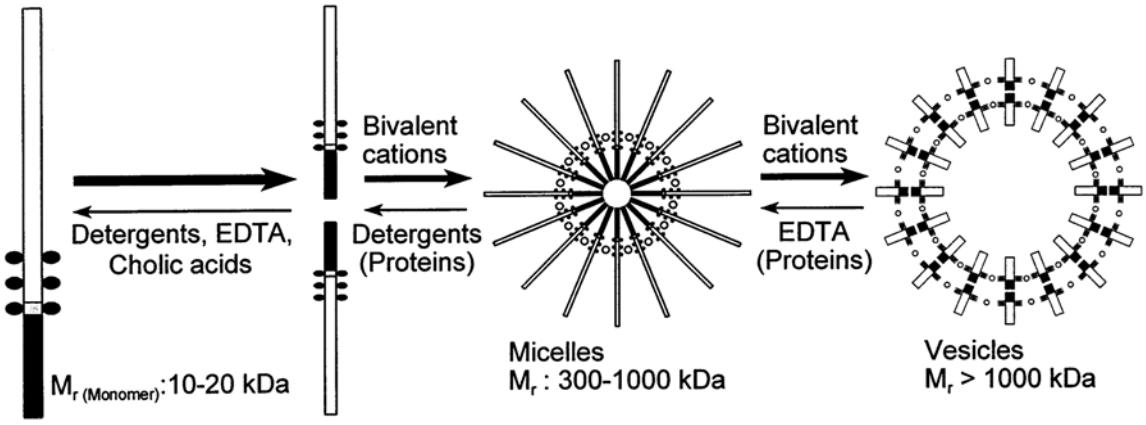

FIG. 1.4. Structures of LPS aggregates in aqueous solutions. An LPS monomer is depicted on the left with lipid A (black rod), phosphate groups (black circles), and saccharide group (white rod). Bivalent cations (white circles) facilitate formation of micelles and vesicles. (Reprinted from Journal of Biotechnology, 76, Petsch D, Anspach FB, Endotoxin removal from protein solutions, 97-119, Copyright (2000), with permission from Elsevier (35).

Bacteria in solutions

Because minute traces of bacteria or LPS can cause adverse immune system reactions, it is important to prevent any possible contamination of water sources in

dialysate and remove any LPS contamination when isolating recombinant proteins from gram-negative bacteria.

The most sensitive technique to measure LPS concentrations in solution is the limulus amebocyte lysate (LAL) assay. This assay is based on the coagulation of cell lysate of the horseshoe crab *Limulus polyphemus* in contact with very low concentrations of LPS. LPS concentrations measured with this test are generally reported in endotoxin units (EU) per ml, where one EU is equivalent to 0.1 ng of LAL reactivity of the U.S. Pharmacopoeia reference standard endotoxin, EC-5 from *E. coli* 0113:h10:K (38).

Bacterial contamination in dialysate fluids and clinical water sources has been documented (39-42). A diverse community of culturable bacteria has been found in dialysate fluids, of which *Pseudomonas* is most common (43-46). Robust, sessile bacterial communities, called biofilms, may present a persistent source of contamination in dialysate water production lines because they are difficult to detect and remove (40-42). Several studies on water and dialysate quality in clinics in the U.S. and Europe have shown that as many as 20% of the samples tested were above the limit of the recommended standards (45, 47-48). While small quantities of contamination may not always elicit a pyrogenic response, continued exposure to contaminated dialysate is of great concern because a typical patient on hemodialysis therapy will be directly exposed to 18,000-30,000 liters of water annually (46, 49). Reported pyrogenic reactions up to 0.7 per 1000 treatments have been reported (14, 46, 50).

LPS contamination is prevalent in other sources besides that of water used in dialysate. Tap and mineral water have been reported to contain 1-20 EU/ml, while water in an open-air swimming pool contained over 25,000 EU/ml (51). Ingestion of LPS

poses little risk as compared to direct introduction into the blood, as in dialysis, or injection of contaminated recombinant therapeutics. Still a higher possibility of LPS contamination exists in solutions prepared from gram-negative bacteria. A solution of proteins from high cell density cultures of *E. coli* contained over 2 million EU/ml, while proteins from shaking flask cultures of *E. coli* contained 70,000-500,000 EU/ml (35). Commercial preparations of bovine serum albumin (BSA) contained up to 50 EU/ml (35).

RESEARCH OBJECTIVES

The research is driven by the following hypothesis: "Hollow fiber membranes exhibit properties favorable to secondary functionality, such as endotoxin removal, during primary application in dialysis or isolation of therapeutics from recombinant bacteria."

To test this hypothesis, a series of experiments were designed to explore physicochemical characteristics of HFMs undergoing several sterilization procedures. Also, chemical modifications to hollow fibers were explored based on the theory that membrane surface chemistry can act as an endotoxin adsorption matrix in both dialysis and filtration applications. To achieve these goals, the experimental work of this research was divided into three specific aims:

1. *Effect of sterilization techniques on physicochemical properties of polysulfone hollow fibers*. Polysulfone hollow fibers subjected to ethylene oxide, bleach and electron-beam sterilization treatments were characterized to deduce the overall

effects to surface hydrophilicity, surface morphology, and membrane sorption abilities.

2. *Hemodialysis membrane surface chemistry as a barrier to endotoxin transfer*. Membrane surface chemistry, more specifically polyvinylpyrrolidone content in the polymer structure, was investigated as a mechanism to adsorb bacterial endotoxin and prevent possible back-filtration in hemodialysis conditions.
3. *Hollow fiber membranes modified with poly-L-lysine as endotoxin scavengers*. The addition of poly-L-lysine to polysulfone hollow fiber membranes was investigated as a potential tool for scavenging endotoxin from both dialysate solutions and biological solutions prepared from gram-negative bacterial cultures. Interactions of poly-L-lysine and endotoxin were investigated using several analytical techniques.

Chapter 2 will discuss current research being done on hollow fiber membranes including material choice, membrane analysis techniques, and cleaning of membranes. Another section will discuss current techniques of removing LPS from solutions including using hollow fiber membranes. The following three chapters will present new research as per the three objectives outlined above. The final chapter will include general conclusions and recommendations for further research.

REFERENCES

1. U.S. Renal Data System, USRDS 2008 Annual Report: Atlas of chronic kidney disease and end-stage renal disease in the United States, Bethesda, MD: National Institutes of Health, National Institute of Diabetes and Digestive and Kidney Diseases, 2008.

2. Levey AS, Coresh J, Balk E, Kausz AT, Levin A, Steffes MW, et al. National kidney foundation practice guidelines for chronic kidney disease: Evaluation, classification, and stratification. *Ann Intern Med* 2003;139:137-47.

3. K/DOQI clinical practice guidelines for chornic kidney disease: evaluation, classification, and stratification. Kidney disease outcome quality initiative. *Am J Kidney Dis* 2002;39:S1-246.

4. Keane W, Eknoyan G. Proteinuria, albuminuria, risk, assessment, detection, elimination (PARADE): A position paper of the National Kidney Foundation. *Am J Kidney Dis* 1999;33:1004-10.

5. Smith HW. Comparative physiology of the kidney. In: Smith HW, ed. *The Kidney: Structure and Function in Health and Disease*. New York: Oxford University Press, 1951:520-74.

6. Rowe JW, Andres R, Tobin JD, Norris AH, Shock NW. The effect of age on creatinine clearance in men: A cross-sectional and longitudinal study. *J Gerontol* 1976;31:155-63.

7. Fissell WH, Fleischman AJ, Humes HD, Roy S. Development of continuous implantable renal replacement: Past and future. *Translational Research* 2007;150:327-36.

8. Hamilton RW. Principles of dialysis: Diffusion, convection and dialysis machines. In: Henrich WL, Bennet WM, eds. *Atlas of diseases of the kidney*. Philadelphia: Blackwell Science, 1999:1.1-1.6.

9. Woodrow G, Turney JH, Brownjohn AM. Technique failure in peritoneal dialysis and its impact on patient survival. *Perit Dial Int* 1997;17:360-4.

10. Augustine T, Brown PW, Davies SD, Summers AM, Wilkie ME. Encapsulating peritoneal sclerosis: Clinical significance and implications. *Nephron Clin Pract* 2009;111:c149-c54.

11. Nodaira Y, Ikeda N, Watanabe K, Inoue T, Gen S, Kanno Y, et al. Risk factors and cause of removal of peritoneal dialysis catheter in patients on continuous ambulatory peritoneal dialysis. *Adv Perit Dial* 2008;24:65-8.

12. Rosner MH. Hemodialysis for the non-nephrologist. *Southern Med J* 2005;98:785-91.

13. Palmer BF. Dialysate composition in hemodialysis and peritoneal dialysis. In: Henrich WL, Bennet WM, eds. *Atlas of Diseases of the Kidney*. Philadelphia: Blackwell Science, 1999:2.1-2.8.

14. Gordon SM, Oettinger CW, Bland LA, Oliver JC, Arduino MJ, Aguero SM, et al. Pyrogenic reactions in patients receiving conventional, high-efficiency, or high-flux hemodialysis treatments with bicarbonate dialysate containing high concentrations of bacteria and endotoxin. *J Am Soc Nephrol* 1992;2:1436-44.

15. Williams AJ, Dittmer ID, McArley A, Clarke J. High bicarbonate dialysate in haemodialysis patients: Effects on acidosis and nutritional status. *Nephrol Dial Transplant* 1997;12:2633-7.

16. Kobrin SM, Raja RM. Effect of varying dialysate bicarbonate concentration on serum phosphate. *ASAIO Trans* 1989;35:423-5.

17. Vienken J, Bowry S. Quo vadis dialysis membrane? *Artif Organs* 2002;26:152-9.

18. Graham FL, Eb AJvd. A new technique for the assay of infectivity of human adenovirus 5 DNA. *Virology* 1973;52:456-67.

19. Midoux P, Breuzard G, Gomez JP, Pichon C. Polymer-based gene delivery: A current review on the uptake and intracellular trafficking of polyplexes. *Curr Gene Ther* 2008;8:335-52.

20. Reisinger H, Sevcsik E, Vorauer-Uhl K, Lohner K, Katinger H, Kunert R. Serum-free transfection of CHO-cells with tailor-made unilamellar vesicles. *Cytotechnology* 2007;54:157-68.

21. Dingermann T. Recombinant therapeutic proteins: Production platforms and challenges. *Biotechnol J* 2007;3:90-7.

22. Graumann K, Premstaller A. Manufacturing of recombinant therapeutic proteins in microbial systems. *Biotechnol J* 2006;1:164-86.

23. Raetz CRH. Biochemistry of endotoxins. *Annu Rev Biochem* 1990;59:129-70.

24. Vaara M, Nikaido H. Outer membrane organization. In: Rietschel ET, ed. *Handbook of Endotoxin*. Amsterdam: Elsevier, 1984:1-45.

25. Gorbet MB, Sefton MV. Endotoxin: The uninvited guest. *Biomaterials* 2005;26:6811-7.

26. Ohno N, Morrison DC. Lipopolysaccharide interaction with lysozyme. *J Biol Chem* 1989;264:4434-41.

27. Rietschel ET, Kirikae T, Schade FU, Mamat U, Schmidt G, Loppnow H, et al. Bacterial endotoxin: Molecular relationships of structure to activity and function. *FASEB J* 1994;8:217-25.

28. Bland LA, Oliver JC, Arduino MJ, Oettinger CW, McAllister SK, Favero MS. Potency of endotoxin from bicarbonate dialysate compared with endotoxins from *Escherichia coli* and *Shigella flexneri*. *J Am Soc Nephrol* 1994;5:1634-7.

29. Gunn JS. Bacterial modification of LPS and resistance to antimicrobial peptides. *J Endotoxin Res* 2001;7:57-62.

30. Qureshi N, Kutuzova G, Takayama K, Rice PA, Golenbock TT. Structure of lipid A and cell activation. *J Endotoxin Research* 1999;5:147-50.

31. Yamamoto K-i, Matsuda M, Hayama M, Asutagawa J, Tanaka S, Kohori F, et al. Evaluation of the activity of endotoxin trapped by a hollow-fiber dialysis membrane. *J Membrane Sci* 2006;272:211-6.

32. Darkow R, Groth T, Albrecht W, Lützow K, Paul D. Functionalized nanoparticles for endotoxin binding in aqueous solutions. *Biomaterials* 1999;20:1277-83.

33. Bergstrand A, Svanberg C, Langton M, Nyden M. Aggregation behavior and size of lipopolysaccharide from *Escherichia coli* O55:B5. *Colloid Surface B* 2006;40:99-106.

34. Hayama M, Miyasaka T, Mochizuki S, Asahara H, Tsujioka K, Kohori F, et al. Visualization of distribution of endotoxin trapped in an endotoxin-blocking filtration membrane. *J Membrane Sci* 2002;210:45-53.

35. Petsch D, Anspach FB. Endotoxin removal from protein solutions. *J Biotechnol* 2000;76:97-119.

36. Li L, Luo RG. Protein concentration effect on protein-lipopolysaccharide (LPS) binding and endotoxin removal. *Biotechnol Lett* 1997;19:135-8.

37. Dinarello CA, Cannon JG. Cytokine measurement in septic shock. *Ann Inter Med* 1993;119:853-4.

38. Tellingen Av, Grooteman MPC, Pronk R, Loon Jv, Vervloet MG, Wee PMt, et al. Lipopolysaccharide concentrations during superflux dialysis using unfiltered bicarbonate dialysate. *ASAIO J* 2002;48:383-8.

39. Bambauer R, Walther J, Jung WK. Ultrafiltration of dialysis fluid to obtain a sterile solution during hemodialysis. *Blood Purificat* 1990;8:309-17.

40. Hoenich NA, Levin R. The implications of water quality in hemodialysis. *Semin Dialysis* 2003;16:492-7.

41. Man N-K, Degremont A, Darbord J-C, Collet M, Vaillant P. Evidence of bacterial biofilm in tubing from hydraulic pathway of hemodialysis system. *Artif Organs* 1998;22:596-600.

42. Marion-Ferey K, Leid JG, Bouvier G, Pasmore M, Husson G, Vilagines R. Endotoxin level measurement in hemodialysis biofilm using "the whole blood assay". *Artif Organs* 2005;29:475-81.

43. Gomila M, Gasco J, Busquets A, Gil J, Bernaeu R, Buades JM, et al. Identification of culturable bacteria present in haemodialysis water and fluid. *FEMS Microbiol Ecol* 2005;52:101-14.

44. Tsuchida K, Nakatani T, Sugimura K, Yoshimura R, Matsuyama M, Takemoto Y. Biological reactions resulting from endotoxin adsorbed on dialysis membrane: An in vitro study. *Artif Organs* 2004;28:231-4.

45. Jaber BL, Gonski JA, Cendoroglo M, Balakrishnan VS, Razeghi P, Diniarello CA, et al. New polyether sulfone dialyzers attenuate passage of cytokine-inducing substances from *Pseudomonas aeruginosa* contaminated dialysate. *Blood Purificat* 1998;16:210-9.

46. ANZSN. *Consensus Statement for Maintenance of Chemical and Microbiological Safety of Haemodialysis Water and Dialysate Systems*. Sydney, Australia: Australian and New Zealand Society of Nephrology, 1996.

47. Linnenweber S, Lonnemann G. Pyrogen retention by the Asahi APS-650 polysulfone dialyzer during in vitro dialysis with whole human donor blood. *ASAIO J* 2000;46:444-7.

48. Lonnemann G, Sereni L, Lemke H-D, Tetta C. Pyrogen retention by highly permeable synthetic membranes during in vitro dialysis. *Artif Organs* 2001;25:951-60.

49. Weber V, Linsberger I, Rossmanith E, Weber C, Falkenhagen D. Pyrogen transfer across high- and low-flux hemodialysis membranes. *Artif Organs* 2004;28:210-7.

50. Roth VR, Jarvis WR. Outbreaks of infection and/or pyrogenic reactions in dialysis patients. *Semin Dialysis* 2000;13:92-6.

51. Müller-Calgan H. Der limulustest in der pharmazeutischen praxis. In: Scheer R, ed. *Der Limulustest*. Stuttgart: Wissenschaftliche Verlagsgesellschaft, 1989:51.

CHAPTER 2

LITERATURE REVIEW

HOLLOW FIBER MEMBRANE (HFM) MATERIALS

The first membranes used in dialysis were composed of cellulose (Cuprophan) and were manufactured in a flat-sheet design. In the 1970's, hollow fiber membranes (HFMs) were first introduced offering laminar blood flow, low boundary layer resistance, increased mass transport, and offering less-costly production (1). Cellulose was the gold standard for several years because of ease in manufacturing and transport characteristics. Cellulose membranes and derivatives thereof are currently being investigated for use in dialysis and liver assist bioreactors. Cellulose-acetate hollow fibers modified with phospholipids have shown good permeability, low protein adsorption, and low fouling due to the hydrophilic phospholipids sequestered on the outer surface of the HFM (2-3). Similar membranes also showed better adhesion of hepatocytes and increased urea and albumin synthesis compared to unmodified cellulose-acetate membranes (4). Other cellulose-acetate membranes modified with vitamin E did not demonstrate increased or decreased biocompatibility as measured by standard lipid profiles, oxidized LDL levels, or total antioxidant status, but did show potential decrease in overall middle-molecular weight clearance long term (5).

New issues of biocompatibility and hemocompatibility have caused concerns that membrane material properties could be the cause of leucopenia, complement activation, cell activation, coagulation, and cytokine release (1). The introduction of synthetic membranes formed with polyacrylonitrile (PAN) and polysulfone (PS) helped overcome

these issues. These membranes offered better biocompatibility and the ability to specifically design transport characteristics based on size exclusion (6). PS and PAN are often blended with hydrophilizing agents, such as polyvinylpyrrolidone (PVP) or meth-allylsufonate, to improve biocompatibility and provide the necessary porosity for transport of solutes (6-8).

PS membranes have become increasingly popular for not only hemodialysis applications, but for use in ultrafiltration, plasmapheresis, microfiltration, cell culture, bioreactors, tissue engineering, and controlled drug release devices (4, 9-15). The reason for this is based on the ability to design specific molecular weight cut-offs (MWCO) while remaining structurally intact, biocompatible, chemically inert, and allowing transport of gases, nutrients, and products. Constant improvement is being sought by changing polymer blends to accentuate desired characteristics.

Among the more popular variations of PS is polyethersulfone (PES), which is believed to be better for liquid transport based on increased polarity of PES compared to PS (16). Chitosan and heparin added to PS membranes showed increased wettability and decreased platelet, HSA, and fibrinogen adhesion (17). Surfactants are often added to PS to increase hydrophilicity and decrease protein adsorption (18-20). Addition of SPAN-80 showed decreased macrovoid size and increased pervaporation (21). PES blended with PEO increased water flux (due to decreased hydrophobicity) and decreased fouling (22). The increased wettability of PEO-PS membranes arises from the hydrophilic PEO chain being sequestered on the outer surfaces of the membranes during the phase inversion process (20). Another experimental blend of PS-cellulose-acetate has been shown to

increase water flux, surface porosity, but decrease rejection of proteins and metal ions (23).

Still other membranes made of alumina are being investigated as a potential alternative to other synthetic membranes (24). These membranes offer the advantage of uniform pore size, pore distribution, higher hydraulic conductivity, and resistance to high temperature, making these ceramic membranes a viable alternative.

It must be noted that desired surface and membrane matrix characteristics are specific to the end use of the hollow fiber. HFMs used in HD must possess a MWCO near 60 kD to ensure that major plasma proteins, such as albumin, are retained while toxins, such as urea and β_2-microglobulin (B2M), are removed. Also, HD membranes must disallow adsorption of proteins, cells, and bacteria as this may compromise ultrafiltration rates. Conversely, adsorption of cells is necessary in applications such as cell culture, bioreactors, and tissue engineering.

CHARACTERIZATION OF HFMS

As stated, properties of HFMs must be investigated to determine their surface physicochemistry, biocompatibility, and ability to perform the intended designed job. Characterization techniques are as vast as the properties they investigate. Microscopic methods investigate surface morphology and structure while filtration techniques show the ability of a fiber to selectively remove or retain biological and chemical species.

For membranes used in ultrafiltration, microfiltration, dialysis, and perfusion, ultrafiltration rates and sieving coefficients are vital to overall performance (25-28). Membrane flux is often measured using the ultrafiltration coefficient (KUF) which is

defined as the number of milliliters of fluid per hour that are transferred across a membrane per unit pressure gradient. If the KUF is low, the permeability of water is low. The ability of a HFM to selectively limit the transport of species of different molecular weights is often measured using a range of dextrans. Clearance of urea and B2M, two species of interest in hemodialysis, are also often used.

Microscopy techniques have also proven useful in analyzing pore sizes of HFMs. Scanning electron microscopy (SEM) has been used to image both lumen surfaces and matrix pores of HFMs. Particularly, SEM has been used to measure surface porosity and fouling of membranes used in bioreactors (15-16, 23, 29-30). Atomic force microscopy (AFM) is a powerful tool used to provide three-dimensional images of surfaces on the nanoscale (25, 28, 31-33). AFM has been used to visualize membrane morphology changes from wet to dry states (7). Also, upon phase inversion, polymeric membranes tend to form nodules or nodule aggregates as described by Kesting (34). AFM was also used to measure the size of these nodules as well as pore sizes (29, 32). AFM has also been used to image cross-sections of HFMs, although such images are unclear (35).

Elemental analysis of membranes is often performed using x-ray photoelectron spectroscopy (XPS) and nuclear magnetic resonance (NMR). These techniques are used to deduce distribution of chemicals used in membrane fabrication. For example, XPS has been used to determine the surface composition of PS-PVP membranes based on the distribution of sulfur and nitrogen, components of PS and PVP, respectively (26, 36). NMR has been used to measure bulk chemical characteristics (18).

Water contact angle measurement (CAM) is often used to learn about surface chemistry and wettabililty of a surface (36). However the size and morphology of HFMs

causes an inherent problem with CAM. One method used an instrument to view the meniscus of water in a HFM (29). Another method used a form of goniometry to measure dynamic water contact angle (29). While these methods are useful in measuring advancing and receding contact angle, there are limitations to measuring static water contact angle.

Biocompatibility of HFMs used in dialysis, bioreactors, and cell culture must be addressed for each membrane type used. Often adsorption of blood proteins, platelets, and heparin are investigated (7, 18, 37). Activation of lactate dehydrogenase can also be used to test biocompatibility in vivo (7). Fibrinogen and HSA adsorbed to an AFM tip has yielded data on attraction of proteins to surfaces of PS-PVP membranes (38).

Other methods used to investigate membrane fouling are confocal laser scanning microscopy (CLSM) and time-of-flight secondary ion mass spectroscopy (30, 39-40). While these methods can provide important data on the fouling behavior of HFMs, the resolution of the collected images is generally low.

CLEANING OF HFMS

There exist numerous sterilization procedures used on medical and ultrafiltration devices of which ethylene oxide, irradiation, and steam autoclaving are the most popular (41). Also, filters used in ultrafiltration and dialysis often undergo reprocessing using bleach, citric acid, formaldehyde, and peracetic acid. Choice of sterilization and reprocessing procedure can have dramatic effects on membrane physicochemistry and biocompatibility.

Sterilization techniques

Ethylene oxide (ETO) gas is often used as a sterilant where high temperatures would be detrimental to the properties of the sterilized material. This small gas (MW = 44.1 g/mol), is capable of penetrating most materials, killing any organisms. The unstable structure of ETO allows it to react with various functional groups of proteins and nucleic acids (42). Because the first hollow fiber membranes were composed of cellulose, this method of sterilization was the preferred choice. However, residual ETO can cause adverse reactions in biological environments. In dialysis, "first-use syndrome" was found to be caused by residual ETO in dialyzers following initial sterilization (43).

With the introduction of PS membranes, the choice of steam-sterilization became a possibility. However, there have been conflicting reports about the biocompatibility of steam-sterilized HFMs. In 1992, Link and Büttner suggested steam sterilization was a better option compared to irradiation and ETO (44). Also, in 1998, steam-sterilized dialyzers were shown to be more biocompatible than ETO sterilized membranes based on several markers including white blood cell count and complements C3a and C5a (anaphylatoxins) (45). However, in 2002, another study reported that steam sterilization does not cause a decrease in cytokine release compared to ETO sterilization (46). The debate is ongoing as to the most appropriate sterilization technique for HFMs.

Irradiation is becoming an increasingly popular method of sterilizing medical equipment. An advantage to using irradiation is that the material may be packaged and sealed prior to sterilization. While gamma-irradiation has been the most commonly used method, electron beam (e-beam) sterilization is becoming increasingly popular due to cost-efficiency and quick turnaround times (as short as 5 minute treatment) (47-48). E-

beam systems use high energy electrons to inactivate any biological substances on a material (48). The energy of the electrons in the beam determines the depth of penetration of the electrons into the material. The power of the beam determines the absorbed dosage of radiation at a given conveyor belt speed. The radiation dosage determines the effectiveness of microbial inactivation. The System International (SI) dose unit is the gray (Gy), defined as 1 joule of energy deposited per kilogram of treated material. Typical dosage used in the United States and Europe is 25 kGy (47, 49), however, dosage is determined by the bioburden of the material being irradiated. At this level, the probability of a viable organism existing on the material (activation coefficient) is 10^{-6}.

E-beam sterilization, however, can potentially cause structural changes to polymeric materials. It has been reported that PS has a high radiation stability under dose conditions as extreme as 10^4 kGy (50). Conversely, cross-linking of polymers, including PVP, and restructuring of chemical bonds using e-beam radiation has been investigated (51-53). While the typical irradiation dosage of 25 kGy is 1% of the dosage necessary to reduce mechanical strength of PS by 50%, it can be suggested that physical and chemical properties may be altered by e-beam systems (50).

While most studies on sterilization procedures focus on biocompatibility issues of materials, changes in physicochemistry are not typically reported. It has been shown that e-beam systems may cause some physical or chemical changes, while steam sterilization may also alter some membrane properties if the glass-transition temperature of the material is lower than the autoclave temperature (42). Chemical and morphological changes to materials undergoing ETO treatment have not typically been investigated.

Reprocessing techniques

Closely related to sterilization procedures is reprocessing techniques. While not all HD clinics reprocess dialyzers, the practice is still in use for HD dialyzers and UF filters. Much like sterilization processes, reprocessing procedures may cause changes in biocompatibility and physicochemistry.

Reprocessing using bleach has been shown to cause dramatic changes in membrane properties and overall performance. Because the reactivity of bleach is high, exposure times need not be long (as low as 2 minutes). However, to understand the effects of bleach, longer exposure times have been investigated, especially for HFMs used in UF applications. Short bleach times (5 minutes) coupled with a formaldehyde rinse showed an increase in B2M clearance (27). Longer bleach times (from 0.5 hours to several days) showed increases in flux, increases in pore size up to 7 times, and embrittlement as measured by fiber tensile strength, and net negative charge in PS membranes (26, 54-56). The increased pore size could be attributed to chain scission of PVP via radical reactions as reported (57). An advantage of using bleach is the ability of such treatments to wash membranes of any residual plasma proteins accrued during HD treatment (55).

Because bleaching has been shown to cause changes in membrane properties, other means of reprocessing have been investigated. Peracetic acid and heated citric acid are widely used because they are less destructive to membrane properties. Renalin®, a solution composed of peracetic acid, acetic acid and hydrogen peroxide, has gained popularity for reprocessing HD dialyzers. Peracetic acid has been shown to restore clearances of urea and vitamin B12 (58). However, peracetic acid has been shown to not

fully wash membranes of accumulated plasma proteins, resulting in decreased clearance of B2M and larger molecular weight dextrans (27, 55, 58). Heated citric acid increased clearances of B2M and fully restored urea clearances in PS membranes.

Much like the choice of sterilization technique, reprocessing of hollow fibers remains a topic of debate. Choosing a reprocessing technique greatly depends on the membrane being used and the desired properties to be attained.

REMOVAL OF LPS FROM SOLUTIONS

Removal of LPS from dialysate and water solutions

Because of the possibility of bacterial and LPS contamination in water and dialysate, these solutions must be sterilized prior to use. LPS molecules exhibit high heat stability, requiring temperatures above 180^{o}C to inactivate (59). Therefore other means of eliminating LPS from solutions have been sought. Removal of LPS from solution is generally achieved using affinity sorbents and filtration. Plasma exchange, charcoal hemoperfusion, and immobilization to polymyxin B (PMB), ceramic membranes, and functionalized nanoparticles have been investigated with varying degrees of success (60-64). Other chemistries exhibiting a high affinity for LPS include poly-L-lysine (PLL), diethylaminoethane, histamine, and histidine (65). Cationic polyelectrolytes presumably bind to the negatively charged phosphate groups on LPS. Ultrafiltration of water prior to dialysate preparation has been shown to be effective in eliminating most LPS and bacteria from solution (66-68).

Because the dialysis membrane represents the final barrier in preventing back-filtration of LPS to the blood side of the membrane, several studies have focused on

bacterial retention properties of HFMs. The means of prevention has been ascribed primarily to adsorption, with filtration also playing a vital role (69-70). Certain PS, polyamide and cellulose membranes have been shown to stop back-filtration (69, 71-72). However, it has also been shown that other PS and PES membranes of similar characteristics prevent back-filtration of LPS to different degrees, indicating that specific membrane characteristics contribute to the overall performance of inhibiting trans-membrane LPS flux (69, 73-74). LPS transfer was shown to occur as quickly as 10 minutes (74). Also, increased LPS loads in the dialysate compartment led to increased back-filtration (75-76).

One study showed that LPS readily bound to hydrophobic domains on polyether polymer alloy (PEPA) and polymethyl-methacrylate (PMMA) membranes, but not to hydrophobic domains (77). Similarly, another study showed that preventing back-filtration of LPS increased when a hydrophobic outer layer existed on the HFM and that the presence of PVP increased chances of LPS leaking into the blood compartment (70). The presence of an outer hydrophobic skin to bind LPS could prove valuable because it has been shown that LPS does not have to be in direct contact with blood to elicit a pyrogenic response (78).

Other researchers have focused on reducing serum levels of LPS due to either LPS back-diffusion or infections. Sevelamer hydrochloride (commonly known under the trade name Renagel®) has been shown to bind free LPS in solution and that free phosphate in solution causes positive cooperative binding of LPS (79). Also, a system using immobilized albumin has been shown to remove LPS in hemoperfusion tests (80).

Removal of LPS from biological solutions

During protein purification of solutions prepared using gram-negative bacteria, it is necessary to remove LPS during a purification step. While extraction of intracellular proteins from whole yeast cells has been reported, destruction of bacterial cells via some external process is usually necessary to remove unsecreted proteins (81). Often disruption of cells is performed by high-pressure homogenization, after which filtration, two-phase extraction, and/or an adsorption process removes LPS (82). Because LPS may interact with proteins in solution, LPS can often be "hidden" from removal processes (83). Also, removal processes largely depend on the properties of the protein of interest as the protein may degrade under extreme pH, temperature, or ionic strength. Current methods of removing LPS using each of these techniques will be briefly discussed.

Because LPS usually exists in micelles, separation from small proteins via ultrafiltration is commonly used. One study showed that adding Ca^{2+} and LPS monomers to a solution caused large aggregates of LPS (as in Fig. 1.4) for easier removal with filtration (84). However, some proteins interact with high concentrations of Ca^{2+}, and therefore, this method is limited in its use. Also, because many proteins are larger, ultrafiltration is not a viable option. Therefore, other methods are more commonly used.

Above a critical micelle concentration, detergent combines with lipid A of LPS forming micelles which separate from solution. A number of detergents are being investigated including those of the Triton X series. Triton X-114 detergents have been shown to be effective at removing LPS from solution (85-87). Above a "cloud point" temperature, micelles separate to the bottom of a solution into a micelle-rich phase, while the upper portion of the lipid contains a micelle-poor phase. Centrifugation is commonly

used to facilitate further separation. Subsequent additions of detergent and centrifugation steps can eliminate LPS further.

Perhaps the most common methods of removing LPS from solutions involve the use of an adsorbent (polycationic, immunoaffinity) either in conjunction with filtration or through chromatography. Numerous studies have explored the use of each of these techniques. However, it must be noted that preferred methods are usually dependent on the properties of the proteins in solution.

Linking an adsorbent to a chromatographic membrane has been shown to be effective at selectively removing LPS from a solution (65, 88). Anspach and Hilbeck (65) coated sepharose beads with PLL, PMB, histidine, histamine, and DEAE. They showed excellent removal of LPS from solution at low and neutral pH, but weak adsorption at a pH of 8.5, possibly due to the some deprotonation of the adsorbents (only histidine and histamine have pKa lower than 8.5). Also, all showed good recovery (> 90%) of lysozyme at low and neutral pH, but less (< 90%) recovery at pH 8.5. PLL showed the best recovery of BSA at low and neutral pH, while DEAE performed worst. Another group bound Iron(III) to a chromatographic matrix for LPS removal (89).

While chromatographic methods are often used, it has been shown that under certain conditions, use of an adsorbent-linked filter was more effective at removing LPS from solution (90). It was shown that PEI and PLL removed more LPS, while maintaining over 90% BSA recovery. However, as with similar chromatographic methods, removal of LPS and recovery of protein was highly pH dependent. Similarly, another study showed over 99% removal of LPS from a solution containing BSA using a nylon membrane containing several adsorbents including PLL, PMB, PEI, and DEAE

(91). Addition of a chelating agent increased LPS adsorption slightly in all cases except DEAE. Others have used polycationic adsorbents attached to cellulosic membranes to remove over 90% of LPS while allowing over 90% recovery of BSA (92).

While most methods of binding an adsorbent to a filter membrane often use cross-linking agents, one group has explored the idea of including a charged monomer during the formation of a membrane to provide a charged surface for binding LPS (93). This method could prove valuable as filtration characteristics of the membrane can be custom tailored. Adsorbent-based filtration membranes modified through cross-linking may experience clogging of pores, thus lowering effective pore size.

Others have explored adding adsorbents directly to solutions to first bind LPS in solution, then using filters to remove large aggregates. Cross-linked granular chitosan and water insoluble poly-ε-lysine have both been used for this purpose (94-95). The poly-ε-lysine also allowed excellent recovery of a diverse array of proteins (including BSA, insulin, myoglobin, gamma-globulin, and cytochrome c) after filtration through cellulose acetate membranes. Submicron-sized polystyrene-coglycidyl-methacrylate beads modified with several chemistries were explored for LPS-binding capabilities (64). Cross-linked lysine monomers were shown to be very effective, whereas PEI and PMB were less effective.

As shown, lysine represents an effective adsorbent for LPS. Modifications, using this polyelectrolyte, to hollow fiber membranes used in filtration will be explored in Chapter 5.

REFERENCES

1. Vienken J, Bowry S. Quo vadis dialysis membrane? *Artif Organs* 2002;26:152-9.

2. Ye SH, Watanabe J, Ishihara K. Cellulose acetate hollow fiber membranes blended with phospholipid polymer and their performance for hemopurification. *J Biomat Sci-Polym E* 2004;15:981-1001.

3. Ye SH, Watanabe J, Takai M, Iwasaki Y, Ishihara K. Design of functional hollow fiber membranes modified with phospholipid polymers for application in total hemopurification system. *Biomaterials* 2005;26:5032-41.

4. Ye SH, Watanabe J, Takai M, Iwasaki Y, Ishihara K. High functional hollow fiber membrane modified with phospholipid polymers for a liver assist bioreactor. *Biomaterials* 2006;27:1955-62.

5. MacGinley R, Westhuyzen J, Saltissi D, Morgan C, Healy H, Thirlwell GK, et al. Evaluation of a novel vitamin E coated cellulosic membrane hollow fiber dialyzer. *ASAIO J* 2001;47:66-73.

6. Mulder M. *Basic Principles of Membrane Technology*. The Netherlands: Kluwer Academic Publishers, 1996.

7. Hayama M, Yamamoto K-i, Kohori F, Sakai K. How polysulfone dialysis membranes containing polyvinylpyrrolidone achieve excellent biocompatibility? *J Membrane Sci* 2004;234:41-9.

8. Mujais SK, Schmidt B, Hacker H, Opatrny K, Gurland HJ. Synthetic modification of PAN membrane: Biocompatibility and functional characterization. *Nephrol Dial Transplant* 1995;10 Suppl 3:46-51.

9. Khayet M, Feng CY, Khulbe KC, Matsuura T. Preparation and characterization of polyvinylidene fluoride hollow fiber membranes for ultrafiltration. *Polymer* 2002;43:3879-90.

10. Ronco C, Ballestri M, Brendolan A. New developments in hemodialyzers. *Blood Purificat* 2000;18:267-75.

11. Darnige L, Legallais C, Arvieux J, Pitiot O, Vijayalakshmi MA. Functionalized hollow fiber membrane cartridge for adsorption of anticofactor/antiphospholipid antibodies: A potential tool for treatment. *Artif Organs* 1999;23:834-9.

12. Beck J, Angus R, Madsen B, Britt D, Vernon B, Nguyen KT. Islet encapsulation: Strategies to enhance islet cell functions. *Tissue Eng* 2007;13:589-99.

13. Wolfe SP, Hsu E, Reid LM, Macdonald JM. A novel multi-coaxial hollow fiber bioreactor for adherent cell types. Part 1: Hydrodynamic studies. *Biotechnol Bioeng* 2002;77:83-90.

14. Yang P, Teo W-K, Ting Y-P. Design and performance study of a novel immobilized hollow fiber membrane bioreactor. *Bioresource Technol* 2006;97:39-46.

15. Bhattacharya R, Phaniraj TN, Shailaja D. Polysulfone and polyvinyl pyrrolidone blend membranes with reverse phase morphology as controlled release systems: Experimental and theoretical studies. *J Membrane Sci* 2003;227:23-37.

16. Barth C, Gonçalves MC, Pires ATN, Roeder J, Wolf BA. Asymmetric polysulfone and polyethersulfone membranes: Effects of thermodynamic conditions during formation on their performance. *J Membrane Sci* 2000;169:287-99.

17. Yang M-C, Lin W-C. Protein adsorption and platelet adhesion of polysulfone membrane immobilized with chitosan and heparin conjugate. *Polym Advan Technol* 2003;14:103-13.

18. Hancock LF, Fagen SM, Ziolo MS. Hydrophilic, semipermeable membranes fabricated with poly(ethylene oxide)-polysulfone block copolymer. *Biomaterials* 2000;21:725-33.

19. Kim Y-W, Kim J-J, Kim YH. Surface characterization of biocompatible polysulfone membranes modified with poly(ethylene glycol) derivatives. *Korean J Chem Eng* 2003;20:1158-65.

20. Park JY, Acar MH, Akthakul A, Kuhlman W, Mayes AM. Polysulfone-*graft*-poly(ethylene glycol) graft copolymers for surface modification of polysulfone membranes. *Biomaterials* 2006;27:856-65.

21. Tsai HA, Li LD, Lee KR, Wang YC, Li CL, Huang J, et al. Effect of surfactant addition on the morphology and pervaporation performance of asymmetric polysulfone membranes. *J Membrane Sci* 2000;176:97-103.

22. Wang Y-Q, Su Y-L, Ma X-L, Sun Q, Jiang Z-Y. Pluronic polymers and polyethersulfone blend membranes with improved fouling-resistant ability and ultrafiltration performance. *J Membrane Sci* 2006;283:440-7.

23. Sivakumar M, Mohan DR, Rangarajan R. Studies on cellulose acetate-polysulfone ultrafiltration membranes II. Effect of additive concentration. *J Membrane Sci* 2006;268:208-19.

24. Huang Z, Zhang W, Yu J, Gao D. Nanoporous alumina membranes for enhancing hemodialysis. *J Med Devices* 2007;1:79-83.

25. Barzin J, Feng C, Khulbe KC, Matsuura T, Madaeni SS, Mirzadeh H. Characterization of polyethersulfone hemodialysis membrane by ultrafiltration and atomic force microscopy. *J Membrane Sci* 2004;237:77-85.

26. Wolff SH, Zydney AL. Effect of bleach on the transport characteristics of polysulfone hemodialyzers. *J Membrane Sci* 2004;243:389-99.

27. Cheung AK, Agodoa LY, Daugirdas JT, Depner TA, Gotch FA, Greene T, et al. Effects of hemodialyzer reuse on clearances of urea and β_2-microglobulin. *J Am Soc Nephrol* 1999;10:117-27.

28. Khayet M, Matsuura T. Determination of surface and bulk pore sizes of flat-sheet and hollow-fiber membranes by atomic force microscopy, gas permeation and solute transport methods. *Desalination* 2003;158:57-64.

29. Rafat M, De D, Khulbe KC, Nguyen T, Matsuura T. Surface characterization of hollow fiber membranes used in artificial kidney. *J Appl Polym Sci* 2006;101:4386-400.

30. Le-Clech P, Marselina Y, Ye Y, Stuetz MM, Chen V. Visualisation of polysaccharide fouling on microporous membrane using different characterisation techniques. *J Membrane Sci* 2007;290:36-45.

31. Bowen WR, Hilal N, Lovitt RW, Williams PM. Atomic force microscope studies of membranes: Surface pore structures of Cyclopore and Anopore membranes. *J Membrane Sci* 1996;110:233-8.

32. Hayama M, Kohori F, Sakai K. AFM observation of small surface pores of hollow-fiber dialysis membrane using highly sharpened probe. *J Membrane Sci* 2002;197:243-9.

33. Ochoa NA, Prádanos P, Palacio L, Pagliero C, Marchese J, Hernández A. Pore size distributions based on AFM imaging and retention of multidisperse polymer solutes Characterisation of polyethersulfone UF membranes with dopes containing different PVP. *J Membrane Sci* 2001;187:227-37.

34. Kesting RE. The four tiers of structure in integrally skinned phase inversion membranes and their relevance to the various separation regimes. *J Appl Polym Sci* 1990;41:2739-52.

35. Khulbe KC, Feng C, Matsuura T, Khayet M. AFM images of the cross-section of polyetherimide hollow fibers. *Desalination* 2006;201:130-7.

36. Hayama M, Yamamoto K-i, Kohori F, Uesaka T, Ueno Y, Sugaya H, et al. Nanoscopic behavior of polyvinylpyrrolidone particles on polysulfone/polyvinylpyrrolidone film. *Biomaterials* 2004;25:1019-28.

37. Chanard J, Lavaud S, Randoux C, Rieu P. New insights in dialysis membrane biocompatibility: Relevance of adsorption properties and heparin binding. *Nephrol Dial Transpl* 2003;18:252-7.

38. Matsuda M, Yamamoto K-i, Yakushiji T, Fukuda M, Miyasaka T, Sakai K. Nanotechnological evaluation of protein adsorption on dialysis membrane surface hydrophilized with polyvinylpyrrolidone. *J Membrane Sci* 2008;310:219-28.

39. Ferrando M, Rożek A, Zator M, López F, Güell C. An approach to membrane fouling characterization by confocal scanning laser microscopy. *J Membrane Sci* 2005;250:283-93.

40. Aoyagi S, Hayama M, Hasegawa U, Sakai K, Hoshi T, Kudo M. TOF-SIMS imaging of protein adsorption on dialysis membrane. *Appl Surf Sci* 2004;231-232:411-5.

41. Booth AF, ed. *Sterilization of Medical Devices*. Buffalo Grove, IL: Interpharm Press, 1999.

42. Nair PD. Currently practised sterilization methods - some inadvertent consequences. *J Biomater Appl* 1995;10:121-35.

43. Bommer J, Barth H, Wilhelms O, Schindele H. Anaphylactoid reactions in dialysis patients: Role of ethylene oxide. *Lancet* 1985;2:1382.

44. Link A, Büttner K. Steam sterilization: A suitable alternative? *Med Device Technol* 1992;3:45-7.

45. Müller TF, Seitz M, Eckle I, Lange H, Kolb G. Biocompatibility differences with respect to the dialyzer sterilization method. *Nephron* 1998;78:139-42.

46. Aucella F, Tetta C, Tessore V, Nitte CD, Vigilante M, Gatta G, et al. Is steam sterilization really making any difference in dialysis-induced cytokine release? *Int J Artif Organs* 2002;25:832-7.

47. Clough RL. High-energy radiation and polymers: A review of commercial processes and emerging applications. *Nucl Instrum Meth B* 2001;185:8-33.

48. Bowser GF, Tchougounov AA, Tchougounova AA. On-site electron beam sterilization: A compelling option for today and tomorrow. In: Booth AF, ed. *Sterilization of Medical Devices*. Buffalo Grove, IL: Interpharm Press, 1999:151-9.

49. Hagman DE. Sterilization. In: Troy DB, Beringer P, eds. *Remington: The Science and Practice of Pharmacy*. 21 ed. Baltimore, MD: Lippincott Williams & Wilkins, 2005:776-801.

50. Clough RL, Gillen KT, Dole M. Radiation resistance of polymers and composites. In: Clegg DW, Collyer AA, eds. *Irradiation Effects on Polymers*. New York: Elsevier, 1991:79-156.

51. Meinhold D, Schweiss R, Zschoche S, Janke A, Baier A, Simon F, et al. Hydrogel characteristics of electron-beam-immobilized poly(vinylpyrrolidone) films on poly(ethylene terephthalate) supports. *Langmuir* 2004;20:396-401.

52. Jiang B, Wu Z, Zhao H, Tang F, Lu J, Wei Q, et al. Electron beam irradiation modification of collagen membrane. *Biomaterials* 2006;27:15-23.

53. Kim CO, Kim DH, Kim JS, Park JW. Self-assembly of a diblock copolymer on a patterned surface with low-energy electron beam. *Langmuir* 2006;22:4131-5.

54. Qin J-J, Wong F-S. Hypochlorite treatment of hydrophilic hollow fiber ultrafiltration membranes for high fluxes. *Desalination* 2002;146:307-9.

55. Shao J, Wolff SH, Zydney AL. In vitro comparison of peracetic acid and bleach cleaning of polysulfone hemodialysis membranes. *Artif Organs* 2007;31:452-60.

56. Gaudichet-Maurin E, Thominette F. Ageing of polysulfone ultrafiltration membranes in contact with bleach solutions. *J Membrane Sci* 2006;282:198-204.

57. Wienk IM, Meuleman EEB, Borneman Z, Boomgaard Tvd, Smolders CA. Chemical treatment of membranes of a polymer blend: Mechanism of the reaction of hypochlorite with poly(vinyl pyrrolidone). *J Polym Sci Pol Chem* 1995;33:49-54.

58. Wolff SH, Zydney AL. Effect of peracetic acid reprocessing on the transport characteristics of polysulfone hemodialyzers. *Artif Organs* 2005;29:166-73.

59. Petsch D, Anspach FB. Endotoxin removal from protein solutions. *J Biotechnol* 2000;76:97-119.

60. Bender H, Pflänzel A, Saunders N, Czermak P, Catapano G, Vienken J. Membranes for endotoxin removal from dialysate: Considerations on feasibility of commercial ceramic membranes. *Artif Organs* 2000;24:826-9.

61. Tetta C, Bellomo R, Inguaaggiato R, Wratten ML, Ronco C. Endotoxin and cytokine removal in sepsis. *Therap Apher Dial* 2002;6:109-15.

62. Sato T, Shoji H, Koga N. Endotoxin adsorption by polymyxin B immobilized fiber column in patients with systemic inflammatory response syndrome. *Therap Apher Dial* 2003;7:252-8.

63. Linnenweber S, Lonnemann G. Pyrogen retention by the Asahi APS-650 polysulfone dialyzer during in vitro dialysis with whole human donor blood. *ASAIO J* 2000;46:444-7.

64. Darkow R, Groth T, Albrecht W, Lützow K, Paul D. Functionalized nanoparticles for endotoxin binding in aqueous solutions. *Biomaterials* 1999;20:1277-83.

65. Anspach FB, Hilbeck O. Removal of endotoxins by affinity sorbents. *J Chromatogr A* 1995;711:81-92.

66. Bambauer R, Walther J, Jung WK. Ultrafiltration of dialysis fluid to obtain a sterile solution during hemodialysis. *Blood Purificat* 1990;8:309-17.

67. Oliver JC, Bland LA, Oettinger CW, Arduino MJ, Garrard M, Pegues DA, et al. Bacteria and endotoxin removal from bicarbonate dialysis fluids for use in conventional, high-efficiency, and high-flux hemodialysis. *Artif Organs* 1992;16:141-5.

68. Rafiee-Tehrani M, Farrokhnia R, Falkenhagen D, Weber C. Removal of lipid A and *Pseudomonas aeruginosa* endotoxin from dialysis fluids by high-flux polysulfone ultrafilter (dialyzer). *PDA J Pharm Sci Tech* 1996;50:306-10.

69. Henrie M, Ford C, Andersen M, Stroup E, Diaz-Buxo J, Madsen B, et al. In vitro assessment of dialysis membrane as an endotoxin transfer barrier: Geometry, morphology, and permeability. *Artif Organs* 2008;32:701-10.

70. Hayama M, Miyasaka T, Mochizuki S, Asahara H, Yamamoto K-i, Kohori F, et al. Optimum dialysis membrane for endotoxin blocking. *J Membrane Sci* 2003;219:15-25.

71. Rietschel ET, Kirikae T, Schade FU, Mamat U, Schmidt G, Loppnow H, et al. Bacterial endotoxin: Molecular relationships of structure to activity and function. *FASEB J* 1994;8:217-25.

72. Tellingen Av, Grooteman MPC, Pronk R, Loon Jv, Vervloet MG, Wee PMt, et al. Lipopolysaccharide concentrations during superflux dialysis using unfiltered bicarbonate dialysate. *ASAIO J* 2002;48:383-8.

73. Takemoto Y, Nakatani T, Sugimura K, Yoshimura R, Tsuchida K. Endotoxin adsorption of various dialysis membranes: In vitro study. *Artif Organs* 2003;27:1134-7.

74. Weber V, Linsberger I, Rossmanith E, Weber C, Falkenhagen D. Pyrogen transfer across high- and low-flux hemodialysis membranes. *Artif Organs* 2004;28:210-7.

75. Bommer J, Becker KP, Urbaschek R. Potential transfer of endotoxin across high-flux polysulfone membranes. *J Am Soc Nephrol* 1996;7:883-8.

76. Lonnemann G, Sereni L, Lemke H-D, Tetta C. Pyrogen retention by highly permeable synthetic membranes during in vitro dialysis. *Artif Organs* 2001;25:951-60.

77. Nakatani T, Tsuchida K, Sugimura K, Yoshimura R, Takemoto Y. Investigation of endotoxin adsorption with polyether polymer alloy dialysis membranes. *Int J Mol Med* 2003;11:195-7.

78. Yamamoto K-i, Matsuda M, Hayama M, Asutagawa J, Tanaka S, Kohori F, et al. Evaluation of the activity of endotoxin trapped by a hollow-fiber dialysis membrane. *J Membrane Sci* 2006;272:211-6.

79. Perianayagam MC, Jaber BL. Endotoxin-binding affinity of sevelamer hydrochloride. *Am J Nephrol* 2008;28:802-7.

80. Stauback K-H, Boehme M, Zimmermann M, Otto V. A new endotoxin adsorption device in gram-negative sepsis: Use of immobilized albumin with the MATISSE adsorber. *Transfus Apher Sci* 2003;29:93-8.

81. Shepard SR, STone C, Cook S, Bouvier A, Boyd G, Weatherly G, et al. Recovery of intracellular recombinant proteins from the yeast *Pichia pastoris* by cell permeabilization. *J Biotechnol* 2002;99:149-60.

82. Graumann K, Premstaller A. Manufacturing of recombinant therapeutic proteins in microbial systems. *Biotechnol J* 2006;1:164-86.

83. Magalhães PO, Lopes AM, Mazzola PG, Rangel-Yagui C, Penna TCV, Jr. AP. Methods of endotoxin removal from biological preparations: A review. *J Pharm Pharm Sci* 2007;10:388-404.

84. Li L, Luo RG. Use of Ca2+ to re-aggregate lipopolysaccharide (LPS) in hemoglobin solutions and the subsequent removal of endotoxin by ultrafiltration. *Biotechnol Tech* 1198;12:119-22.

85. Bordier C. Phase separation of integral membrane proteins in Triton X-114 solution. *J Biol Chem* 1981;256:1604-7.

86. Aida Y, Pabst MJ. Removal of endotoxin from protein solutions by phase separation using Triton X-114. *J Immunol Methods* 1990;132:191-5.

87. Colpan M, Moritz P, Schorr J. Process for the depletion or removal of endotoxins. United States Patent Nr. 5,747,663, May 5, 1998.

88. Davies JR. Process for removing endotoxins. United States Patent Nr. 5,917,022, June 29, 1999.

89. Luo RG, Kang Y. Methods for removing endotoxins from biological solutions using immobilized metal affinity chromatography. United States Patent Nr. 6,365,147, Apr. 2, 2002.

90. Petsch D, Beeskow TC, Anspach FB, Deckwer W-D. Membrane adsorbers for selective removal of bacterial endotoxin. *J Chromatogr B* 1997;693:79-91.

91. Anspach FB, Petsch D, Deckwer W-D. Model studies on the mechanism of endotoxin adsorption on flat-sheet microfiltration membrane adsorbers. *Can J Chem Eng* 1999;77:921-30.

92. Todokoro M, Hirayama C, Kunitake M, Sakata M. Endotoxin adsorbent, and a method of removing endotoxin by using the same. United States Patent Nr. 6,699,386, Mar. 2, 2004.

93. Wu X, Joe L. Kinsey J, Ishee M, Konstantin P, Shertok J, Yang Y. Charged membrane. United States Patent Nr. 6,849,185, Feb. 1, 2005.

94. Adachi T, Ida J, Hashimoto M. Method of removing endotoxin. United States Patent Nr. 5,169,535, Dec. 8, 1992.

95. Hirayama C, Sakata M, Nakamura M, Ihara H, Kunitake M, Todokoro M. Preparation of poly(ε-lysine) adsorbents and application to selective removal of lipopolysaccharides. *J Chromatogr B* 1999;721:187-95.

CHAPTER 3

EFFECT OF STERILIZATION TECHNIQUES ON PHYSICOCHEMICAL PROPERTIES OF POLYSULFONE HOLLOW FIBERS[1]

ABSTRACT: Sterilized hollow fiber membranes are used in hemodialysis, ultrafiltration, bioprocessing, and tissue engineering applications that require a stable and biocompatible surface. Here we demonstrate significant changes in fiber physicochemical properties depending on method of sterilization. Commercial polysulfone hollow fibers containing poly(vinylpyrrolidone) were subjected to ethylene oxide (ETO), sodium hypochlorite (bleach), and electron-beam (e-beam) sterilization techniques followed by analysis of surface hydrophilicity, morphology, and water retention ability. E-beam sterilized fibers had contact angles near 48° compared to the ETO and bleach treated fibers, which were each near 56°. Atomic force microscopy revealed lumen RMS roughness values near 19 nm for all three sterilization methods; however, e-beam sterilized and bleach treated fibers had significantly higher (~106 nm) RMS values for the outer wall as compared to the ETO sterilized fibers (~39 nm). The increased hydrophilicity and surface area of the e-beam sterilized fiber was reflected by a greater water evaporation rate than the ETO treated fiber. These results demonstrate common sterilization methods may significantly alter polymer membrane physicochemical properties, which may in turn impact surface fouling. For tissue engineering and bioprocessing applications, these changes may be leveraged to promote cell adhesion and spreading.

[1] Coauthored by Benjamin Madsen, David W. Britt, Floyd Griffiths, Elise McKenna, and Chih-Hu Ho

INTRODUCTION

The surface physicochemical properties of hollow fiber membranes (HFMs) are of significant importance as they influence ultrafiltration rates, as well as dictate whether biological components (proteins, cells, bacteria) adsorb to the membrane, which may be favorable in cell culture, bioreactor, and tissue engineering applications (1-3), but less desirable in ultrafiltration applications where biofouling diminishes filtration efficiency (4-7). HFM fabrication procedures, including polymer/copolymer and solvent selection, as well as post-fabrication processing and sterilization methods, influence HFM surface chemical and physical properties, impacting overall performance of the membrane.

Polysulfone (PS) and cellulose acetate are the most common materials used in HFM production, chosen based on their structural integrity, ease in manufacture, and biocompatibility. Common copolymer additives include poly(vinylpyrrolidone) (PVP), polyvinylidene fluoride, polyetherimide, poly(ethylene oxide), and phosphorylcholine polymer (1, 8-12). These copolymers are necessary to form the pore structure in the membrane through phase inversion. Because PS membranes are used in many applications, particular interest has been given to analyzing and altering membranes containing this polymer and the commonly-used hydrophilic additive, PVP. Here we characterize the physicochemical properties of pure PS and PS-PVP membranes following several common sterilization methods.

The influence of sterilization on HFM properties and performance is of significant importance, especially for multi-use devices subjected to repeated sterilization cycles. As this is the last step before application (or re-use), its influence is often overlooked. Common biomedical material sterilization methods include steam autoclaving, ETO gas,

irradiation, or exposure to several chemical sanitizers such as sodium hypochlorite, hydrogen peroxide, sodium hydroxide, or ethanol. Here we focus on ETO, e-beam, and bleach treatments to compare common gas, irradiation, and chemical sterilization methods.

Several methods have been used to study the properties of HFMs including scanning electron microscopy (SEM), atomic force microscopy (AFM), contact angle measurement (CAM), X-ray photoelectron spectrometry (XPS), ultrafiltration rate, protein adsorption, and tensile strength (4, 8, 10-18). We present a method for sectioning hollow fibers to expose the lumen as a flat surface for CAM and AFM analysis. Additionally, water evaporation rate from the membrane is presented as a sensitive method to characterize membrane hydrophilicity and sorption properties.

Applying AFM, CAM, and water evaporation techniques we demonstrate dramatic changes in HFM surface roughness and hydrophilicity as a function of initial chemistry and sterilization technique. The results demonstrate how common sterilization methods may inadvertently change membrane properties, as well as provide simple post-fabrication methods to tune properties toward specific applications.

MATERIALS AND METHODS

Membrane preparation

All hollow fiber membranes used in this study were prepared by Fresenius Medical Care North America. ETO and e-beam sterilized fibers were obtained from the commercial dialysis cassettes Fresenius Optiflux® F200NR and F200NR^{e}, respectively, with each having an aqueous KUF of 200 mL/h·mm Hg and an albumin sieving

coefficient of 0.45%. These membranes are manufactured using a polymer blend of PS and PVP; their respective structures are shown below:

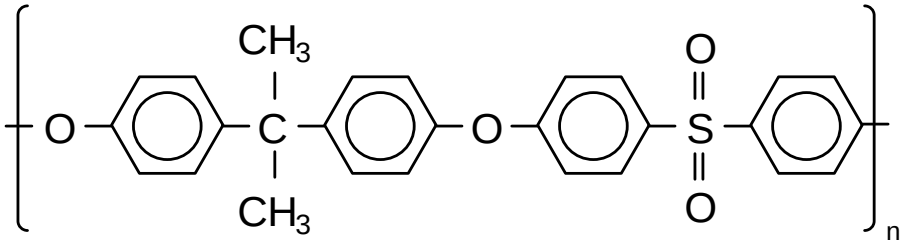

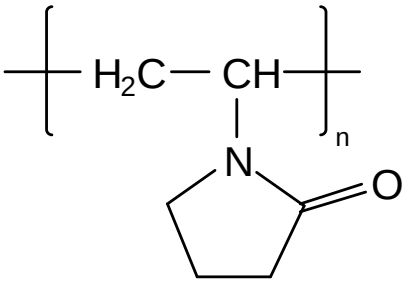

.

PS hollow fiber membranes were fabricated on a pilot line using polysulfone without any other polymer additives. This fiber group was not subjected to any sterilization technique, serving only as a control to compare with PS-PVP membranes. Bleach treated F200NR fibers were subjected to 0.57% effective sodium hypochlorite content from the dialysate side at 70^{o}C for 2 minutes. All hollow fiber membranes were prepared with the same spinning parameters (spinneret size, air gap, bore fluid, rinsing time), producing asymmetric membranes similar to that shown in Fig. 3.1, with a compact filtering layer at the inner surface and a porous matrix structure through the remainder of the fiber cross section.

Hollow fibers were sectioned to access the lumen for both AFM and CAM with the aid of a stereo microscope (SMZ645, Nikon Corp.). Fibers were fixed on double-sided tape, cut longitudinally with a razor blade, spread open, and rolled flat using a clean

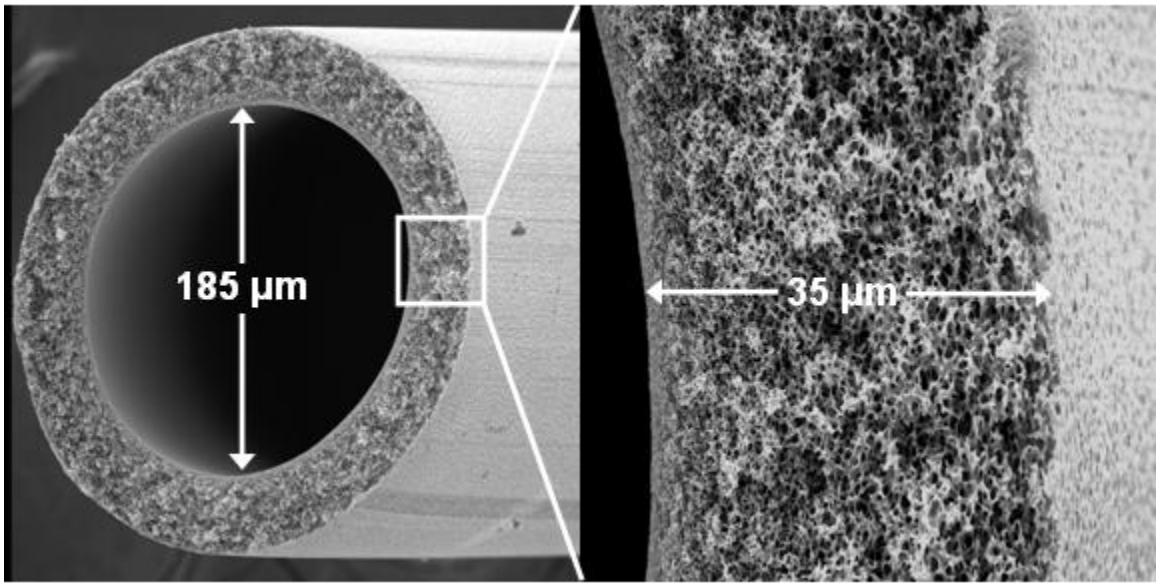

FIG. 3.1. SEM of PS-PVP asymmetric dialysis hollow fiber [19].

glass test tube. Intact fibers were also rolled flat on double-sided tape to present the outside of the fiber as a flat surface.

Water contact angle measurement

Water contact angles of fibers were obtained using a VCA Optima (AST Products, Inc.). Measurements (n = 8) were made on both the lumen and outside of hollow fibers with 0.25 µl droplets of double distilled water (MP-3A, Barnstead Intl.) at 25^{o}C. Statistical analysis was performed on WCA measurements and all subsequent data sets using two-population t-tests in Origin® software (v6.1052, OriginLab Corporation).

AFM morphology

Sample surface morphology and roughness were observed using a Bioscope AFM (Nanoscope IIIa, Digital Instruments, Inc.) in tapping mode using a silicon nitride cantilever (40 N/m, Tap300, Budget Sensors). A scan size of 2 x 2 µm^2 for the lumen of

the fibers was chosen to show the nanostructure of the membranes. A scan size of 10 x 10 μm^2 for the outside of the fibers was chosen to show macrostructures of the porous membranes. The root mean square (RMS) roughness was measured (n = 5) using Nanoscope III imaging software (version 5.30r3, Digital Instruments, Inc.). Lumen particle sizes were calculated using a previously described method ($n \geq 30$) (14).

Water evaporation rate

Water evaporation rates for hollow fibers were obtained using a tensiometer, μtrough S (Kibron, Inc.). One-inch lengths of hollow fibers were affixed to the tensiometer wire probe using a small piece of double-sided tape, brought into contact with water in a reservoir, and allowed to equilibrate for at least two minutes to reach maximum absorption capacity (25^oC, 24% relative humidity). Upon removal from the water reservoir, the evaporation induced and change in mass was recorded over time. Water evaporation rates for the fibers were calculated from the change in mass over 2 minute time periods. This method offers distinct advantages over using a standard analytical balance in terms of sensitivity of the instrument (< 0.1 μg), instrument equilibration time, and reduced variability due to sample transfer and user error.

RESULTS

Surface hydrophilicity by CAM

Contact angle measurements were performed on the lumen and outside of PS and PS-PVP fibers to compare wettability of each surface. Results for the contact angle measurements are presented in Fig. 3.2. Statistical analysis was conducted to show significant difference between outer and lumen contact angles and among the different

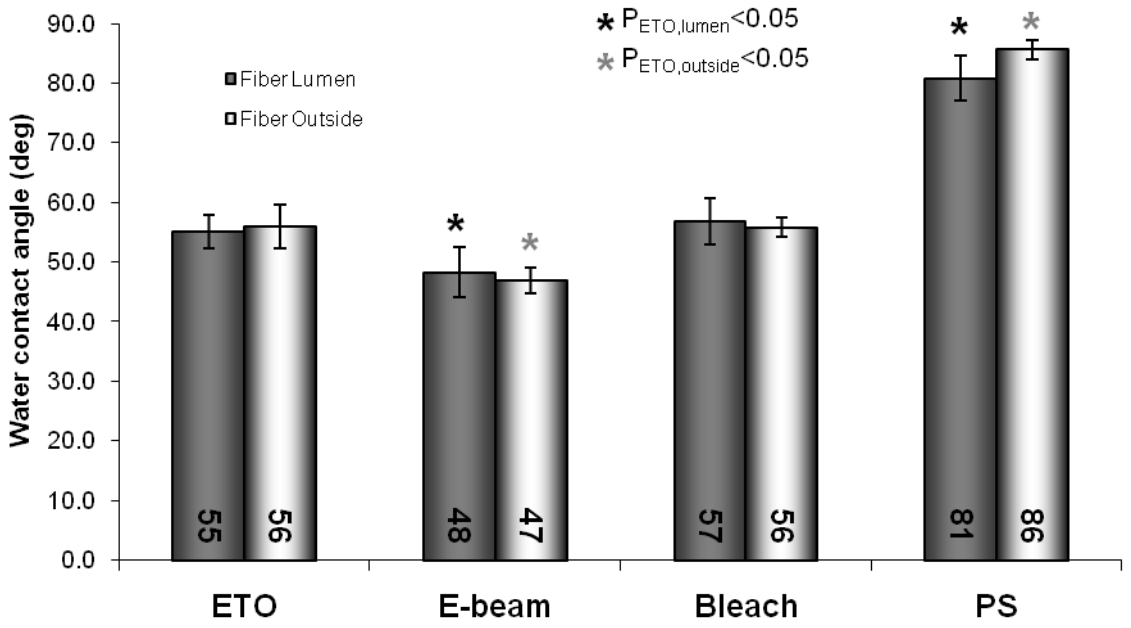

FIG. 3.2. CAM of hollow fibers, both lumen (dark) and outside (light). Mean ± s.d., n = 8. PS and e-beam sterilized fibers show higher and lower contact angles, respectively, than the ETO sterilized and bleach treated fibers ($p < 0.05$). The 2-minute bleach treated fiber had identical contact angle to the ETO fiber. Fibers bleached for 1 hour showed contact angles approaching those of PS fibers (data not shown).

membrane types. The ETO sterilized and 2-minute bleach treated membranes had nearly identical contact angles (~56^o), suggesting similar fiber surface properties. Longer (1 hour) bleaching times significantly increased the contact angle to 73^o (data not shown) suggesting loss of hydrophilic PVP with time. Contact angles for bleached flat-sheet membranes formed using the same polymer chemistry are shown in Fig. A.1 (Appendix A). In contrast, e-beam sterilization led to a significant lowering of water contact angle (~47^0) as compared to the ETO sterilized and bleach treated membranes ($p < 0.05$). As expected, the pure PS fiber had significantly higher water contact angle (> 80^o) than any other membrane due to lack of PVP. There was no significant difference between inner skin and outer membrane for each fiber type.

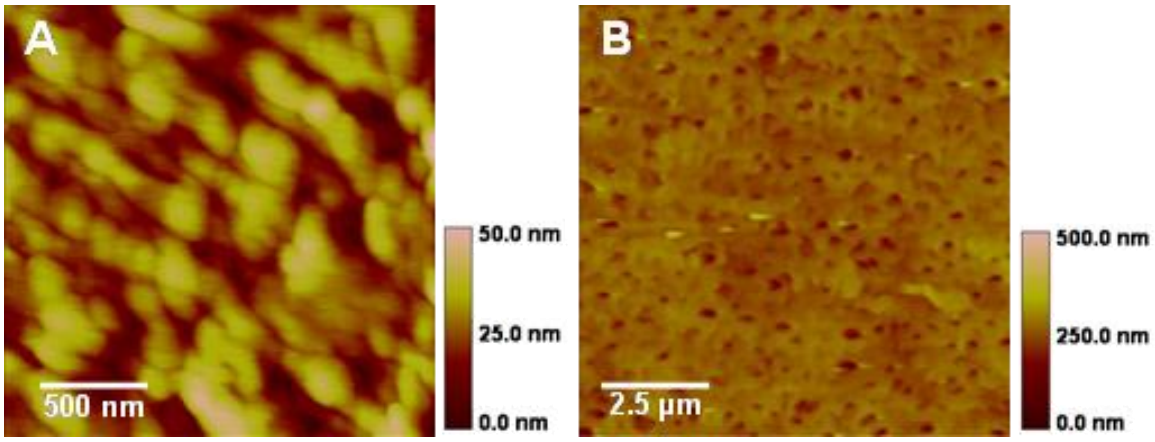

FIG. 3.3. AFM images of the ETO sterilized hollow fiber, lumen (A) and outside (B). The asymmetrical membrane shows nodule aggregates on lumen and porous structure on outside.

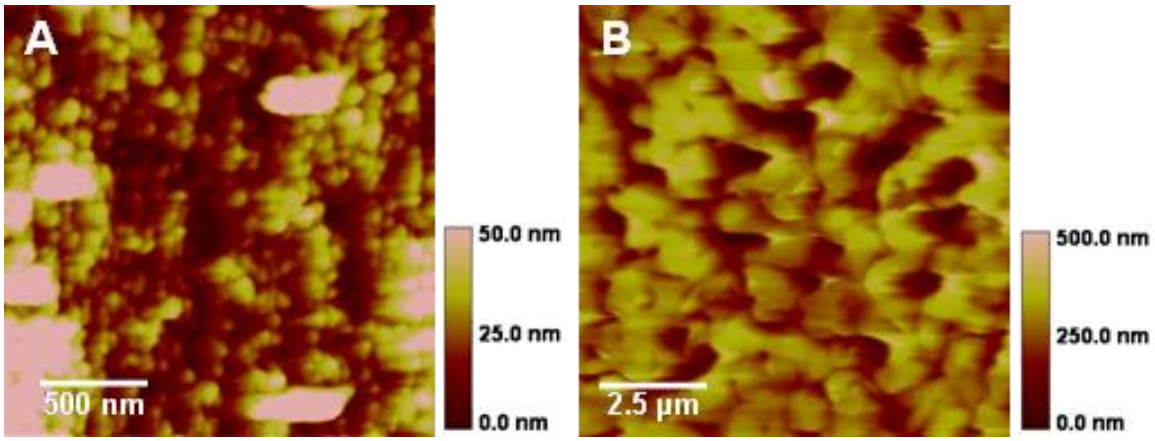

FIG. 3.4. AFM images of e-beam sterilized hollow fiber, lumen (A) and outside (B). Nodule aggregates for this membrane are significantly smaller than those on the ETO sterilized membrane. Pores on the outside are also larger than those on the ETO sterilized membrane.

AFM morphology

AFM images of the lumen and outside of each membrane type are shown in Figs. 3.3-3.6. Images presented here were representative of all images taken for each membrane type (n = 5). The bead-like structures seen in the lumen images of each membrane type can be classified as nodule aggregates based on the four superimposed

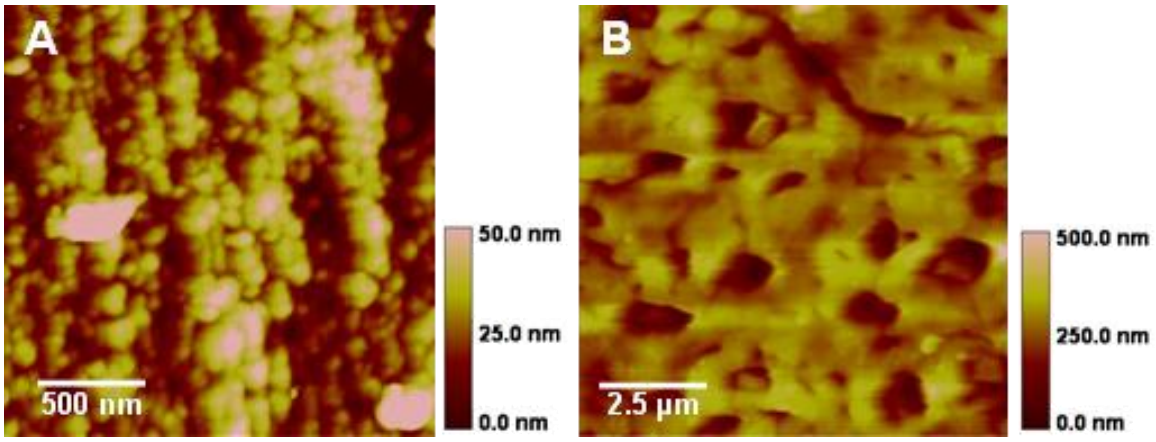

FIG. 3.5. AFM images of bleach treated hollow fiber, lumen (A) and outside (B). The membrane is structurally very similar to e-beam sterilized hollow fibers on both lumen and outside.

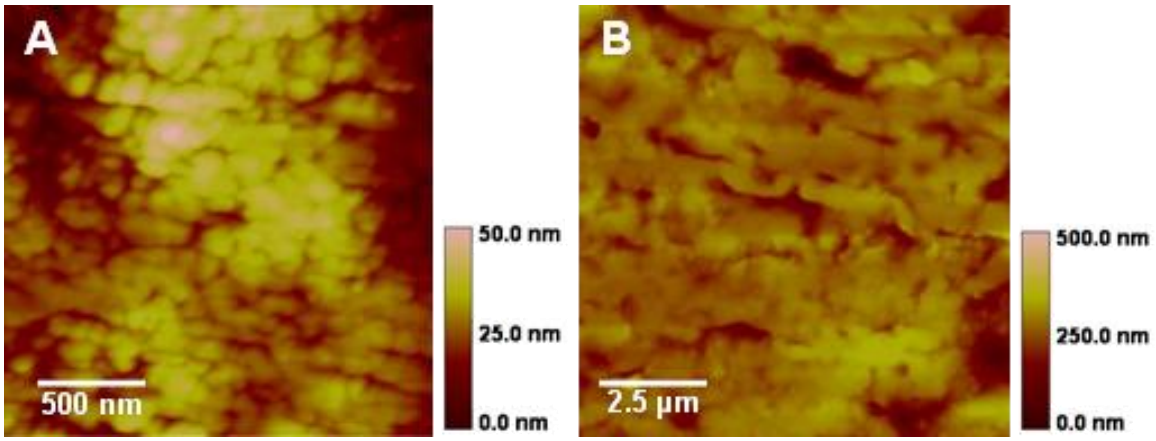

FIG. 3.6. AFM images of PS hollow fiber, lumen (A) and outside (B). Membrane is structurally different, especially on the outside, than other fibers due to chemical differences of PS polymer versus PS-PVP polymer blend.

tiers of structure in integrally skinned phase inversion membranes described by Kesting [20]. Nodule aggregates are described as spherical clumps of coalesced macromolecule groups, between which are pores responsible for membrane ultrafiltration characteristics. Nodule aggregate sizes for the lumens of the membranes were as follows ($n \geq 30$): ETO, 153 ± 49 nm; e-beam, 97 ± 32 nm; bleach, 104 ± 36 nm; PS, 130 ± 53 nm. Nodule

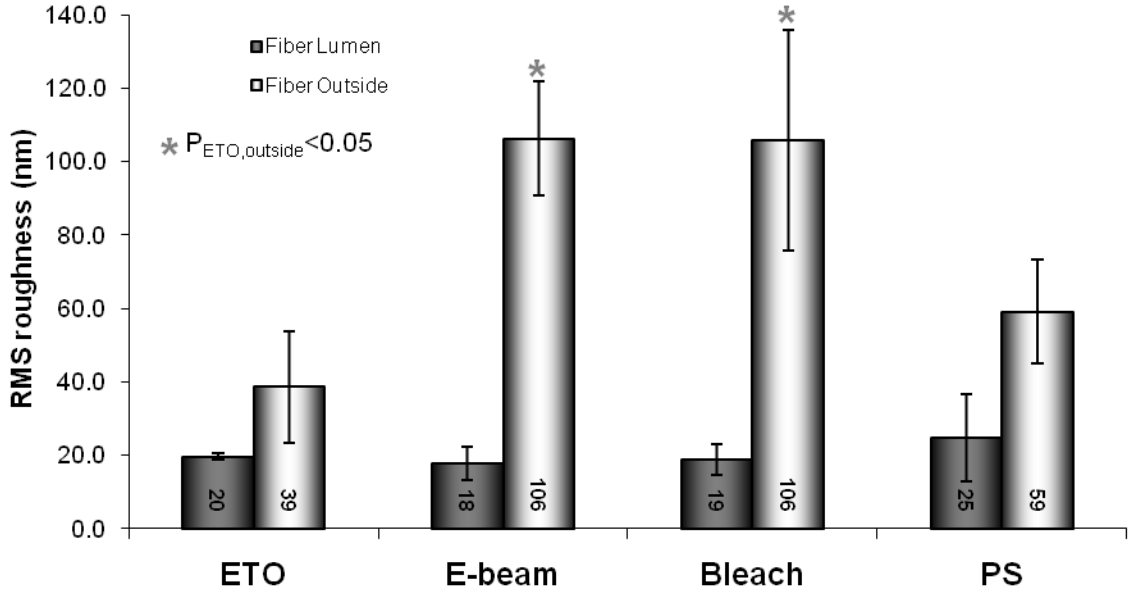

FIG. 3.7. RMS roughness of hollow fibers, both lumen (dark) and outside (light). Mean ± s.d., n = 5. No significant difference among lumen RMS values is reported ($p < 0.05$). Bleach treated and e-beam sterilized fibers show significantly higher RMS values than ETO sterilized and PS fibers.

aggregate sizes for the ETO and PS membranes were similar, whereas the nodule aggregates for bleach treated and e-beam sterilized fibers were significantly smaller ($p < 0.05$).

AFM images reported here show varying size and structure of the porous membranes depending on sterilization method. Similar to the trends seen for the lumens, the outsides of the bleach treated and e-beam sterilized fibers were significantly different than the ETO sterilized fiber; pore sizes for these membranes were much larger. Also, the outside of the PS membrane exhibited ill-defined pores and a skin-like structure, due to lack of PVP during the phase inversion process.

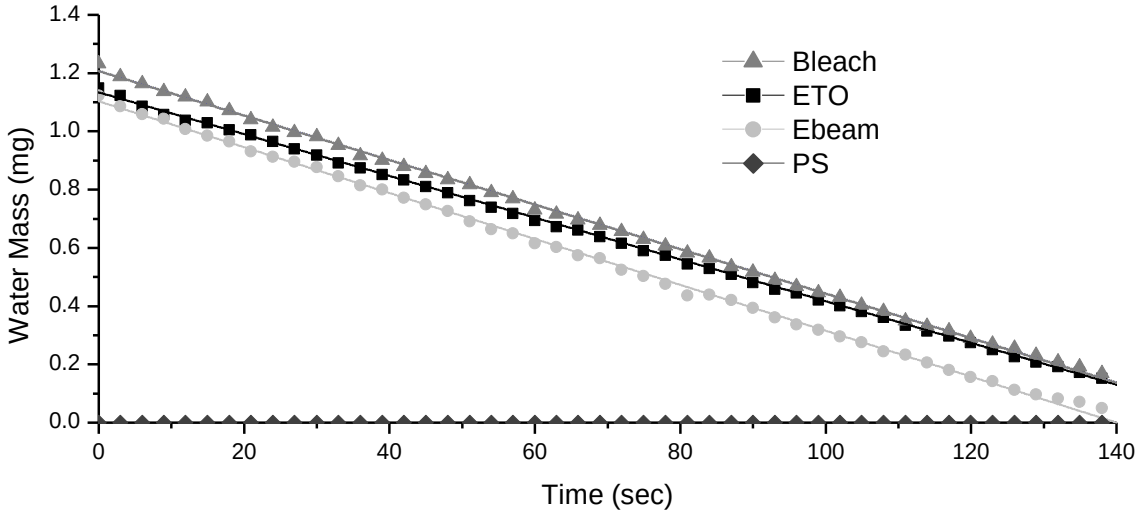

FIG. 3.8. Averaged evaporation profiles of hollow fibers measured by tensiometer, with mass of absorbed water in the hollow fiber versus time (n = 9). Sensitivity of the tensiometer probe allows for highly accurate measurements (< 0.1 μg). Error bars have been removed for clarity.

Table 3.1. Experimental results for water evaporation rate and water absorption of hollow fibers (n = 9).

Hollow fiber	Absorbed Water (mg)	Water Evaporation Rate (μg/s)
ETO	1.13 ± 0.02	7.17 ± 0.56
E-beam	1.10 ± 0.04	7.88 ± 0.46
Bleach	1.21 ± 0.02	7.64 ± 0.40
PS	–	–

RMS roughness of the lumen and outside of each fiber is reported in Fig. 3.7. No significant difference was found among any membranes on the lumen side. However, both bleach treated and e-beam sterilized fibers had significantly higher roughness on the outside surfaces compared to the ETO sterilized and PS fibers. This large increase in surface roughness arises from increased pore size as seen in the AFM images. The large particles seen on the lumen images of both the e-beam sterilized and bleach treated

membranes were observed on all PS-PVP membranes and were included in the calculation of surface roughness.

Water evaporation rate

Averaged evaporation profiles for the sterilized fibers are shown in Fig. 3.8. Calculated evaporation rates of water for hollow fibers as well as the mass of water absorbed by the fibers are shown in Table 3.1. Due to the hydrophobic nature of the PS polymer, no water was absorbed in the PS membranes, whereas fibers containing PVP exhibited different degrees of water absorption. The e-beam sterilized fiber exhibited a faster evaporation rate than the ETO sterilized fiber, while the bleach treated fiber was not significantly different from either the ETO or e-beam sterilized fiber. All membranes were statistically significant from all others in the amount of water absorbed. An increase in absorbed water could indicate a larger porosity while a faster evaporation rate likely reflects increased porosity and hydrophilicity.

DISCUSSION

Differential effects of e-beam and ETO sterilization, and bleach treatment on PS-PVP membranes are observed. In particular, e-beam and 2-minute bleach treatments significantly increased the porosity (roughness) of the outer surfaces and decreased the nodule size on the lumens as compared to ETO sterilization. Contact angles, however, did not differ drastically for these three sterilization methods, although e-beam treated fibers were slightly more hydrophilic (47-48^{o}) compared to both ETO and bleached fibers (55-57^{o}). Extended bleach sanitation time beyond two minutes increased fiber hydrophobicity, with 1-2 hour bleach treatments yielding surface hydrophobicities

approaching that of pure PS (81-86^{o}) , which are similar to previously reported values (9, 21). Thus fiber hydrophobicity may be selectively increased or decreased through post-fabrication bleach treatment or e-beam exposure, respectively.

Sterilization methods have the potential to cause slight to major transformations in membrane chemistry and overall performance of polymeric HFMs including membrane shrinkage, changes in permeability, increases in pore size, and changes in surface chemistry and charge (22-24). In addition to potentially altering membrane pore size and ultrafiltration rate, sterilization may also compromise biocompatibility due to changes in physicochemical properties or retention of toxic residuals, such as the case for ETO (25-26). Alternatively, modified surface properties may potentially favor cell spreading and proliferation, as desired in tissue culture applications (4). Surface roughness and energy are key parameters determining cell-surface interactions. As compared to gas sterilization with ETO, e-beam and bleach treatments increased outside surface RMS, decrease lumen nodule size, and can be used to tune the hydrophobicity in PS-PVP membranes. Similar surface features have been observed previously using SEM and AFM (8-9, 13-14, 27).

It has been reported that PS has a high radiation stability under dose conditions as extreme as 10^4 kG (28). Conversely, cross-linking of polymers, including PVP, and restructuring of chemical bonds at lower dosages (10-100 kG) using electron beam radiation has been investigated (29-31). The radiation dosage used in this study (25 kG) is similar to that used in current sterilizing medical equipment (32-33). While this dosage is approximately 1% of the dosage necessary to reduce mechanical strength of PS by 50% (28), it can be suggested that physical and chemical properties of membranes are indeed

altered here. E-beam sterilization in this study lowered contact angle for the lumen and outside surfaces by approximately 8^{o} (compared to the ETO sterilized and bleach treated membranes), and increased surface roughness on the outside of the membrane by 2.7 times relative to the ETO sterilized membrane. Also, decreased nodule aggregate size compared to the ETO sterilized membrane may indicate changes in polymer interactions. While the e-beam radiation dosage used in this study was small, it was sufficient to cause slight, but significant, chemical changes throughout the fiber matrix and physical restructuring on the outside and lumen of the membrane.

Bleaching of HFMs as a sterilization or reprocessing technique has been shown to affect many membrane characteristics including surface chemistry, membrane permeability, pore size, and polymer chain molecular weight (18, 22, 34-36). While reprocessing times often differ based on technique, bleaching times of 2 minutes used in this study are within the time frames tested previously (35, 37-38). It has been shown that PVP is washed from membranes treated with bleach for long periods of time (48 hours) due to chain scission via radical reactions (39), and that luminal and outer surface nitrogen content (due solely to PVP) decreased significantly with bleach times from 1 hour (22). We found one hour of bleach treatment led to contact angles of 73.3^{o} for the outside of fibers, approaching that of PS membranes. Due to some PVP being washed out of the bleach treated membranes, a larger percentage of the membrane surface would consist of the more hydrophobic PS. Results presented here for fibers bleached for 2 minutes show no significant change in contact angle of hollow fiber membranes compared to the ETO fibers, implying little change in surface chemistry due to PVP removal from the polymer matrix. Thus, the increased roughness and porosity in the

outer membrane and decreased nodule size in the lumen following bleaching is unlikely the result of PVP removal.

HFMs treated with solutions containing bleach for 2 minutes have been shown to increase clearances of β_2-microglobulin, suggesting increased pore sizes and/or decreased nodule aggregate sizes on the lumen surface of the membrane (35). Rearrangement of polymer molecules upon bleach treatment may have caused a decrease in polymer aggregate size as seen here and in previous reports, but left the overall chemistry of the polymer membrane unaffected, yielding a membrane of equal surface hydrophilicity to the ETO sterilized membrane (9, 18).

That the bleach treated and e-beam sterilized fibers were much different than the ETO sterilized fiber could be explained by the methods of polymer restructuring discussed above for these sterilization techniques. Larger pore sizes for the outside of these membranes could cause an increase in solute transfer and weakening of the fiber structure (18, 22, 35). Increased solute transport could be of importance in both filtration and cell culture applications, while weakening of fiber structure is of concern in applications where high trans-membrane pressures are used.

Water evaporation rates of hollow fibers can give an indication of surface and bulk properties, such as porosity and wettability. In cases such as vapor permeation, the ability of a membrane to retain certain liquids, including water, can be very useful (40-41). Results shown in Fig. 3.8 and Table 3.1 indicate different evaporation profiles for ETO and e-beam sterilized fibers. Restructuring of fiber morphology, as previously discussed, could indicate an increase in surface area of the e-beam sterilized fiber compared to the ETO sterilized fiber. E-beam induced chemical changes as inferred by

decreased water contact angle likely enhance wicking or spreading of water. The increased surface area and hydrophilicity thus facilitate water evaporation from the e-beam sterilized fiber. Based on the data, it can be noted that water retention abilities (water evaporation rates) can be altered based on sterilization technique.

The mass of water absorbed by each fiber type was significantly different in each case. As noted in Table 3.1, the bleach treated fibers absorbed the largest quantity of water. The breakdown of the matrix of hollow fibers in contact with hypochlorite solutions as seen in SEM micrographs has been reported (34). Although the exposure time of hypochlorite tested in that study was significantly longer than the exposure time here, it can be assumed that a similar, yet less intense, breakdown would occur. Because of this increase in membrane porosity, more water would be absorbed. Conversely, despite having a surface morphology similar to that of the bleach treated fiber, the e-beam sterilized membrane absorbed less water than the ETO sterilized and bleach treated membranes. Fiber matrix properties not observed in the AFM images may have been slightly changed upon e-beam treatment, allowing less water to be absorbed.

The changes described here for sterilized PS-PVP HFMs have specific application to their fields of use. HFMs used in ultrafiltration, especially hemodialysis, must exhibit specific physicochemical characteristics including pore size, surface wettability, and biocompatibility. The fibers investigated showed hydrophilic surfaces with porous inner membranes similar to those used in clinical application. Because PS-PVP membranes have become an interesting surface for cell culture, bioreactors, and tissue engineering due to the ability of the polymer to be formed into specific geometries (i.e. for cell encapsulation), it is necessary to consider physicochemical changes in these membranes

post-sterilization. PS-PVP membrane biocompatibility has been attributed to a “cushion effect”, where an increase in regularity of polymer structures in wet conditions led to decreased platelet and fibrinogen adhesion (8, 9). The largest increase in platelet adhesion was achieved by more hydrophobic surfaces that had a smaller concentration of PVP at the surface of the membrane. However, it has also been shown that islet cells better adhere to PS and PS-PVP films than to more hydrophobic polystyrene, indicating surface wettability is just one factor affecting cell adhesion to a surface (4).

CONCLUSION

The present study focused on characterizing and comparing physicochemical properties of hollow fiber membranes subjected to several sterilization procedures using contact angle measurement, atomic force microscopy, and water evaporation rate. The e-beam sterilized fiber exhibited a modest decrease in water contact angle compared to both ETO sterilized and bleach treated membranes and a higher water evaporation rate than that of the ETO sterilized membrane. Also, the e-beam sterilized and bleach treated membranes both had larger outside surface RMS values and smaller lumen nodule aggregate sizes compared to the ETO sterilized membrane. These findings indicate significant changes in both physical and chemical properties of the membrane surface and possible changes to the porous matrix for different sterilization techniques. This has significant implications regarding selection of sterilization methods given the diverse range of hollow fiber applications, including ultrafiltration, cell culture, and tissue engineering. While detrimental effects to membranes such as altered mechanical properties, surface fouling ability, and ultrafiltration must be considered, sterilization-

induced changes to surface characteristics also provide a facile means to altering membrane surface roughness and energy, which may be leveraged to promote cell adhesion and spreading for tissue engineering and bioprocessing applications.

REFERENCES

1. Khayet M, Feng CY, Khulbe KC, Matsuura T. Preparation and characterization of polyvinylidene fluoride hollow fiber membranes for ultrafiltration. *Polymer* 2002;43:3879-90.

2. Ronco C, Ballestri M, Brendolan A. New developments in hemodialyzers. *Blood Purificat* 2000;18:267-75.

3. Darnige L, Legallais C, Arvieux J, Pitiot O, Vijayalakshmi MA. Functionalized hollow fiber membrane cartridge for adsorption of anticofactor/antiphospholipid antibodies: A potential tool for treatment. *Artif Organs* 1999;23:834-9.

4. Beck J, Angus R, Madsen B, Britt D, Vernon B, Nguyen KT. Islet encapsulation: Strategies to enhance islet cell functions. *Tissue Eng* 2007;13:589-99.

5. Wolfe SP, Hsu E, Reid LM, Macdonald JM. A novel multi-coaxial hollow fiber bioreactor for adherent cell types. Part 1: Hydrodynamic studies. *Biotechnol Bioeng* 2002;77:83-90.

6. Yang P, Teo W-K, Ting Y-P. Design and performance study of a novel immobilized hollow fiber membrane bioreactor. *Bioresource Technol* 2006;97:39-46.

7. Ye SH, Watanabe J, Takai M, Iwasaki Y, Ishihara K. High functional hollow fiber membrane modified with phospholipid polymers for a liver assist bioreactor. *Biomaterials* 2006;27:1955-62.

8. Hayama M, Yamamoto K-i, Kohori F, Sakai K. How polysulfone dialysis membranes containing polyvinylpyrrolidone achieve excellent biocompatibility? *J Membrane Sci* 2004;234:41-9.

9. Hayama M, Yamamoto K-i, Kohori F, Uesaka T, Ueno Y, Sugaya H, et al. Nanoscopic behavior of polyvinylpyrrolidone particles on polysulfone/polyvinylpyrrolidone film. *Biomaterials* 2004;25:1019-28.

10. Khayet M, Matsuura T. Determination of surface and bulk pore sizes of flat-sheet and hollow-fiber membranes by atomic force microscopy, gas permeation and solute transport methods. *Desalination* 2003;158:57-64.

11. Hancock LF, Fagen SM, Ziolo MS. Hydrophilic, semipermeable membranes fabricated with poly(ethylene oxide)-polysulfone block copolymer. *Biomaterials* 2000;21:725-33.

12. Ye SH, Watanabe J, Ishihara K. Cellulose acetate hollow fiber membranes blended with phospholipid polymer and their performance for hemopurification. *J Biomat Sci-Polym E* 2004;15:981-1001.

13. Hayama M, Kohori F, Sakai K. AFM observation of small surface pores of hollow-fiber dialysis membrane using highly sharpened probe. *J Membrane Sci* 2002;197:243-9.

14. Rafat M, De D, Khulbe KC, Nguyen T, Matsuura T. Surface characterization of hollow fiber membranes used in artificial kidney. *J Appl Polym Sci* 2006;101:4386-400.

15. Bowen WR, Hilal N, Lovitt RW, Williams PM. Atomic force microscope studies of membranes: Surface pore structures of Cyclopore and Anopore membranes. *J Membrane Sci* 1996;110:233-8.

16. Barzin J, Feng C, Khulbe KC, Matsuura T, Madaeni SS, Mirzadeh H. Characterization of polyethersulfone hemodialysis membrane by ultrafiltration and atomic force microscopy. *J Membrane Sci* 2004;237:77-85.

17. Matsuda M, Yamamoto K-i, Yakushiji T, Fukuda M, Miyasaka T, Sakai K. Nanotechnological evaluation of protein adsorption on dialysis membrane surface hydrophilized with polyvinylpyrrolidone. *J Membrane Sci* 2008;310:219-28.

18. Gaudichet-Maurin E, Thominette F. Ageing of polysulfone ultrafiltration membranes in contact with bleach solutions. *J Membrane Sci* 2006;282:198-204.

19. Henrie M, Ford C, Andersen M, Stroup E, Diaz-Buxo J, Madsen B, et al. In vitro assessment of dialysis membrane as an endotoxin transfer barrier: Geometry, morphology, and permeability. *Artif Organs* 2008;32:701-10.

20. Kesting RE. The four tiers of structure in integrally skinned phase inversion membranes and their relevance to the various separation regimes. *J Appl Polym Sci* 1990;41:2739 - 52.

21. Kim Y-W, Kim J-J, Kim YH. Surface characterization of biocompatible polysulfone membranes modified with poly(ethylene glycol) derivatives. *Korean J Chem Eng* 2003;20:1158-65.

22. Wolff SH, Zydney AL. Effect of bleach on the transport characteristics of polysulfone hemodialyzers. *J Membrane Sci* 2004;243:389-99.

23. Takesawa S, Ohmi S, Konno Y, Sekiguchi M, Shitaokoshi S, Takahashi T, et al. Varying methods of sterilisation, and their effects on the structure and permeability of dialysis membranes. *Nephrol Dial Transpl* 1987;1:254-7.

24. Nair PD. Currently practised sterilization methods - some inadvertent consequences. *J Biomater Appl* 1995;10:121-35.

25. Müller TF, Seitz M, Eckle I, Lange H, Kolb G. Biocompatibility differences with respect to the dialyzer sterilization method. *Nephron* 1998;78:139-42.

26. Pearson F, Bruszer G, Lee W, Sagona M, Sargent H, Woods E, et al. Ethylene oxide sensitivity in hemodialysis patients. *Artif Organs* 1987;11:100-3.

27. Khulbe KC, Feng CY, Matsuura T, Mosqueada-Jimenaez DC, Rafat M, Kingston D, et al. Characterization of surface-modified hollow fiber polyethersulfone membranes prepared at different air gaps. *J Appl Polym Sci* 2007;104:710-21.

28. Clough RL, Gillen KT, Dole M. Radiation resistance of polymers and composites. In: Clegg DW, Collyer AA, eds. *Irradiation Effects on Polymers*. New York: Elsevier, 1991:79-156.

29. Jiang B, Wu Z, Zhao H, Tang F, Lu J, Wei Q, et al. Electron beam irradiation modification of collagen membrane. *Biomaterials* 2006;27:15-23.

30. Kim CO, Kim DH, Kim JS, Park JW. Self-assembly of a diblock copolymer on a patterned surface with low-energy electron beam. *Langmuir* 2006;22:4131-5.

31. Meinhold D, Schweiss R, Zschoche S, Janke A, Baier A, Simon F, et al. Hydrogel characteristics of electron-beam-immobilized poly(vinylpyrrolidone) films on poly(ethylene terephthalate) supports. *Langmuir* 2004;20:396-401.

32. Clough RL. High-energy radiation and polymers: A review of commercial processes and emerging applications. *Nucl Instrum Meth B* 2001;185:8-33.

33. Hagman DE. Sterilization. In: Troy DB, Beringer P, eds. *Remington: The Science and Practice of Pharmacy*. 21 ed. Baltimore, MD: Lippincott Williams & Wilkins, 2005:776-801.

34. Rouaix S, Causserand C, Aimar P. Experimental study of the effects of hypochlorite on polysulfone membrane properties *J Membrane Sci*. 2006;277:137-47.

35. Cheung AK, Agodoa LY, Daugirdas JT, Depner TA, Gotch FA, Greene T, et al. Effects of hemodialyzer reuse on clearances of urea and β_2-microglobulin. *J Am Soc Nephrol* 1999;10:117-27.

36. Qin J-J, Wong F-S. Hypochlorite treatment of hydrophilic hollow fiber ultrafiltration membranes for high fluxes. *Desalination* 2002;146:307-9.

37. Gagnon R, Kaye M. Dialyzer performance over prolonged reuse. *Clin Nephrol* 1985;24:21-7.

38. Murthy B, Sundaram S, Jaber B, Perrella C, Meyer K, Pereira B. Effect of formaldehyde/bleach reprocessing on in vivo performances of high-efficiency cellulose and high-flux polysulfone dialyzers. *J Am Soc Nephrol* 1998;9:464-72.

39. Wienk IM, Meuleman EEB, Borneman Z, Boomgaard Tvd, Smolders CA. Chemical treatment of membranes of a polymer blend: Mechanism of the reaction of hypochlorite with poly(vinyl pyrrolidone). *J Polym Sci Pol Chem* 1995;33:49-54.

40. Shi B, Wu Y, Liu J. Vapor permeation separation of MeOH/MTBE through polyimide/sulfonated poly(ether-sulfone) hollow-fiber membranes. *Desalination* 2004;161:59-66.

41. Fu Y-J, Hu C-C, Lee K-R, Lai J-Y. Separation of ethanol/water mixtures by pervaporation through zeolite-filled polysulfone membrane containing 3-aminopropyltrimethoxysilane. *Desalination* 2006;193:119-28.

CHAPTER 4

HEMODIALYSIS MEMBRANE SURFACE CHEMISTRY AS A BARRIER TO ENDOTOXIN TRANSFER[1]

ABSTRACT: The transfer of bacterial endotoxin (lipopolysaccharide, LPS) from contaminated dialysate solution to a patient's blood during hemodialysis is a serious complication triggering fever and possible systemic shock. This study investigated LPS transfer across native and modified Fresenius Optiflux® F200NR^{e} polysulfone (PS) fibers. Modifications included: bleach-treated, high-PVP, low-PVP, and a copolymer mixture of PS-PEG. Fibers were exposed to 400 EU/ml of LPS from two bacterial sources under conditions modeling a clinical situation (2 hrs countercurrent flow, with saline substituted for blood). Kinetic turbidimetric limulus amoebocyte lysate (LAL) assay of the saline was performed to assess LPS transfer across the membranes. Water contact angle analysis and SEM were performed to correlate LPS transfer to material properties. LPS labeled with AlexaFluor 594 was used for fluorescence studies. Fluorescence images were taken of 10μm sections to observe LPS distribution. LPS adsorbed predominantly near the lumen of all membranes except the copolymer membrane, where LPS localized on the outer wall. LPS was not detected (<0.1 EU/ml) in the blood side of the Optiflux fibers, but was detected in all other samples (>0.1 EU/ml). High-PVP fibers allowed the greatest transfer of LPS to the blood side while adsorbing very little LPS. Low-PVP fibers promoted adsorption of LPS with very little

[1] Coauthored by Benjamin Madsen, David W. Britt, Chih-Hu Ho, Michael Henrie, Cheryl Ford, Eric Stroup, Brent Maltby, Doug Olmstead, and Marion Andersen

transfer to the blood side. Results indicate surface chemistry can be tuned during fiber production to control LPS adsorption and distribution across hollow fibers.

INTRODUCTION

Recent attention in the dialysis community has focused on back-filtration of bacterial endotoxin from contaminated dialysate (1-3). The trend toward high-flux dialyzers, because of their ability to remove large percentages of middle molecular weight toxins such as β_2-microglobulin (MW 11 kDa), has increased the concern of possible bacterial contamination in dialysate (4-5). Bicarbonate dialysate, an ideal environment for bacterial growth, is usually used in conjunction with high-flux membranes due to its biocompatibility (6).

Bacterial endotoxin (lipopolysaccharide, LPS) is a surface-recognition constituent of gram-negative bacterial membranes consisting of 3 main parts: an outer-membrane-integrated lipid (lipid A), a core oligosaccharide, and a long heteropolysaccharide chain (O-antigen) (7). The O-antigen varies among different bacterial strains and is the recognition site for blood-borne antibodies. The lipid A portion is generally conserved among bacterial types and is responsible for causing pyrogenic reactions. LPS is an amphiphilic molecule that has been shown to preferentially adsorb to hydrophobic surfaces (3). Endotoxin size varies from monomers of 10 kDa, to micelles of 1000 kDa or larger (7-9).

Bacterial contamination in dialysate fluids and clinical water sources has been documented (10-13). A diverse community of culturable bacteria has been found in dialysate fluids, of which *Pseudomonas* is most common (14-17). Robust, sessile

bacterial communities, called biofilms, may present a persistent source of contamination in dialysate water production lines because they are difficult to detect and remove (11-13). Several studies on water and dialysate quality in clinics in the U.S. and Europe have shown that as many as 20% of the samples tested were above the limit of the recommended standards (4, 16, 18). While small quantities of contamination may not always elicit a pyrogenic response, continued exposure to contaminated dialysate is of great concern because a typical patient on hemodialysis therapy will be exposed to 18,000-30,000 liters of water annually (17, 19). Reported pyrogenic reactions up to 0.7 per 1000 treatments have been reported, due mainly to pre-treatment issues with dialysis water (6, 17, 20).

Removal of LPS from solution is generally achieved using affinity sorbents and filtration. Plasma exchange and charcoal hemoperfusion, as well as immobilization to polymyxin B, ceramic membranes, and functionalized nanoparticles, have been investigated with varying degrees of success (4-5, 9, 21-22). Other chemistries exhibiting a high affinity for LPS include poly-L-lysine, diethylaminoethane, histamine, and histidine (23). Cationic polyelectrolytes presumably bind to the negatively charged phosphate groups on LPS.

The physicochemical properties of dialysis membranes are also explored to prevent back-filtration of LPS to the blood side of the membrane. The dialyzer represents the final barrier in preventing back-filtration of cytokine-inducing substances, such as LPS. Studies have shown that membranes of polysulfone (PS), polyamide, and cellulosic tri-acetate were effective at stopping back-filtration (1, 10, 24-26). The means of prevention has been ascribed primarily to adsorption, with filtration also playing a

significant role (1-2). However, it has also been shown that membranes of similar characteristics prevent back-filtration of LPS to different degrees, indicating that specific membrane characteristics contribute to the overall performance of inhibiting trans-membrane LPS flux (1, 3, 19).

The present study focuses on the mechanism by which several membranes of different chemical properties remove LPS, utilizing endotoxin from cultured sources and fluorescently-labeled conjugates. The membranes were challenged using both convective and diffusive experimental setups, as previously described (1). We present here how polyvinylpyrrolidone (PVP) content can be altered to encourage LPS adsorption and limit back-filtration. Furthermore we show how fiber sterilization via bleaching, as well as the addition of polyethyleneglycol (PEG) to polysulfone (PS) membranes, affects LPS adsorbing capabilities of dialysis membranes.

MATERIALS AND METHODS

Membranes

All experimental fibers were produced using the phase-inversion solution precipitation method (27) with the same spinning parameters (spinneret size, air gap, bore fluid, rinsing time). Fresenius Optiflux® F200NR^{e} membranes (Fresenius Medical Care North America), PS-PVP membranes sterilized via electron-beam irradiation, were used as the control against which experimental fiber membranes produced on a pilot line (FMCNA, Ogden, UT) were compared. Three experimental fibers were produced using PS as the base polymer with PVP as an additive or PEG as copolymer: High-PVP, Low-PVP, and PEG-Copolymer. “High” and “low” PVP content is with respect to that in the

commercial Optiflux membranes (28). Bleach-treated Optiflux fibers were prepared through exposure to 0.57% effective sodium hypochlorite content from the dialysate side at 70^{o}C for 2 minutes. Short bleach times were used similar to previous studies in order to limit possible membrane damage (29-30). Seiving coefficients for the different fibers used in this study are shown in Fig. C.1. (Appendix C).

Dialysate with bacterial culture filtrates

The contaminated dialysate challenge solution was prepared by inoculating two solutions of Trypticase soy broth (TSB) media with *Stenotrophomonas maltophilia* ATCC 13637 and *Pseudomonas aeruginosa* ATCC 27853, respectively. Following 48 hours of incubation, cultures were ultrasonicated (2 minutes at room temperature) and successively filtered using decreasing pore size, with a resulting final filtration at 0.45 μm. The large pore size used here maximized LPS fraction with no noticeable activity aberrations during the testing period. The remaining bacterial culture filtrates were then combined, rendering a challenge solution with LPS from both organisms. From this concentrated stock, bicarbonate dialysate was spiked to obtain LPS concentrations between 200-500 EU/ml in the dialysate. Challenge dialysate was kept at 4^{o}C until used.

***In vitro* dialysis circuit**

A model of *in vitro* dialysis previously described was modified for this study (Fig. 4.1) (19). Standard-sized dialysis cassettes were used for the *in vitro* studies (n = 3). Pumps connected to the blood compartment (BC) and dialysate compartment (DC) were first calibrated using sterile saline. Standard dialysis tubing sets (Medisystems) were sterilized and assembled prior to running the dialysis simulation, according to the

experimental setup in Fig. 4.1. Both the BC and DC were then rinsed with pyrogen-free saline for 15 minutes, to remove any residual endotoxins. Following the saline rinse, the simulation commenced by closing the BC circuit (closed loop) and introducing the dialysate challenge solution to the DC circuit (420 ± 24 EU/ml). The flow through the BC circuit was held constant at 200 ml/min, using a reservoir of approximately 140 ml, while flow through the DC circuit was 500 ml/min. After 60 minutes, the BC return line was placed in the dialysate challenge reservoir and the inlet blocked, forming a convective circuit as shown in Fig. 4.1. The flow from the BC was lowered to 37 ml/min and the simulation was run for an additional 60 minutes, followed by a saline rinse.

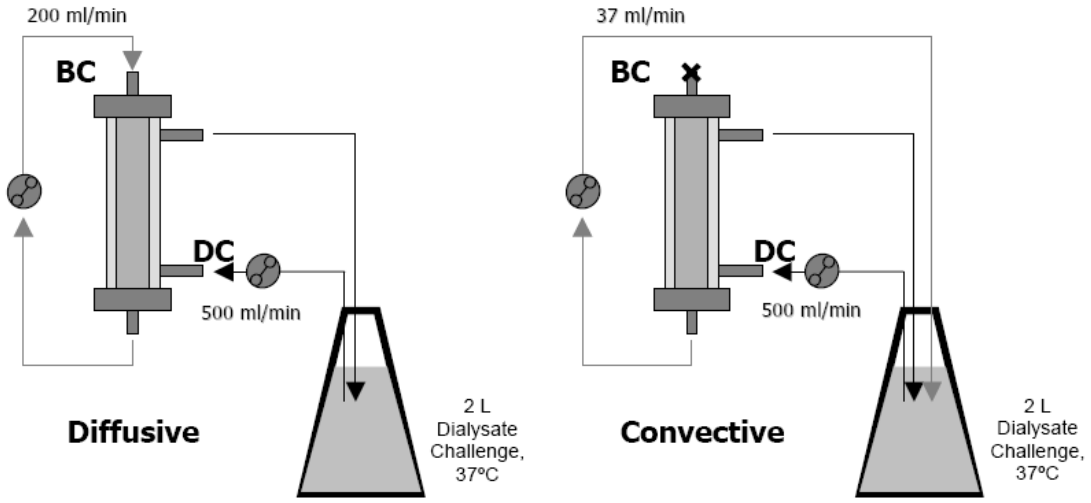

FIG. 4.1. Experimental dialysis simulation setups for the LPS challenge tests. The diffusive setup is first run for 60 minutes, after which the system is changed to the convective setup and run for an additional 60 minutes.

Samples of 10 ml were collected from both the BC and DC following the priming saline rinse, and at time 0, 7, 15, 60, 67, 75, and 120 min during the LPS challenges. LPS concentration in all samples and the original culture filtrate was determined by kinetic

turbidimetric LAL assay (Charles River Labs). The detection limit of LPS concentration in solution was 0.1 EU/ml.

Fluorescent imaging

Fluorescent-labeled LPS conjugate (AlexaFluor® 594 conjugate, Invitrogen) was used to study the areas where LPS binding occurred throughout the membrane wall. Prior studies have shown that a fluorescent label attached to the LPS molecule does not affect the behavior of the LPS (31). Mini-modules (Fig. 4.2) were constructed for the fluorescent imaging portion of the study, to reduce the amount of fluorescent-labeled LPS conjugate required. Thirty fibers of each type were placed in a polycarbonate tube (15 cm in length, 2.4 mm inside diameter) and potted using UV-curable epoxy resin (Dymax Corp.). Mini-modules were subjected to the same experimental simulation setup as the other membranes, with 60 minutes of diffusive and 60 minutes of convective testing. However, fluorescent-labeled LPS was used to contaminate the dialysate. Each mini-module was subjected to a challenge of 800 EU/ml of labeled LPS conjugate, with the simulation run in a controlled dark environment. Flow rates used with the mini-modules similar in proportion to the larger dialyzers: 1 ml/min for the BC, 2 ml/min for the DC.

After the simulations were complete, mini-modules were placed in a drying oven overnight to prepare for sectioning and imaging. The process of embedding, slicing and imaging the samples used a previously described protocol modified for this study (2, 32). Fiber membranes were removed from their housings and sectioned to 10 μm using tissue freezing media (Triangle Biomedical Sciences), a low-profile microtome blade (SEC 35e, Richard-Allan Scientific) and a cryostat (Leica 1850, Leica Microsystems). Sectioned

fibers were imaged using a fluorescence microscope (Nikon TE2000-S, Nikon Corp.) with a Resorufin filter set (Chroma Technology). This filter set was used to minimize membrane auto-fluorescence and maximize fluorescence of the AlexaFluor® 594 conjugate. Images of the membrane samples were obtained with a 12 megapixel camera (Nikon DXM1200, Nikon Corp.) at a resolution of 1280 X 1024 using a 60-second image integration time and analyzed with ACT-1 software (Nikon Corp.). Fluorescence intensity through the cross-section of each fiber was measured using ImageJ software (National Institutes of Health).

FIG. 4.2. Mini-module used for fluorescence imaging, showing polycarbonate housing and T's, with UV curable epoxy for potting material. Approximately 30 fibers, 15 cm in length, provide the mini-module with about 15 cm^2 of surface area.

Surface characterization by water contact angle

For all membranes tested, sessile drop contact angle analysis was performed on both the outer surface and lumen of the fibers. To access the lumen, the fiber was cut longitudinally and spread open onto double-sided tape. A goniometer (VCA Optima, AST Products) was used to image 0.25 μl droplets of double-distilled water on the

surface. Immediately following the application of the droplet, a digital image was captured; from this image the contact angle of the droplet was determined (n = 8).

SEM imaging

Fiber membranes were prepared for SEM by dipping the fibers in liquid nitrogen and snapping them with a quick motion, yielding a 90^{o} break. Membranes were then placed onto an imaging stage and coated with gold to 20 nm thick using a sputter coater (Lesker 108, Kurt J. Lesker Co.) and a thickness monitor (Cressington MTM10, Cressington Scientific Instruments Ltd.). Membranes were then imaged using a field emission scanning electron microscope (Hitachi F-4000, Hitachi, Ltd.).

RESULTS

Dialysis simulations using bacterial culture filtrates as challenge material

Dialysis simulation data for all membranes tested are shown in Figs. 4.3-4.5, with curves representing LPS levels measured from the blood compartment and dialysate compartment. All plots use a semi-log scale for the LPS concentration. Maximum LPS levels in the DC typically occurred from minute 7 to minute 15, attributed to the time required for the LPS to equilibrate throughout the system. All graphs show a decrease in free LPS in the DC with time due to adsorption to the membrane.

Initial LPS levels in the dialysate reservoirs measured by the LAL assay were as follows: Optiflux, 455 ± 44 EU/ml; low-PVP, 446 ± 73 EU/ml; high-PVP, 410 ± 107 EU/ml; bleach, 467 ± 224 EU/ml; copolymer, 241 ± 43 EU/ml. During the dialysis simulations no LPS was detected in the BC samples from the Optiflux membrane (Fig.

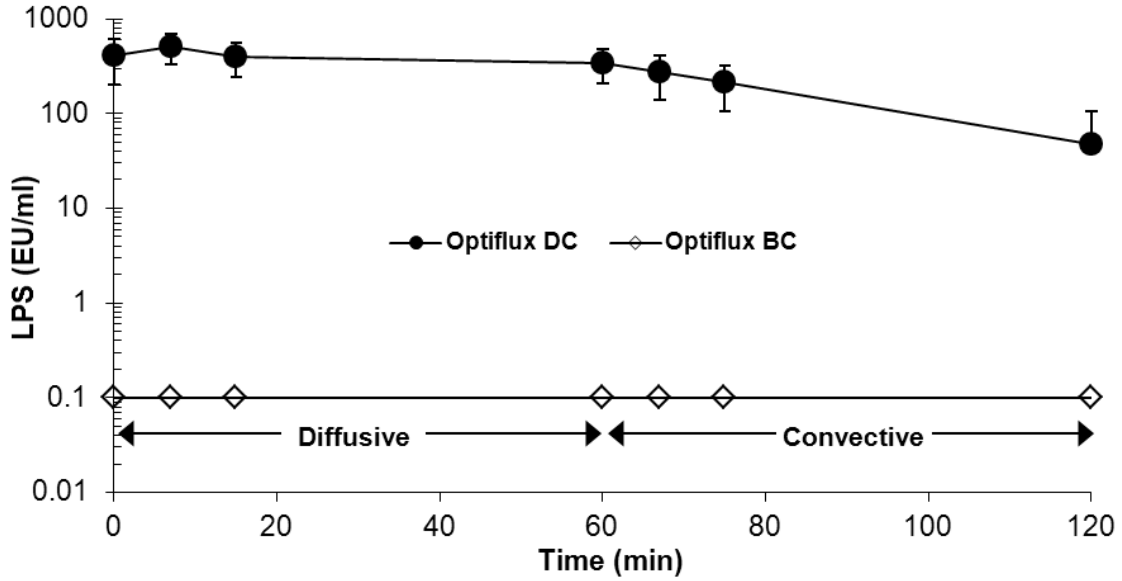

FIG. 4.3. Semi-log plot of LPS concentrations in the DC (closed circle) and BC (open circle) for Optiflux (control) membrane (mean ± s.d., n = 3).

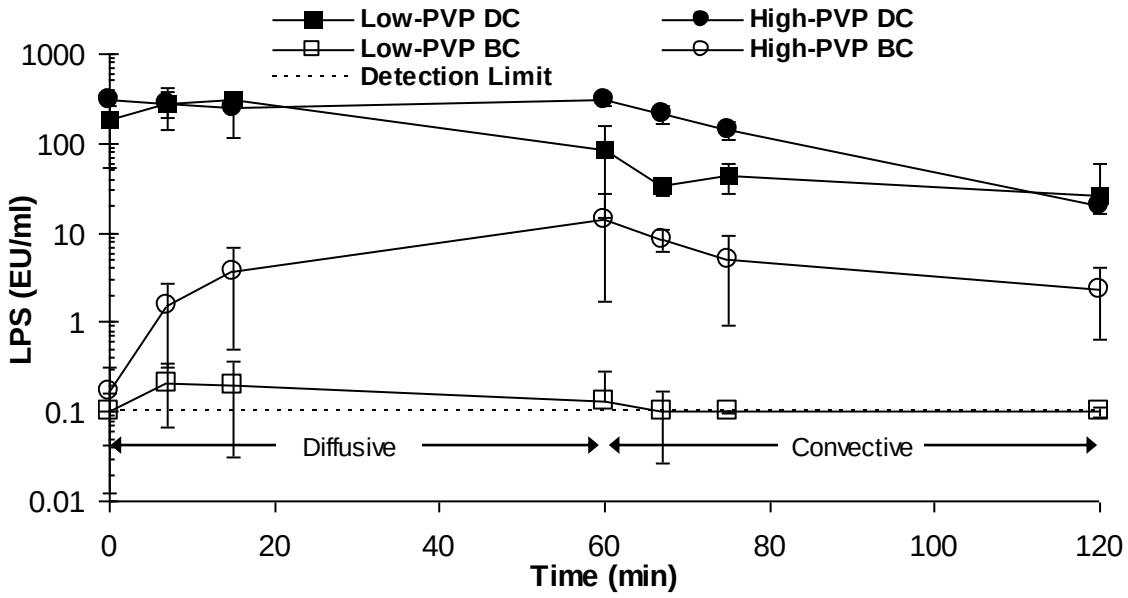

FIG. 4.4. Semi-log plot of LPS concentration in BC and DC of high-PVP and low-PVP membranes (mean ± s.d., n = 3).

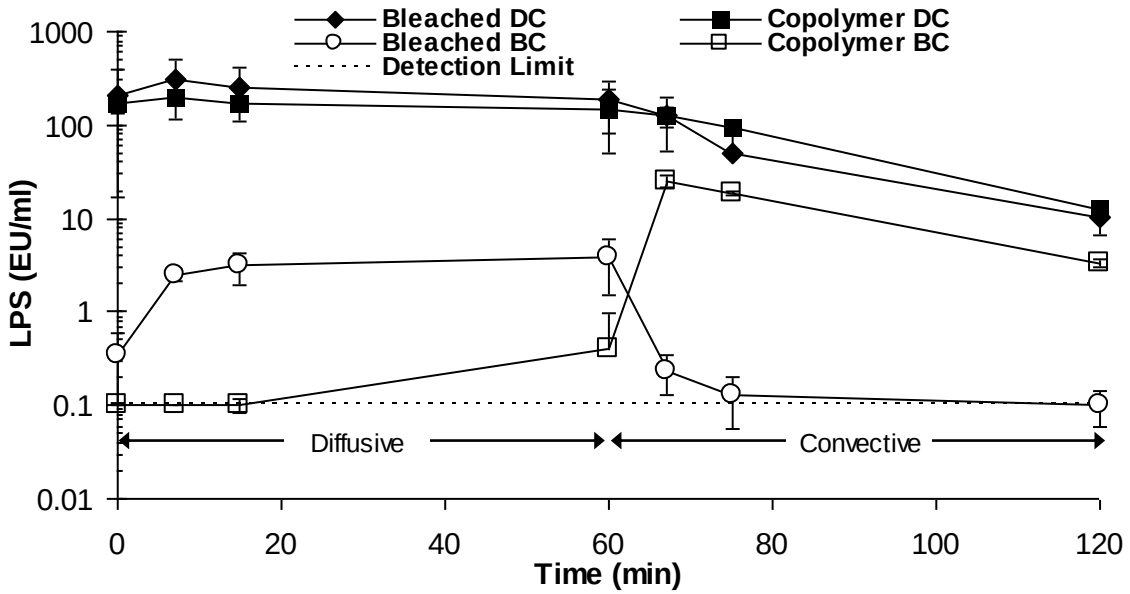

FIG. 4.5. Semi-log plot of LPS concentration in BC and DC of bleached and PS-PEG copolymer membranes (mean ± s.d., n = 3).

4.3), indicating any LPS back-filtrate was below 0.1 EU/ml. In contrast, LPS was detected to varying degrees in the BC in all of the modified membranes following the initial LPS challenge (Figs. 4.4-4.5). Maximum LPS BC concentrations occurred during diffusive conditions for the low-PVP, high-PVP, and bleach treated membranes, whereas LPS concentrations were highest during convective flow for the copolymer fibers. BC peak LPS concentrations were as follows: low-PVP, 0.2 EU/ml @ 7 min.; high-PVP, 14.4 EU/ml @ 60 min.; bleached, 3.8 EU/ml @ 60 min.; copolymer, 24.8 EU/ml @ 67 min.

Surface hydrophobicity by contact angle analysis

Contact angle measurements were performed on both the outer and inner skin of the fiber membrane. Results for the contact angle measurements are presented in Fig. 4.6, with mean ± standard deviation (n = 8). Statistical analysis showed significant

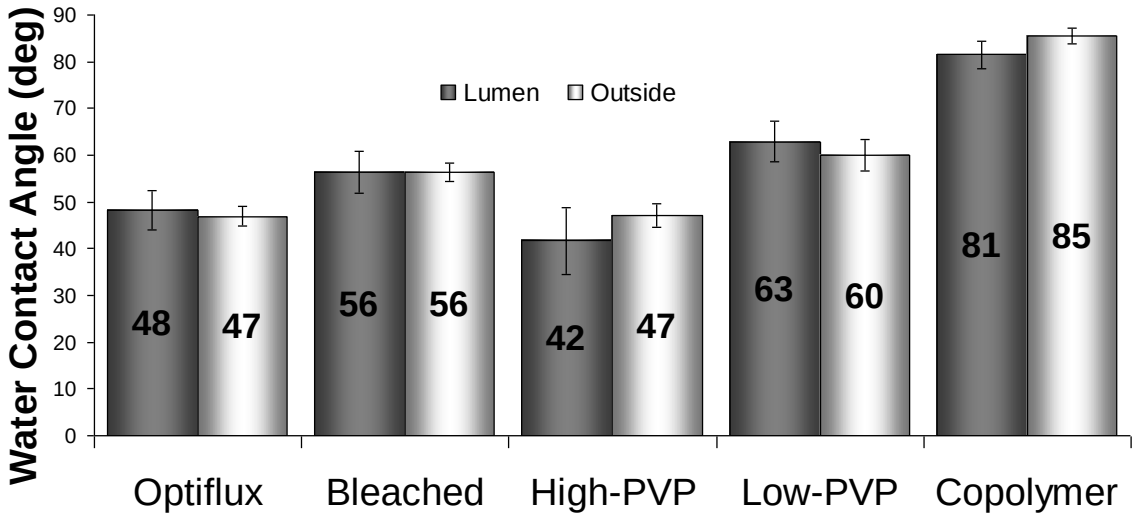

FIG. 4.6. Contact angle measurements of both inner lumen and outside of fiber membranes (mean ± s.d., n = 8). Statistical analysis revealed significant difference ($p < 0.05$) among all samples. Significant difference between the outside and lumen side contact angle was found only in the copolymer and high-PVP membranes.

differences between outer surface and inner lumen contact angles and among the different membrane types. Results indicate that the copolymer and high-PVP membranes exhibited significant differences between the outer and inner skin contact angles ($p < 0.05$). All lumen contact angles were significantly different from each other, while all outside contact angles were significantly different except Optiflux and high-PVP membranes. Differences in contact angle arise from physicochemical differences among fibers, namely surface roughness, porosity, and concentration and location of the hydrophilizing agent, PVP.

Imaging of dialysis membranes

Fluorescence and SEM images, as well as intensity profiles for all membranes tested, are presented in Figs. 4.7-4.11, to illustrate LPS distribution, general membrane geometry, morphologies of the membrane cross sections near the lumen and outside

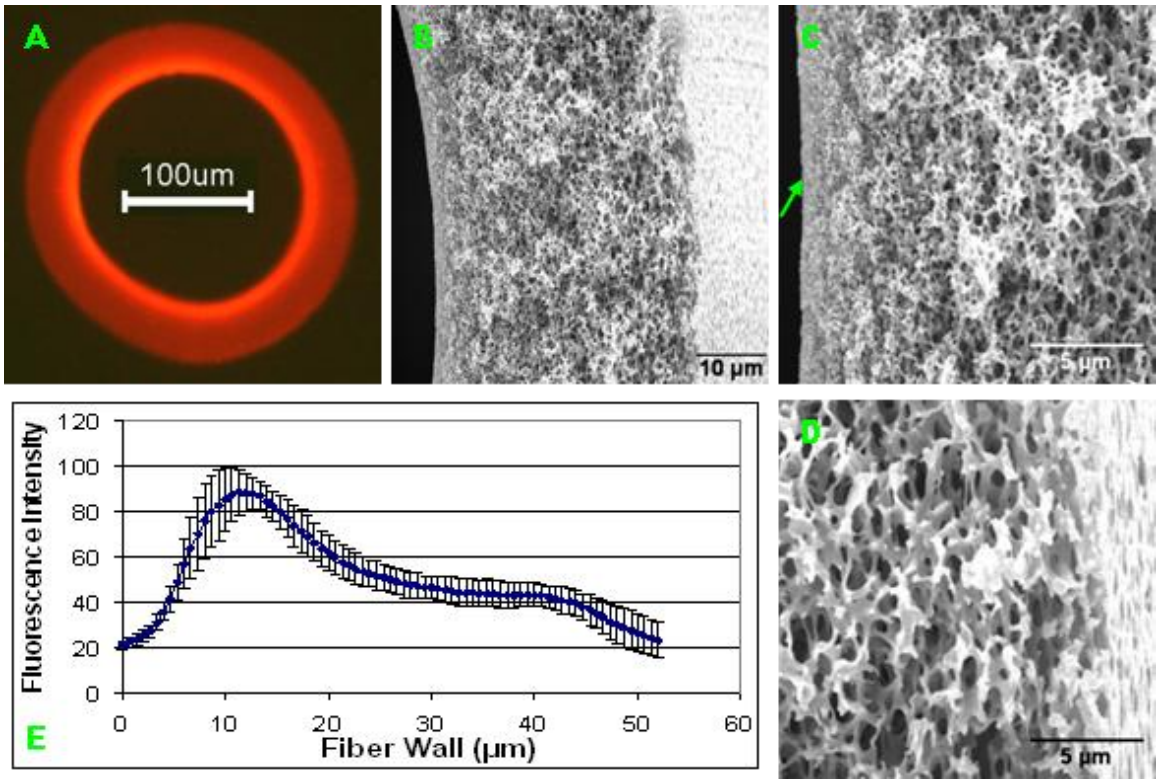

FIG. 4.7. Optiflux membrane: Fluorescence image (A), SEM images of the cross section (B), near the lumen (C), and near the outer wall (D), and fluorescence intensity profile (E). Fluorescent-labeled LPS conjugate is distributed throughout the entire membrane cross-section, accumulating near the inner lumen surface. The intensity profile shows the distribution of LPS adsorption from lumen (left) to outside (right). The arrow in Panel C indicates the boundary of the lumen wall.

surfaces. The arrow in Panel C of Figs. 4.7-4.11 indicates the boundary of the lumen wall.

As seen in the fluorescence microscopy images in Figs. 4.7-4.11, AlexaFluor-LPS aggregated near the lumen for all fibers except the PS-PEG copolymer, where a reverse trend was observed. The low-PVP membrane exhibited a higher LPS affinity as indicated by overall image intensity and a more uniform distribution of LPS throughout the fiber spongy matrix as compared to the other fibers. The presented images were representative of all imaged samples ($n \geq 3$ for each fiber type); no atypical fluorescent

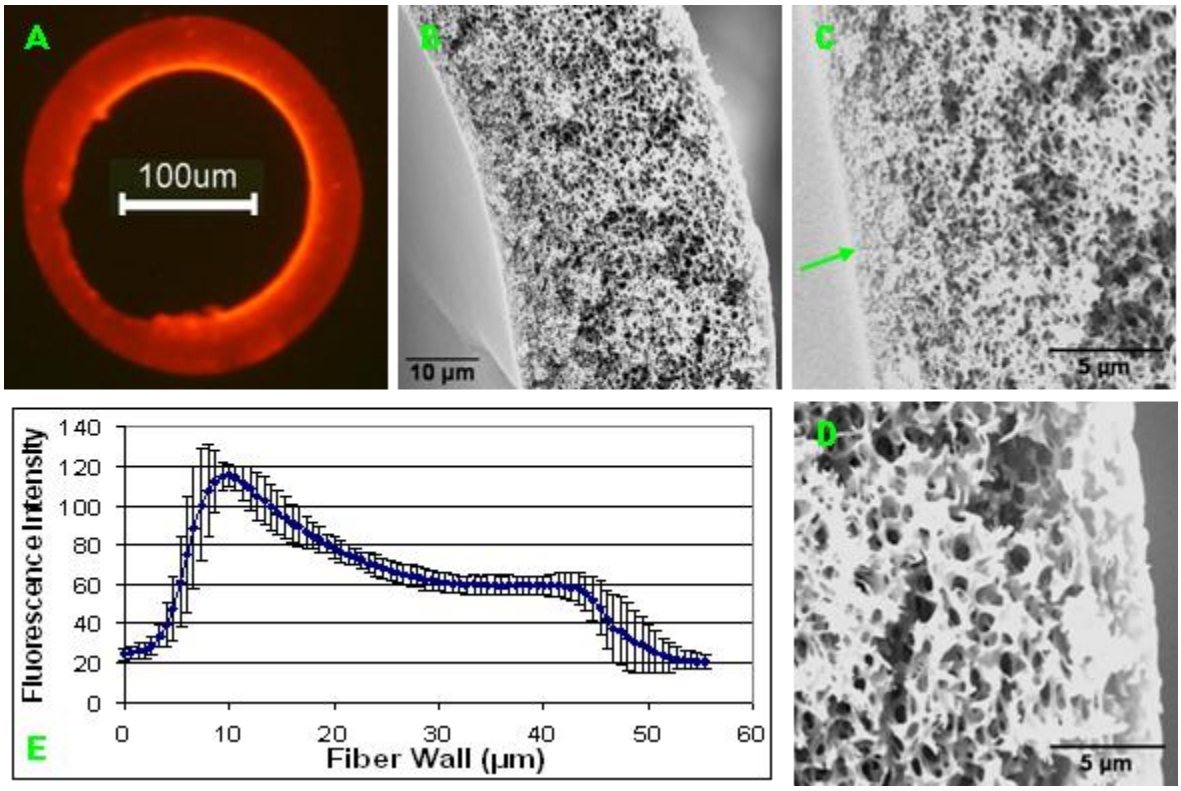

FIG. 4.8. Bleached fiber membrane: Fluorescence image (A), SEM images of the cross-section (B), near the lumen (C), and near the outer wall (D), and fluorescence intensity profile (E). Fluorescence distribution and surface structure were similar to the Optiflux membrane. The different structure in the bottom left of the fluorescence image is due to cryostat cutting artifact.

patterns were observed. Intensity profiles (Panel E, Figs. 4.7-4.11) all show relative fluorescence intensity through the cross section of the fiber from lumen (left) to outside (right).

The cross-sectional SEM images in Figs. 4.7-4.11 show similar spongy asymmetric matrix structures for the Optiflux, bleached, high-PVP, and low-PVP membranes. For these membranes the lumen exhibited a less porous wall while the outside structure was a highly porous polymer network. The copolymer membrane (Fig. 4.11) exhibited a "three-layer" structure with a spongy matrix in the outer half of the membrane, a macroporous structure in the inner half, and a molecular weight cut-off

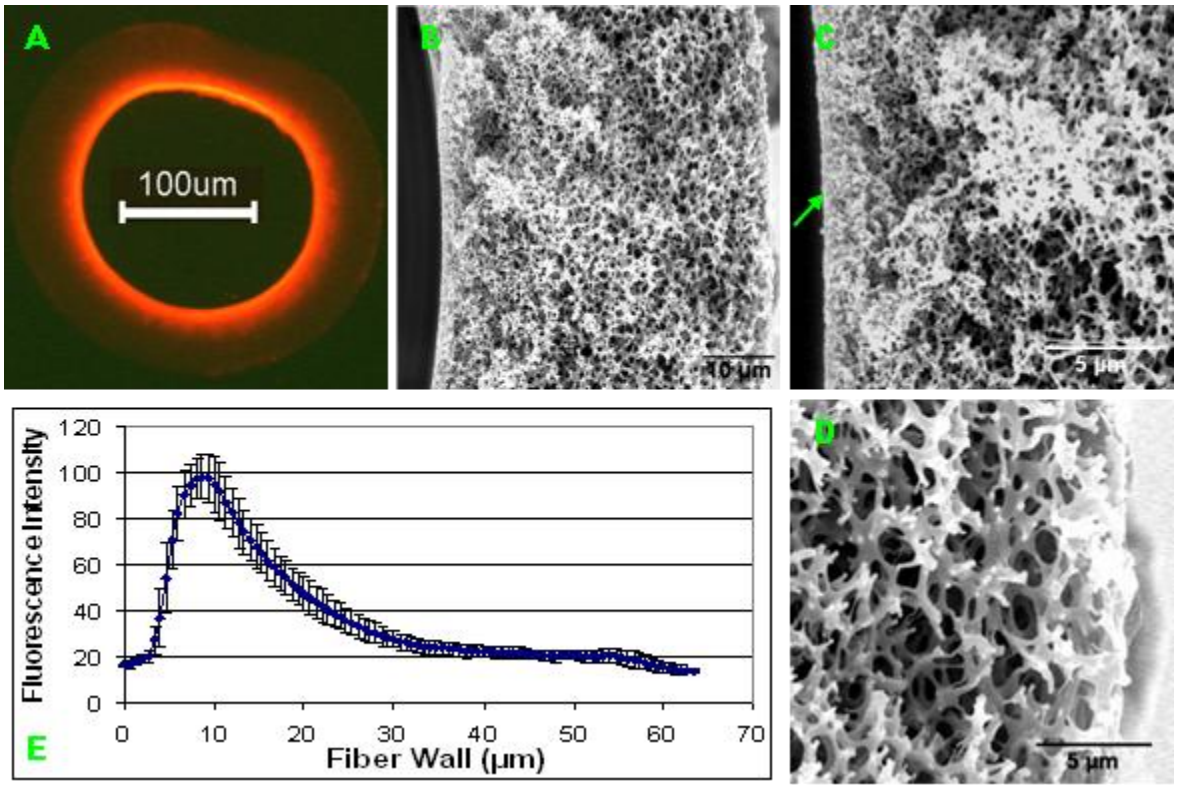

FIG. 4.9. High-PVP membrane: Fluorescence image (A), SEM images of the cross-section (B), near the lumen (C), and near the outer wall (D), and fluorescence intensity profile (E). Fluorescence intensity for the matrix portion of the membrane is much lower for this sample compared to the other samples indicating less adsorption of LPS.

region near the lumen. Fig. 4.11 reveals macropores extending to the inner wall of the membrane as well as a less porous exterior wall. A clear demarcation in the transition from macropores to spongy matrix is seen in Fig. 4.11B. The difference in the structure of this membrane can be attributed to distinct thermodynamics of the phase inversion arising from the use of the PS-PEG copolymer as compared to PVP.

AFM and SEM images of the lumen and outside surfaces are presented in Figs. B.1-B.5 (Appendix B). RMS values for presented AFM images are shown in Table B.1 (Appendix B), with a discussion of such in Appendix B.

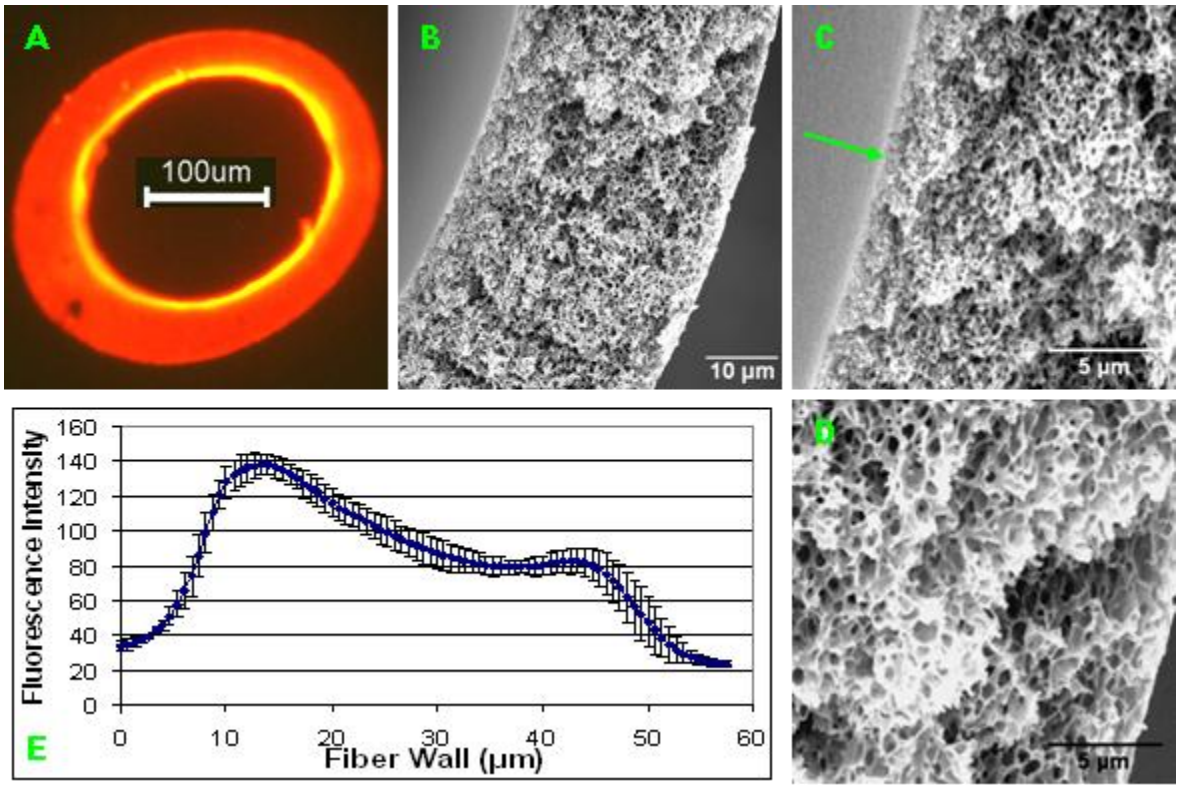

FIG. 4.10. Low-PVP fiber membrane: Fluorescence image (A), SEM images of the cross-section (B), near the lumen (C), and near the outer wall (D), and fluorescence intensity profile (E). Distribution of LPS for this membrane is similar to the Optiflux membrane. However, intensity is much stronger here indicating a higher affinity of the LPS to the membrane.

DISCUSSION

Much attention has recently been given not only to the quality of dialysis water, but to using the dialyzer as a mechanism to prevent back-filtration of bacterial LPS. This study focused on the latter, with attention to investigating how chemical changes in the filter membranes cause LPS to preferentially bind to certain areas and in what quantities.

While studies have shown that incidents of pyrogenic reactions are fairly low, the possibility of back-diffusion of bacterial fragments should be considered great due to the difficulty of detecting and removing biofilms in water purification systems, as previously

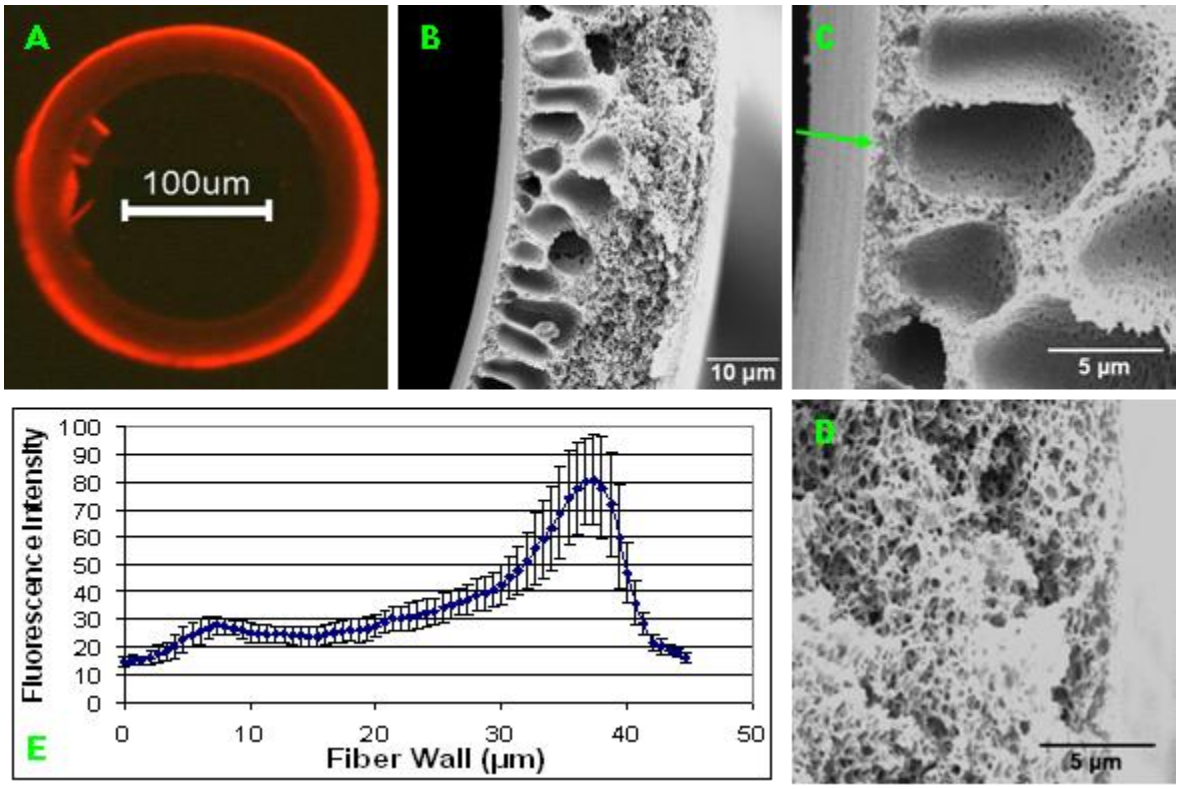

FIG. 4.11. PS-PEG Copolymer fiber membrane: Fluorescence image (A), SEM images of the cross-section (B), near the lumen (C), and near the outer wall (D), and fluorescence intensity profile (E). In contrast to the other fiber types, a distinct transition in the porosity of the spongy matrix is observed and LPS is restricted to the outer surface.

discussed. Should a large portion of one of these biofilms become dislodged, the increase in LPS levels in dialysate could be dramatic. In this study, high concentrations of LPS (roughly 20 times the allowable amount for medical devices) were used to show the ability of hollow fiber membranes to adsorb and filter LPS from solution and to represent a "worst case scenario." However, because experiments were performed at concentrations well below the critical aggregation concentration of LPS similar trends in LPS backfiltration and adsorption would be expected exist at lower concentrations (33, 34).

Results from the high- and low-PVP simulations (Fig. 4.4) show increases in LPS back-diffusion compared to the Optiflux (control) membrane, especially under diffusive conditions. The low-PVP membrane also adsorbed more LPS through the diffusive portion of the simulation, as observed by the sharp decrease in LPS concentration in the dialysate compartment and bright intensity in the corresponding fluorescence image. It is noted that the LPS levels in the blood compartment decreased with time during diffusive conditions and immediately dropped below the detection limit during convective conditions for the low-PVP membrane. This decrease in BC LPS levels during diffusive conditions suggests that LPS in the BC may have adsorbed to the membrane or reentered the dialysis circuit solution. During convective flow all LPS is likely adsorbed or forced into fiber pores. The high-PVP membrane allowed the most LPS transfer into the BC compared to all other membranes. SEM images show a thicker wall structure for the high-PVP membrane (46 μm) than all others (< 38 μm), demonstrating that wall thickness does not necessarily contribute to preventing LPS back-diffusion.

It has been shown previously that dialyzers reprocessed using Renalin® (a sterilant composed of hydrogen peroxide, peracetic acid, acetic acid, and water) resisted trans-membrane passage of LPS during treatments (35). Similarly, polysulfone dialyzers subjected to 13 volumes of a bleach solution were able to remove endotoxin from a challenge solution (36). Bleached membranes in this study allowed LPS back-diffusion immediately upon commencement of the diffusive simulation, but less under convective conditions. This confirms other findings that solute transport characteristics are greatly dependent on the dialyzer being studied and the reprocessing technique (29, 37).

PEG is often added to surfaces as a protein-repellant layer (38). PS-PEG copolymers have previously been incorporated into PS filter membranes to repel proteins and to enhance surface wettability (39-40). PS-PEG copolymer was investigated here for its ability to repel bacterial LPS challenges. The fluorescence, SEM, and contact angle data indicate that during coagulation of the spin-mass a unique three-layer structure formed that readily bound LPS, but restricted adsorption to the outer spongy portion of the membrane. Back-diffusion of LPS, however, was observed after minute 7 of the diffusive simulation. Under convective conditions the membrane allowed a greater diffusion of LPS to the BC, while also adsorbing most of the LPS in the challenge solution as noted by the decrease in DC LPS concentration. It is observed that the LPS concentration in the BC remained at or near the detection limit for most of the diffusive conditions for the copolymer membrane, then increased to about 0.4 EU/ml by 60 min. In contrast to the other membranes, the BC LPS concentration increased upon switching to convective conditions for the copolymer fiber. It is also seen in the SEM cross-section that the spongy matrix pores in the copolymer fiber are much smaller near the outer wall, which may prevent the transport of LPS into the BC during diffusive conditions. These scenarios are being addressed in ongoing work where fiber cross-sections are examined using SEM and fluorescence microscopy after diffusive and convective conditions.

Previous studies have shown that hollow fibers have a great capacity to remove LPS from solution during dialysis simulations (1, 41). The average reduction in LPS from the DC for all membranes tested was 93.7%, similar to previous studies (1). Of note is the continual decrease in LPS concentration (based on negative slope of the

simulation data at minute 120) in the DC for all membrane types, indicating that all membranes had not reached their adsorptive capacities for LPS.

To address the distribution of PVP and PEG we employed water contact angle analysis of fiber lumens and outside walls (Fig. 4.6). PVP, a common additive to PS membranes, is used to decrease hydrophobicity, increase biocompatibility, and create pores during the phase inversion process (42). The water contact angles for lumen and outer wall for the Optiflux membrane were 48 and 47, respectively, similar to values previously reported (1). The addition or reduction of PVP concentration is reflected in the lower and higher contact angles for the high- and low-PVP membranes, respectively, compared to the Optiflux standard. Bleaching of PS-PVP membranes has been shown to cause an increase in hydrophobicity and net negative charge, attributed to chain scission of PVP via radical reactions (35, 43-45). Bleaching Optiflux fibers for 2 minutes increased hydrophobicity as shown in the increase in contact angle.

Unlike PVP, the PS-PEG additive is an amphiphilic copolymer, which will influence phase separation during the fiber precipitation process, as suggested by the "3-layer" structure observed in the SEM cross-section. The higher contact angles observed for the PS-PEG membrane are indicative of more hydrophobic domains (likely due to hydrophobic polysulfone) on these surfaces. It is possible that the PEG chains are sequestered in the fiber matrix while PS is concentrated at the interfaces (outside wall and lumen), thus causing an increase in contact angle of these surfaces, and subsequently less LPS adsorption through the spongy matrix. The increase in outside membrane contact angle is different than a previous study that suggested that PEG chains segregated to the outside surfaces of the membrane causing a more hydrophilic membrane (39-40).

However, due to the sensitive nature of the phase inversion process, small changes can dramatically alter thermodynamic partitioning of the polymers in the spin-mass (27). Continuing research will focus on varying ratios of PS:PEG and refining spinning conditions to obtain a membrane structure more similar to the Optiflux fiber while eliminating LPS entry into the BC and continuing to favor LPS adsorption to the outer wall.

It has been shown that LPS preferentially binds to hydrophobic membranes and that PVP restricts adsorption of proteins to PS membranes (42, 46). Therefore it would be expected, based on contact angles, that the bleached, low-PVP, and copolymer membranes would bind more LPS than the Optiflux control. Fluorescence images and intensity profiles show that LPS bound extensively through the matrix of the low-PVP membrane but only to the outside of the copolymer membrane. LPS also bound more prevalently through the matrix of the bleached membrane compared to the Optiflux membrane, suggesting a chemical makeup in the spongy matrix similar to the low-PVP membrane. PVP content is likely diminished throughout the membrane as indicated by the increase in contact angle compared to the Optiflux membrane. Also, LPS bound only near the lumen of the more hydrophilic high-PVP membrane and not through the matrix of the hollow fiber. SEM images for all membranes but the copolymer show a thick lumen wall. It is likely that LPS in these membranes was trapped near the lumen because of this wall structure. Conversely, the copolymer fiber had much larger macropores near the lumen that likely allowed LPS to easily pass through to the BC. Therefore, adsorption of LPS is likely due to both hydrophobic interactions as well as physical entrapment by pores.

All modified membranes allowed some back-filtration of LPS in the simulation. Because the copolymer membrane bound most LPS on the outer membrane it can be inferred that LPS that breached the outer part of the copolymer membrane did not bind to the matrix of the hollow fiber, rather it continued through to the BC. Restricting LPS adsorption to the outside wall of the copolymer membrane is viewed as beneficial as it has been shown that LPS does not need to be in direct contact with blood to elicit a pyrogenic response (8). Although LPS was not detected in the BC of the Optiflux fiber, the possibility of pyrogenic response is still of concern as LPS bound strongly near the lumen and LPS may still exist in the BC below detection limits. Thus, the PS-PEG copolymer formulation employed here is very intriguing as it may afford a means to restrict LPS to the outer membrane.

CONCLUSION

The evolution toward high-flux dialysis membranes coupled with bicarbonate dialysate in hemodialysis necessitates validation of these membranes as pyrogen adsorbers and/or filters. It is important to assess chemical properties of membranes that specifically adsorb and prevent back-filtration of LPS into the BC of dialyzers. Also, it is of interest to determine the effect of reprocessing on LPS back-filtration and adsorption characteristics.

It has been shown in this study that the chemical means by which dialysis membranes adsorb and filter LPS from contaminated dialysate can be tuned through hydrophobic interactions. It has also been shown that bleach treatments at low concentration and short exposure time can cause dramatic changes in back-filtration and

surface physicochemistry of dialysis membranes. Furthermore, it was shown that the addition of PS-PEG to PS caused changes in membrane porosity, surface chemistry, and LPS adsorption characteristics. Of most importance with the PS-PEG copolymer membrane was the ability of the membrane to adsorb LPS primarily on the outside of the membrane, reducing the possibility of pyrogenic reactions with blood.

From these studies it is clear that LPS can be trapped selectively at fiber lumens or outer walls through minor modifications in the PVP content of the spin mass as well as through addition of PS-PEG copolymer. Mixtures of PVP with the copolymer are also of interest as this may allow us to more specifically tune surface properties as well as optimize the morphology of the spongy matrix to selectively trap LPS at the outside wall without allowing any LPS to enter the BC as observed for all chemical modifications presented here.

REFERENCES

1. Henrie M, Ford C, Andersen M, Stroup E, Diaz-Buxo J, Madsen B, et al. In vitro assessment of dialysis membrane as an endotoxin transfer barrier: Geometry, morphology, and permeability. *Artif Organs* 2008;32:701-10.

2. Hayama M, Miyasaka T, Mochizuki S, Asahara H, Yamamoto K-i, Kohori F, et al. Optimum dialysis membrane for endotoxin blocking. *J Membrane Sci* 2003;219:15-25.

3. Takemoto Y, Nakatani T, Sugimura K, Yoshimura R, Tsuchida K. Endotoxin adsorption of various dialysis membranes: In vitro study. *Artif Organs* 2003;27:1134-7.

4. Linnenweber S, Lonnemann G. Pyrogen retention by the Asahi APS-650 polysulfone dialyzer during in vitro dialysis with whole human donor blood. *ASAIO J* 2000;46:444-7.

5. Bender H, Pflänzel A, Saunders N, Czermak P, Catapano G, Vienken J. Membranes for endotoxin removal from dialysate: Considerations on feasibility of commercial ceramic membranes. *Artif Organs* 2000;24:826-9.

6. Gordon SM, Oettinger CW, Bland LA, Oliver JC, Arduino MJ, Aguero SM, et al. Pyrogenic reactions in patients receiving conventional, high-efficiency, or high-flux hemodialysis treatments with bicarbonate dialysate containing high concentrations of bacteria and endotoxin. *J Am Soc Nephrol* 1992;2:1436-44.

7. Gorbet MB, Sefton MV. Endotoxin: The uninvited guest. *Biomaterials* 2005;26:6811-7.

8. Yamamoto K-i, Matsuda M, Hayama M, Asutagawa J, Tanaka S, Kohori F, et al. Evaluation of the activity of endotoxin trapped by a hollow-fiber dialysis membrane. *J Membrane Sci* 2006;272:211-6.

9. Darkow R, Groth T, Albrecht W, Lützow K, Paul D. Functionalized nanoparticles for endotoxin binding in aqueous solutions. *Biomaterials* 1999;20:1277-83.

10. Bambauer R, Walther J, Jung WK. Ultrafiltration of dialysis fluid to obtain a sterile solution during hemodialysis. *Blood Purificat* 1990;8:309-17.

11. Hoenich NA, Levin R. The implications of water quality in hemodialysis. *Semin Dialysis* 2003;16:492-7.

12. Man N-K, Degremont A, Darbord J-C, Collet M, Vaillant P. Evidence of bacterial biofilm in tubing from hydraulic pathway of hemodialysis system. *Artif Organs* 1998;22:596-600.

13. Marion-Ferey K, Leid JG, Bouvier G, Pasmore M, Husson G, Vilagines R. Endotoxin level measurement in hemodialysis biofilm using "the whole blood assay". *Artif Organs* 2005;29:475-81.

14. Gomila M, Gasco J, Busquets A, Gil J, Bernaeu R, Buades JM, et al. Identification of culturable bacteria present in haemodialysis water and fluid. *FEMS Microbiol Ecol* 2005;52:101-14.

15. Tsuchida K, Nakatani T, Sugimura K, Yoshimura R, Matsuyama M, Takemoto Y. Biological reactions resulting from endotoxin adsorbed on dialysis membrane: An in vitro study. *Artif Organs* 2004;28:231-4.

16. Jaber BL, Gonski JA, Cendoroglo M, Balakrishnan VS, Razeghi P, Diniarello CA, et al. New polyether sulfone dialyzers attenuate passage of cytokine-inducing substances from *Pseudomonas aeruginosa* contaminated dialysate. *Blood Purificat* 1998;16:210-9.

17. ANZSN. *Consensus Statement for Maintenance of Chemical and Microbiological Safety of Haemodialysis Water and Dialysate Systems*. Sydney, Australia: Australian and New Zealand Society of Nephrology, 1996.

18. Lonnemann G, Sereni L, Lemke H-D, Tetta C. Pyrogen retention by highly permeable synthetic membranes during in vitro dialysis. *Artif Organs* 2001;25:951-60.

19. Weber V, Linsberger I, Rossmanith E, Weber C, Falkenhagen D. Pyrogen transfer across high- and low-flux hemodialysis membranes. *Artif Organs* 2004;28:210-7.

20. Roth VR, Jarvis WR. Outbreaks of infection and/or pyrogenic reactions in dialysis patients. *Semin Dialysis* 2000;13:92-6.

21. Tetta C, Bellomo R, Inguaaggiato R, Wratten ML, Ronco C. Endotoxin and cytokine removal in sepsis. *Therap Apher Dial* 2002;6:109-15.

22. Sato T, Shoji H, Koga N. Endotoxin adsorption by polymyxin B immobilized fiber column in patients with systemic inflammatory response syndrome. *Therap Apher Dial* 2003;7:252-8.

23. Anspach FB, Hilbeck O. Removal of endotoxins by affinity sorbents. *J Chromatogr A* 1995;711:81-92.

24. Oliver JC, Bland LA, Oettinger CW, Arduino MJ, Garrard M, Pegues DA, et al. Bacteria and endotoxin removal from bicarbonate dialysis fluids for use in conventional, high-efficiency, and high-flux hemodialysis. *Artif Organs* 1992;16:141-5.

25. Rietschel ET, Kirikae T, Schade FU, Mamat U, Schmidt G, Loppnow H, et al. Bacterial endotoxin: Molecular relationships of structure to activity and function. *FASEB J* 1994;8:217-25.

26. Tellingen Av, Grooteman MPC, Pronk R, Loon Jv, Vervloet MG, Wee PMt, et al. Lipopolysaccharide concentrations during superflux dialysis using unfiltered bicarbonate dialysate. *ASAIO J* 2002;48:383-8.

27. Mulder M. *Basic Principles of Membrane Technology*. The Netherlands: Kluwer Academic Publishers, 1996.

28. Heilmann K. Asymmetrical microporous hollow fiber for hemodialysis. United States Patent Nr. Apr. 29, 1988.

29. Cheung AK, Agodoa LY, Daugirdas JT, Depner TA, Gotch FA, Greene T, et al. Effects of hemodialyzer reuse on clearances of urea and β_2-microglobulin. *J Am Soc Nephrol* 1999;10:117-27.

30. Sundaram S, Barrett TW, Meyer KB, Perrella C. Transmembrane passage of cytokine-inducing bacterial products across new and reprocessed polysulfone dialyzers. *J Am Soc Nephrol* 1996;7:2183-91.

31. Levels JHM, Abraham PR, Ende Avd, Deventer SJHv. Distribution and kinetics of lipoprotein-bound endotoxin. *Infect Immun* 2001;69:2821-8.

32. Hayama M, Miyasaka T, Mochizuki S, Asahara H, Tsujioka K, Kohori F, et al. Visualization of distribution of endotoxin trapped in an endotoxin-blocking filtration membrane. *J Membrane Sci* 2002;210:45-53.

33. Bergstrand A, Svanberg C, Langton M, Nyden M. Aggregation behavior and size of lipopolysaccharide from Escherichia coli O55:B5. *Colloid Surface B* 2006;40:99-106.

34. Aurell CA, Wistrom AO. Critical aggregation concentrations of gram-negative bacterial lipopolysaccharides (LPS). *Biochem Biophys Res Commun* 1998;253:119-23.

35. Teehan GS, Guo D, Perianayagam MC, Balakrishnan VS, Pereira BJG, Jaber BL. Reprocessed (high-flux) Polyflux® dialyzers resist trans-membrane endotoxin passage and attenuate inflammatory markers. *Blood Purificat* 2004;22:329-37.

36. Weber C, Groetsch W, Schlotter S, Mitteregger R, Falkenhagen D. Novel online infusate-assisted dialysis system performs microbiologically safely. *Artif Organs* 2001;24:323-8.

37. Shao J, Wolff SH, Zydney AL. In vitro comparison of peracetic acid and bleach cleaning of polysulfone hemodialysis membranes. *Artif Organs* 2007;31:452-60.

38. Leckband D, Sheth S, Halperin A. Grafted poly(ethylene oxide) brushes as nonfouling surface coatings. *J Biomater Sci, Polym Ed* 1999;10:1125-47.

39. Park JY, Acar MH, Akthakul A, Kuhlman W, Mayes AM. Polysulfone-*graft*-poly(ethylene glycol) graft copolymers for surface modification of polysulfone membranes. *Biomaterials* 2006;27:856-65.

40. Hancock LF, Fagen SM, Ziolo MS. Hydrophilic, semipermeable membranes fabricated with poly(ethylene oxide)-polysulfone block copolymer. *Biomaterials* 2000;21:725-33.

41. Nakatani T, Tsuchida K, Sugimura K, Yoshimura R, Takemoto Y. Investigation of endotoxin adsorption with polyether polymer alloy dialysis membranes. *Int J Mol Med* 2003;11:195-7.

42. Hayama M, Yamamoto K-i, Kohori F, Sakai K. How polysulfone dialysis membranes containing polyvinylpyrrolidone achieve excellent biocompatibility? *J Membrane Sci* 2004;234:41-9.

43. Wolff SH, Zydney AL. Effect of bleach on the transport characteristics of polysulfone hemodialyzers. *J Membrane Sci* 2004;243:389-99.

44. Rouaix S, Causserand C, Aimar P. Experimental study of the effects of hypochlorite on polysulfone membrane properties. *J Membrane Sci* 2006;277:137-47.

45. Wienk IM, Meuleman EEB, Borneman Z, Boomgaard Tvd, Smolders CA. Chemical treatment of membranes of a polymer blend: Mechanism of the reaction of hypochlorite with poly(vinyl pyrrolidone). *J Polym Sci Pol Chem* 1995;33:49-54.

46. Yamamoto C, Kim S-T. Endotoxin rejection by ultrafiltration through high-flux hollow fiber filters. *J Biomed Mater Res A* 1996;32:467-71.

CHAPTER 5

POLY-L-LYSINE AS SCAVENGER OF BACTERIAL ENDOTOXIN: CHARACTERIZATION OF SOLUTIONS AND APPLICATION

ABSTRACT: The removal of bacterial endotoxin (lipopolysaccharide, LPS) from solutions is an important step in the purification of biological products and the prevention of pyrogenic reactions during hemodialysis treatment. This study focused on characterizing the interactions of LPS and poly-L-lysine (PLL) in solutions and using these interactions to bind LPS to PLL-modified polymer membranes. Interactions were described using surface tension measurement of solutions and particle size analysis by dynamic light scattering. Atomic force microscopy (AFM) was used to describe interactions on mica and modified glass. Polymer membranes modified with PLL were subjected to fluorescent-labeled LPS to characterize the adsorption capacities of these modified membranes. PLL caused both a decrease in surface tension of LPS solutions and an increase in solution particle size, with a critical PLL to LPS ratio of 1:1. AFM of hydrophobic and hydrophilic surfaces touched to the air-water interface of solutions containing LPS and PLL revealed large aggregates and strands that increased in size with increasing PLL concentration. Fluorescence microscopy revealed that aggregates of PLL and LPS prevented adsorption to PLL-modified membranes. Also, membranes modified with 1 μg/ml of uncross-linked PLL bound LPS in similar quantities as membranes modified with 100 μg/ml of cross-linked PLL.

INTRODUCTION

The removal of bacterial endotoxin (lipopolysaccharide, LPS) from solutions has become an important topic not only in the production of biological solutions, but in the prevention of LPS transfer during hemodialysis treatments (1-4). Novel chemistries and geometries are being sought to preferentially adsorb LPS to membranes while restricting adsorption of other solution components. Characterizing the interaction of LPS with chemical adsorbents is critical to understanding adsorption properties and optimizing removal methods.

Bacterial endotoxin is a surface-recognition constituent of gram-negative bacterial membranes consisting of three main parts: an outer-membrane-integrated lipid (lipid A), a core oligosaccharide, and a long heteropolysaccharide chain (O-antigen) (5). The O-antigen varies among different bacterial strains and is the recognition site for blood-borne antibodies. The lipid A portion is generally conserved among bacterial types and is responsible for causing pyrogenic reactions. LPS is an amphiphilic molecule that has been shown to preferentially adsorb to hydrophobic surfaces (6). However, the net-negative charge due to the phosphate groups on the lipid A portion also make it susceptible to binding with affinity sorbents (7).

Removal of LPS from solution is generally achieved using affinity sorbents and filtration. Plasma exchange and charcoal hemoperfusion, as well as immobilization to polymyxin B, ceramic membranes, and functionalized nanoparticles, have been investigated with varying degrees of success (8-12). Polycations, more specifically poly-L-lysine (PLL), have been used in conjunction with filtration membranes and chromatography columns to remove LPS from solutions (13-15). However, other

chemistries, such as diethylaminoethane, histamine, and histidine have also been shown to be effective LPS adsorbents (13). Cationic polyelectrolytes presumably bind to the negatively-charged phosphate groups on LPS.

LPS solutions exhibit certain characteristics that have been studied through numerous methods including dynamic light scattering, fluorescence microscopy, atomic force microscopy, fluorescence spectroscopy, and Langmuir isotherm measurements (16-20). The amphiphilic nature of LPS causes it to form micelles and larger aggregates in solution comprised of up to 49 molecules with sizes ranging from 14-300 nm in diameter (16, 21).

The present study aims to introduce surface tension measurement as a new method of characterizing LPS solutions. We also characterize the interaction of LPS and PLL solutions using surface tension measurement, dynamic light scattering, and describe macromolecular interactions based on atomic force microscopy. These interactions of LPS and PLL are used to adsorb LPS to membranes modified with PLL and show that membranes with many available amino groups bind large amounts of LPS from a circulating solution.

MATERIALS AND METHODS

Solutions

LPS from *Escherichia coli* 055:B5 (Sigma-Aldrich) and PLL (70-150 kDa MW, Sigma-Adrich) were dissolved in 10 mM PBS (Perbio) containing 0.14 M NaCl and 0.01 M KCl at pH 7.4. Solutions were mixed at various concentrations and used without

further purification for all tests except particle size analysis using DLS, where solutions were filtered using a 0.45 μm filter.

Surface tension measurement

Surface tension measurements of solutions containing LPS, PLL, and mixtures of the two substances were performed on a tensiometer, μtrough S (Kibron, Inc.). Solutions were dispensed in 1-inch diameter Teflon-coated wells and allowed to equilibrate for 20 minutes prior to measuring. Measurements (n = 9) were made at 25^{o}C and 24% relative humidity.

Particle size with dynamic light scattering

Particle sizes of LPS and PLL in solution were obtained using a Brookhaven BI-200SM goniometer and BI-9000AT digital correlator. Measurements (n = 3) were conducted at a fixed 90^{o} angle, at room temperature, and at a wavelength of 633 nm. The averaging time during the measurement of the correlation function was 2 minutes. Size distributions were determined from the experimental data using the NNLS algorithm in the BIC software (Brookhaven Instruments Corp.) and expressed as hydrodynamic diameter in nm.

Atomic force microscopy of solutions on mica and OTS-modified glass

Solutions of LPS, PLL, and mixtures of the two substances were prepared according to the method used to obtain surface tension measurements. Octadecyltrichlorosilane (OTS)-modified glass cover slips were prepared according to the method described previously (22). Clean mica or OTS-coated glass was gently

touched to the air-water interface and peeled from the surface as to avoid removing large amounts of the solution. Samples were dried prior to imaging with AFM.

Sample surface morphology was observed using a Bioscope AFM (Nanoscope IIIa, Digital Instruments, Inc.) in tapping mode with a silicon nitride cantilever (40 N/m, Tap300, Budget Sensors). Samples (n = 3) were imaged at 2 x 2 μm^2. Analysis of sample features was performed using Nanoscope III imaging software (version 5.30r3, Digital Instruments, Inc.). Fig E.2 contains representative images of profile cuts used to determine feature sizes.

Fluorescence studies

Polymer hollow fiber mini-modules (Fig. 5.1) were constructed by placing 30 Fresenius Optiflux® F200NR^e membranes (Fresenius Medical Care North America), polysulfone membranes sterilized via electron beam, in a polycarbonate tube (15 cm in length, 2.4 mm inside diameter) and potted using UV-curable resin (Dymax Corp.). Optiflux® fibers were chosen based on their effective pore size, selectively limiting filtration at approximately 60 kD.

Fibers were coated with PLL and challenged with LPS according to the setup in Fig. 5.2. PLL coating solutions were prepared by mixing PLL (70-150 kDa MW, Sigma-Aldrich) in endotoxin-free water (ThermoFisher Scientific, Inc.). Tubing was rinsed using DDI water for 10 minutes prior to and between all coatings. Modules were coated for 60 minutes at 44 ml/min. Several modules were then subject to 2.5% glutaraldehyde (GA, Fisher Scientific Co.) in PBS from the outside for 20 minutes to cross-link the PLL to the membranes. Finally all fibers were rinsed with several volumes of 1 M NaCl to

FIG. 5.1. Mini-module showing polycarbonate housing and T's, with UV curable epoxy for potting material. Approximately 30 fibers, 15 cm in length, provide the mini-module with about 15 cm^2 of surface area.

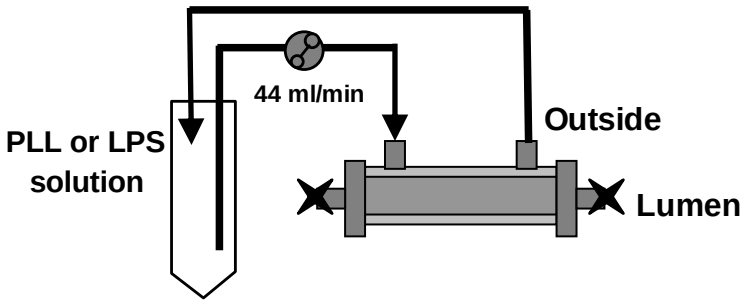

FIG. 5.2. Experimental setup for PLL coatings and LPS challenge tests. Fibers were first coated for 60 minutes with PLL, dried overnight in an oven, and then challenged with LPS for 60 minutes.

remove all unbound PLL and GA, evacuated of fluid, and placed in an oven overnight at 70^{o}C.

Fluorescent-labeled LPS conjugate (AlexaFluor® 594 conjugate, Invitrogen) was used to study the areas where LPS binding occurs throughout the membrane wall. Prior studies have shown that a fluorescent label attached to the LPS molecule does not affect the behavior of the LPS (23). The dialyzers were challenged similar to the PLL-coating procedure. Each module was subjected to a challenge of 100 ng/ml of labeled LPS

conjugate and varying concentrations of PLL, in endotoxin-free water, with the simulation run in a controlled dark environment.

After the simulations were complete, mini-modules were placed in a drying oven overnight to prepare for sectioning and imaging. The process of embedding, slicing, and imaging the samples used a previously described protocol modified for this study (4, 24). Fiber membranes were removed from their housings and sectioned to 10 μm using tissue freezing media (Triangle Biomedical Sciences), a low-profile microtome blade (SEC 35e, Richard-Allan Scientific) and a cryostat (Leica 1850). Sectioned fibers were imaged using fluorescence microscopy (Nikon TE2000-S, Nikon Corp.) with a Resorufin filter set (Chroma Technology). This filter set was used to minimize membrane auto-fluorescence and maximize fluorescence of the AlexaFluor® 594 conjugate. Images of the membrane samples were obtained with a 12 megapixel camera (Nikon DXM1200, Nikon Corp.) at a resolution of 1280 X 1024 using a 60-second image integration time and analyzed with ACT-1 software (Nikon Corp.). Fluorescence intensity analysis was performed using ImageJ software (National Institutes of Health).

RESULTS

Surface tension of solutions

Surface tensions of solutions containing LPS, PLL, and mixtures of the two substances were performed to determine molecular interactions at the air-water interface. Results for measurements of LPS solutions are presented in Fig. 5.3. Solutions containing up to 10 μg/ml LPS behaved similar to that of the PBS solution. From 10-1000 μg/ml LPS, surface tensions dropped logarithmically, thereafter reaching a lower

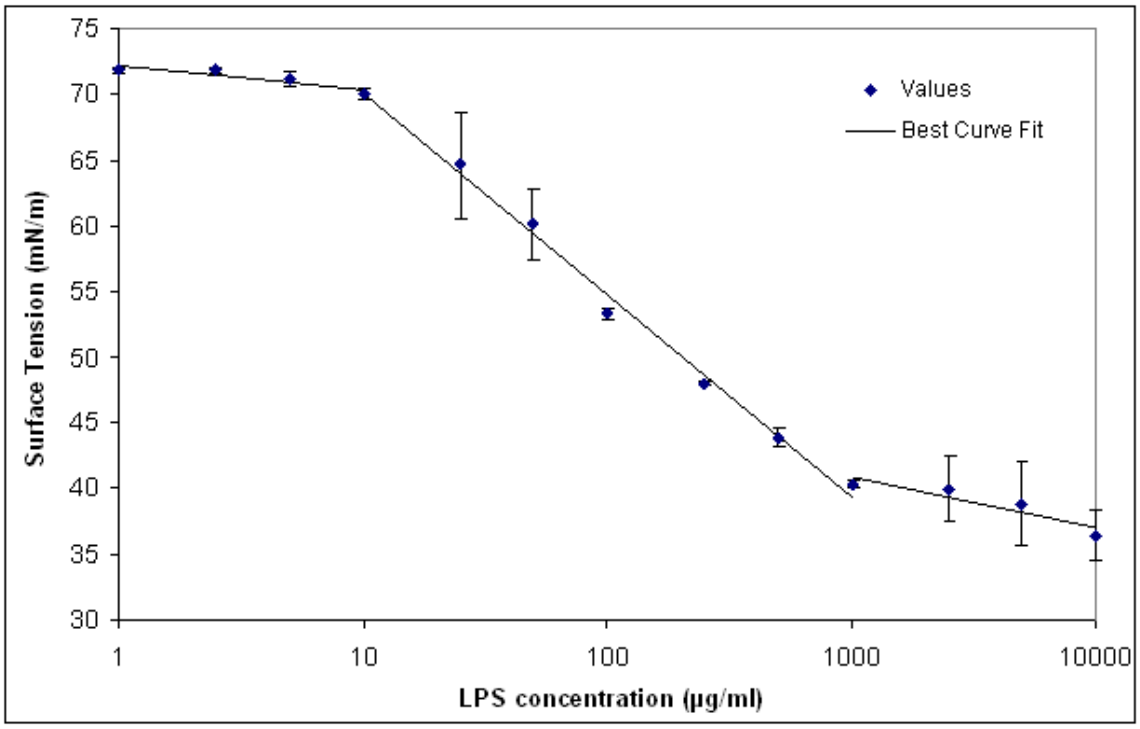

FIG. 5.3. Semi-log plot of LPS surface tension of LPS in PBS (mean ± s.d., n = 3), including best curve fits for upper (below 10 µg/ml LPS) and lower (above 1000 µg/ml LPS) plateaus and logarithmic drop (between 10 and 1000 µg/ml LPS).

plateau of approximately 38 mN/m. At the transition points at both lower and upper extremes, there tended to be a larger variation in surface tension.

Surface tensions of solutions containing LPS and PLL are displayed in Fig. 5.4. PLL was added to LPS to produce solutions containing 47.5 µg/ml of LPS and PLL concentrations of 0.05, 0.5, 5, 50, and 500 µg/ml. It was observed that PLL in PBS (concentrations in PBS ranging from 0.05 µg/ml to 500 µg/ml) did not alter surface tension from that of PBS (data not shown). PLL at low concentrations (≤ 5 µg/ml) did not alter surface tension from that of the LPS solution, while PLL at higher concentrations (from 50 µg/ml) caused a significant drop in surface tension of the LPS solution.

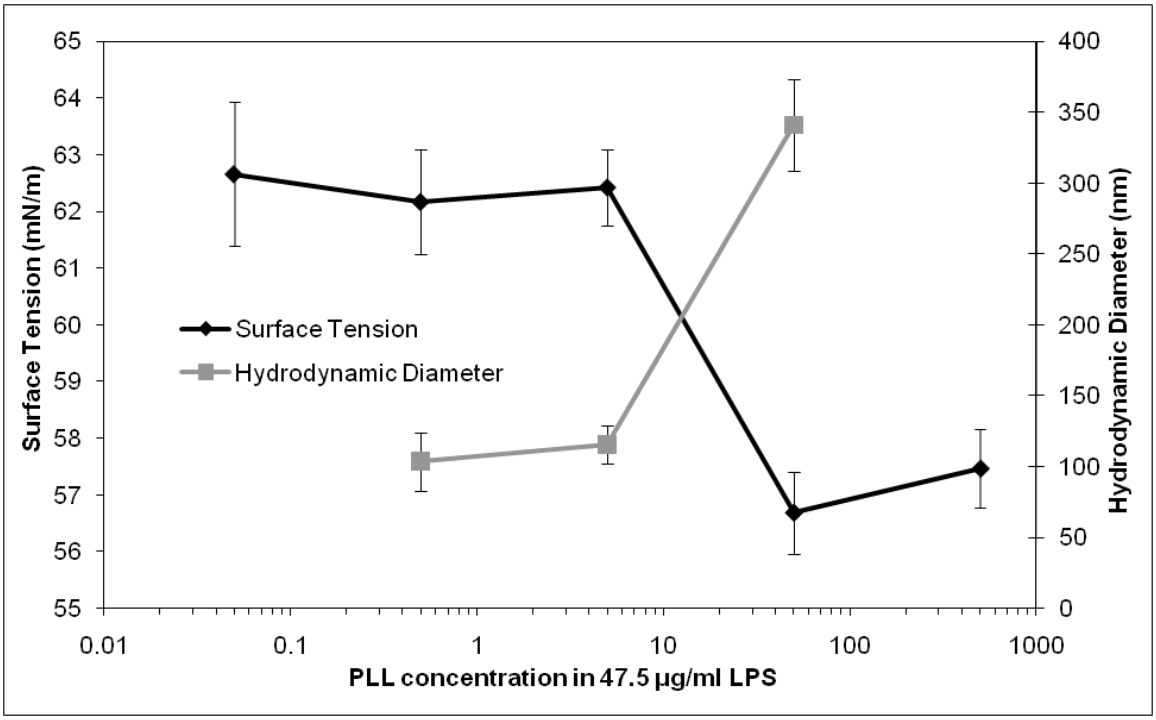

FIG. 5.4. Semi-log plot of surface tensions (mean ± s.d., n = 9) and hydrodynamic diameters (mean ± s.d., n = 3) of solutions containing PLL in 47.5 µg/ml LPS. Surface tension and particle size both showed a transition point between 5 and 50 µg/ml PLL in LPS. Solutions containing PLL only did not alter surface tension from that of PBS (data not shown). Also, solutions containing PLL only did not produce meaningful particle sizes up to 1 mg/ml (data not shown).

Particle sizes from DLS measurements

Particle sizes of solutions containing PLL, LPS, and mixtures of the two substances were measured to determine molecular interactions in solution. While PLL in PBS did not produce meaningful particle sizes up to 1 mg/ml, solutions containing 10, 50, and 100 µg/ml LPS yielded particles with hydrodynamic diameters averaging 65.4 ± 6.9 nm for all solutions. Solutions below these concentrations were too dilute to yield an accurate measurement.

Particle sizes for solutions containing both PLL and LPS are presented in Fig. 5.4. Mixtures containing 0.5 and 5 µg/ml PLL yielded similar particle sizes with

hydrodynamic diameters near 110 nm, while particles for mixtures containing 50 μg/ml PLL were approximately 3 times larger. This transition point corresponds with the transition point for surface tension measurements indicating changes in interaction both in solution and at the air-water interface at this PLL:LPS ratio.

AFM of LPS and PLL solutions on mica and OTS-modified glass

AFM was used to visualize interactions of LPS and PLL pulled from the air-water interface of solutions using mica and OTS-modified glass. Representative images from these tests are shown in Figs. 5.5 and 5.6. Samples from solutions containing 1 and 10 μg/ml LPS (Panels A and B, Fig. 5.5) exhibited salt clusters but no other surface features. Samples from solutions containing 50 and 100 μg/ml LPS (Panels C and D, Fig. 5.5) exhibited small "islands" approximately 0.5-1.3 nm in height. Higher concentrations of LPS led to larger height features and increased overall size of the "islands" on the mica surface. Tests were also performed by transferring films from the air-water interface of LPS solutions to OTS-modified glass, but no changes in surface morphology were observed for these samples (images not shown). Similarly, samples prepared using PLL solutions did not yield any features on the mica surface (images not shown).

Samples from solutions containing both PLL and LPS yielded large features on both mica (Fig. E.1, Appendix E)) and OTS-modified glass (Fig. 5.6). The OTS-modified glass itself exhibited small OTS "anchors," hydrophobic domains formed in preparing the surface of the glass, visible in Panel A of Fig. 5.6. These features were approximately 80 nm in diameter and 6 nm in height. The samples prepared using 0.5 μg/ml PLL and 47.5 μg/ml LPS showed no features beyond that seen in native OTS-

modified glass. The samples prepared using 5 and 50 μg/ml PLL, and 47.5 μg/ml LPS, exhibited large strands, branching between the OTS anchors. These strands increased the height of the OTS anchors to 10.1 ± 3.1 and 16.3 ± 2.9 nm for the 5 and 50 μg/ml PLL samples, respectively. Also, the diameter and height of the strands increased with increasing PLL concentration as follows (n = 8): 25.4 ± 6.9 nm width, 1.5 ± 0.3 nm height for 5 μg/ml PLL; 29.3 ± 5.5 nm width, 3.7 ± 1.2 nm height for 50 μg/ml PLL. The orientation of the connections in Panels B and C in Fig. 5.6 is due to the method of interface transfer and drying.

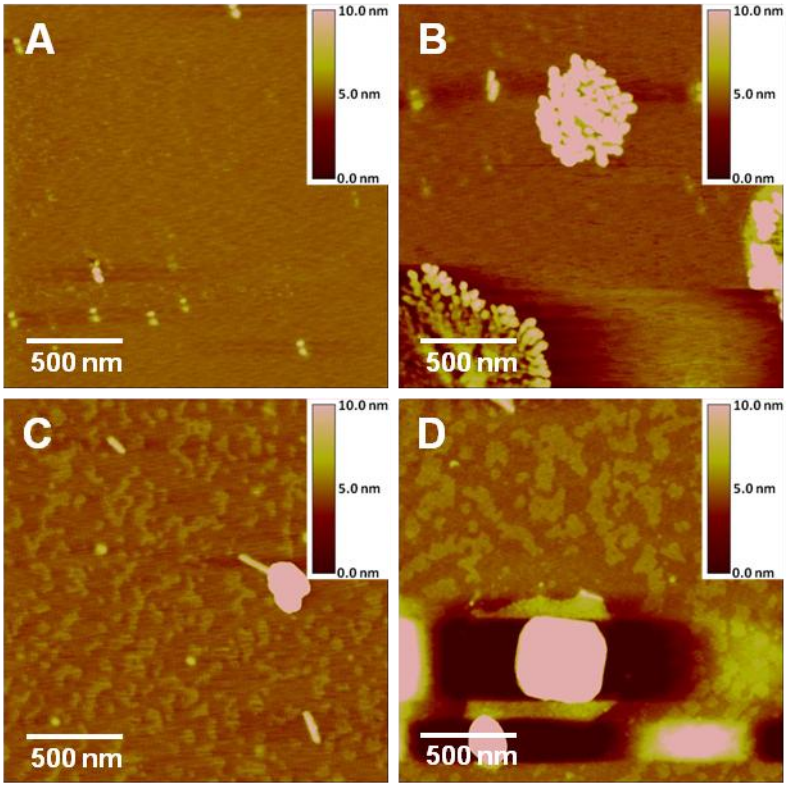

FIG. 5.5. AFM images of LPS on mica from solutions containing (A) 1 μg/ml, (B) 10 μg/ml, (C) 50 μg/ml, and (D) 100 μg/ml LPS in PBS. Solutions containing more than 10 μg/ml LPS led to images containing small "islands," presumably LPS deposits on the mica surface.

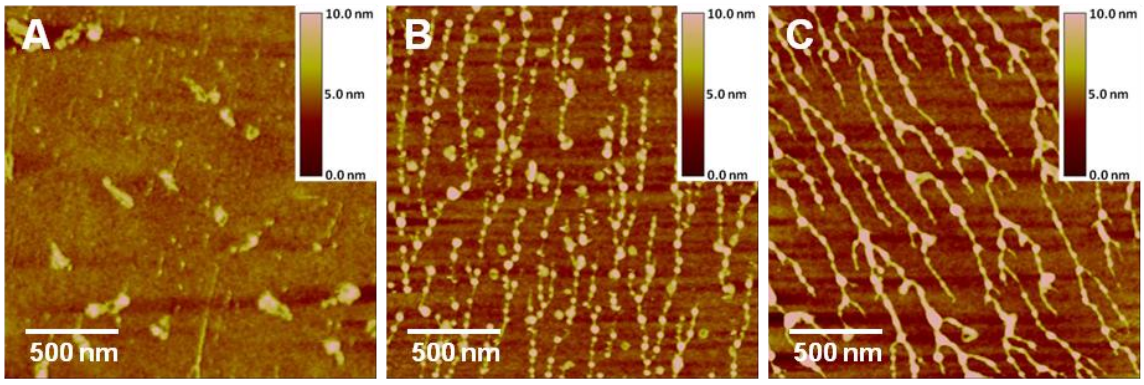

FIG. 5.6. AFM images of LPS and PLL on OTS-modified glass from solutions containing 47.5 μg/ml LPS and (A) 0.5 μg/ml PLL, (B) 5 μg/ml PLL, and (C) 50 μg/ml PLL. OTS "anchors" allowed for LPS and PLL to form organized strands on surface. Increasing PLL concentration led to larger surface features.

Fluorescence studies

Fluorescence images of several challenged membranes are shown in Fig. 5.7. Membranes not subject to PLL or LPS were sectioned and imaged to view the background fluorescence due to the polymer membranes (Panel A, Fig. 5.7). Membranes coated with PLL and challenged with fluorescent-labeled LPS are presented in Panels B-D of Fig. 5.7. Membranes coated with PLL, cross-linked with GA, and challenged with fluorescent-labeled LPS are presented in Panels E-G of Fig. 5.7. Presented images are representative of all membranes imaged for each sample. Fluorescence intensities for all membranes challenged with LPS are presented in Fig. 5.8, with the background fluorescence subtracted from overall intensity values. It must be noted that fluorescence is due solely to the LPS-conjugate and the polymer membranes; PLL did not contribute to fluorescence using the filter set.

As can be seen in Fig. 5.8, membranes not coated with PLL bound LPS to some degree. The membrane coated using 1 μg/ml PLL (Panel C, Fig. 5.7) bound more LPS

than all other membranes not treated with GA, with fluorescence increasing from 2-5 times that of other membranes. Above this concentration of PLL, fluorescence intensity dropped to levels similar to that of uncoated membranes. For membranes treated with GA, fluorescence intensity increased with increasing PLL concentration, with that of the membrane coated with 1000 μg/ml PLL increasing to 18 times the intensity of an uncoated membrane.

The cross-sectional images in Fig. 5.7 also reveal binding of LPS throughout the membrane, with LPS binding more preferentially to the lumen or outside surfaces in most samples. This observation plays a critical role in determining binding characteristics of LPS and PLL as will be discussed.

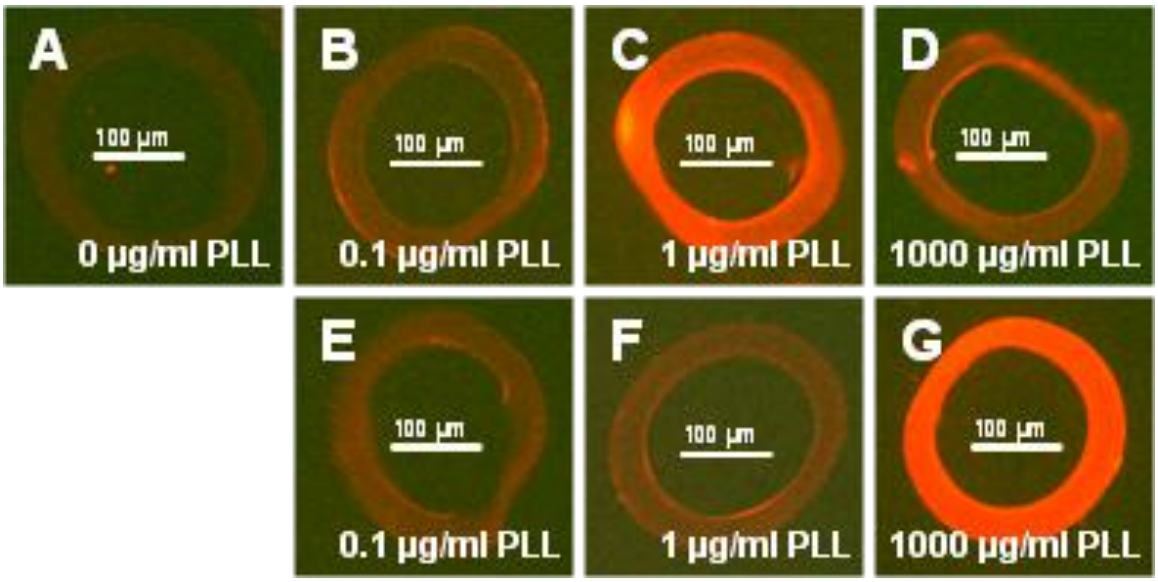

FIG. 5.7. Fluorescence images of polymer hollow fibers modified with PLL and challenged with fluorescent-labeled LPS. (A) Native-unchallenged hollow fiber used to show background fluorescence of polymer membrane. Polymer hollow fibers coated with PLL using (B) 0.1 μg/ml, (C) 1 μg/ml, and (D) 1000 μg/ml PLL. Polymer hollow fibers coated with PLL and cross-linked using GA at PLL concentrations of (E) 0.1 μg/ml, (F) 1 μg/ml, and (G) 1000 μg/ml. Fig. D.1. (Appendix D) contains images of all samples tested.

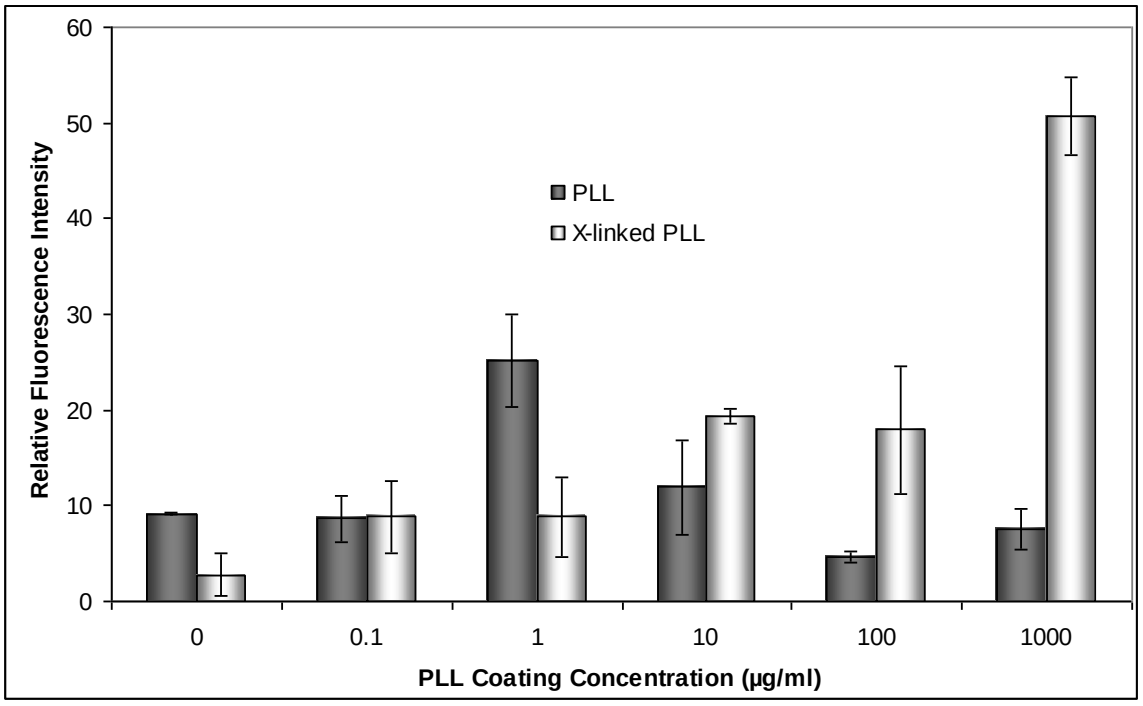

FIG. 5.8. Relative fluorescence intensities of cross-sectional images of hollow fiber membranes (mean ± s.d., n ≥ 3). Background fluorescence due to the membrane has been subtracted from the presented values. Statistical analysis reveals significant difference between the 1 µg/ml PLL only sample and all other PLL samples. Among the cross-linked samples, 10, 100, and 1000 µg/ml PLL were all significantly brighter than lower PLL concentrations.

Several membranes coated with 1 µg/ml were also subjected to a challenge solution containing 100 ng/ml of fluorescent-labeled LPS and varying concentrations of PLL. Fluorescence images of these membranes are shown in Fig. 5.9. Relative fluorescence intensities of each membrane, standardized against membranes not challenged with LPS, were as follows: 0 ng/ml PLL, 25.2 ± 0.6; 10 ng/ml PLL, 27.1 ± 3.7; 100 ng/ml PLL, 6.7 ± 0.2; 1000 ng/ml PLL, 8.6 ± 1.2.

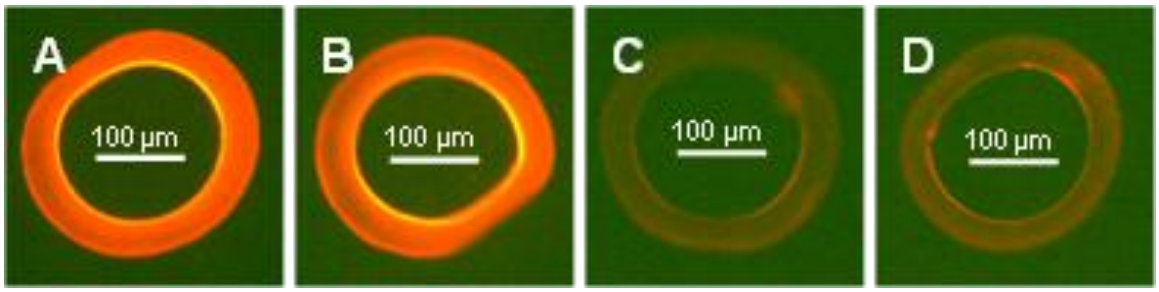

FIG. 5.9. Fluorescence images of polymer hollow fibers modified using a solution containing 1 µg/ml PLL and challenged with solutions containing 100 ng/ml of fluorescent-labeled LPS and (A) 0 ng/ml, (B) 10 ng/ml, (C) 100 ng/ml, and (D) 1000 ng/ml PLL.

DISCUSSION

While numerous methods to remove LPS from solutions exist, few methods have characterized the interactions of LPS with adsorbents. Insights into these interactions can help improve adsorption methods by directing researchers to using materials with appropriate characteristics. This study focused on characterizing the interactions of LPS and PLL and utilizing these interactions to remove LPS from solutions through the use of PLL-modified polymer membranes.

In order to understand the interactions of PLL and LPS in solution, the dynamics of LPS aggregation in solution and on surfaces were quantified. Surface tension measurement and hydrodynamic diameter quantization were performed on LPS solutions. It was found that solutions of LPS have a surface tension similar to that of water (72 mN/m) up to about 10 µg/ml, whereupon surface tension dropped logarithmically up to a concentration of about 1 mg/ml (38 mN/m). It has been proposed that aggregation of LPS molecules is a continuous process starting at 10 µg/ml and proceeding up to 300 µg/ml, with critical aggregation concentrations to be between 1 and 38 µg/ml (16, 18-19,

21). Surface tensions measured here begin dropping at or near the critical aggregation concentration, forcing aggregates to the air-water interface, and continue until the interface becomes saturated.

Particle sizes of LPS solutions, as measured using dynamic light scattering, have been found to vary in size from 26 nm to 190 nm, with little effect due to solution concentration (16, 19). LPS solutions measured in this study were found to be approximately 65 nm with no significant difference over a ten-fold increase in LPS concentration. Particles in LPS solutions above the critical aggregation concentration, then, remain the same size regardless of increased concentration.

Previous studies have shown that LPS preferably binds to hydrophobic surfaces (6, 25). Findings in this study, however, showed that LPS did not bind to hydrophobic OTS-modified glass but did bind to hydrophilic mica. LPS particles measured by dropping LPS solutions on mica at 40 μg/ml have been found to be 19.3 nm in diameter and 1.2 nm in height (24). LPS aggregates on mica observed here using AFM were found to mirror trends seen in surface tension tests; features on mica appeared, starting at 50 μg/ml, with height and diameter of features increasing with increasing concentration. Additionally, the sizes of the "islands" observed in this study were much larger than those previously observed. Higher LPS concentrations at the air-water interface, as observed with surface tension measurements, may have allowed more LPS transfer to the mica surface, leading to large surface features.

Aggregates of PLL and LPS were observed using surface tension, particle size, and AFM. Measurements showed that increasing concentration ratios of PLL and LPS to 1:1 caused a significant decrease in surface tension and an increase in hydrodynamic

diameter. This finding is contrary to previous reports that cationic antibiotics caused an increase in surface tension of LPS monolayers, presumably taking LPS from the surface and pulling it back into solution (26). However, different scavengers, including polyelectrolytes, proteins, and surfactants, may cause varying effects on LPS solutions (7, 27-30). The decrease in surface tension upon increasing concentration of PLL observed here may have forced more LPS to the air-water interface, causing the solution to appear to contain more LPS. DLS measurements showed that PLL caused LPS aggregation, possibly forming clusters of aggregates or increasing aggregate size.

AFM images revealed strands of LPS and PLL on both mica and OTS-modified glass. The OTS-modified glass contained clusters of polymerized OTS on the film surface formed during the coating procedure, similar to those observed previously (31). The hydrophobic clusters formed by OTS were used in hopes of providing "anchors" on which the lipid tails of LPS would preferentially adsorb. The observed strands of LPS and PLL are formed by electrostatic interactions, while hydrophobic interactions allowed adsorption to the OTS. The lack of features in images of PLL or LPS on OTS-modified glass further verifies that these electrostatic interactions give stability to the aggregates of LPS and PLL.

Fluorescent-labeled LPS was used to visualize the distribution of LPS in polymer hollow fiber membranes modified with different amounts of PLL. Similar membranes have been shown to be slightly hydrophilic, with water contact angles of approximately 48^{o} (3). It is interesting to note that images of samples modified with PLL using no cross-linking agent showed the most fluorescence in the sample modified using 1 μg/ml PLL. Images of membranes modified with 1 μg/ml PLL using no cross-linking agent and

subject to LPS solutions containing varying concentrations revealed that at a PLL to LPS ratio of 1:1, adsorption of LPS dropped dramatically. The aggregates of LPS and PLL formed in solution prevented LPS adsorption to the membrane in these samples. Similarly, for those membranes modified with PLL and subjected to LPS challenges, LPS formed aggregates with the PLL molecules, releasing the PLL from the membrane.

The observations seen in DLS and surface tension measurements, as well as images of LPS and PLL on OTS-modified glass and PLL-modified membranes show that the 1:1 ratio of PLL to LPS is of great significance. While the PLL molecules contain between 550 and 1170 phosphate groups, the LPS molecules contain only approximately 7 phosphate groups. Aggregates may be formed similar to a micellar structure, with lipid A tails toward the center of the molecule, and saccharide chains and PLL molecules organized on the outside. The binding of LPS to PLL may sterically hinder further binding of PLL to the LPS molecules. It must also be noted that the concentrations used in the modification and challenging of polymer membranes were much lower than those used in surface tension and DLS measurements, indicating that the 1:1 ratio holds significant value over a wide concentration range.

For cross-linked samples, increased concentrations of PLL led to increased LPS adsorption. PLL was bound more tightly to the membrane due to the cross-linking, however, binding sites were likely taken up by the cross-linking procedure as well. PLL may have bound to the membrane only, or cross-linking may have caused larger aggregates of PLL to form in membrane pores, preventing the release of PLL into the solution upon LPS adsorption.

Analysis of fluorescence images revealed that membranes modified using 1 μg/ml PLL, with no cross-linking agent, adsorbed as much LPS as membranes modified using 10 and 100 μg/ml PLL with GA. PLL binding sites were likely compromised during the cross-linking procedure as discussed, effectively lowering the number of available amine groups for LPS adsorption. This observation suggests that lower concentrations of PLL may be used to bind similar amounts of LPS, as long as binding sites on PLL are not compromised.

Fluorescence images also reveal binding of LPS in larger quantities to the lumen and outside of membranes. Because the setup shown in Fig. 5.2 did not include a counter-current flow, diffusion of PLL and LPS throughout the membrane cross-section would have been expected to be limited to the outside sections of the membrane. Larger particle sizes of LPS formed in solution would have been limited in the depth of penetration into the membrane. However, it is seen that LPS diffused readily to the inner portion of the membrane where it bound in significant quantities in several membranes. As seen in previous SEM images, the membrane has a tight molecular weight cutoff near the lumen, where large aggregates of LPS and PLL molecules may have become embedded in small pores (3). Also, larger aggregates of PLL and LPS formed in solution may not have been able to penetrate the outermost layers of the membrane causing higher fluorescence intensity at this boundary.

CONCLUSION

The present study focused on characterizing the aggregation behavior of LPS and PLL in solution and using these interactions to bind LPS to polymer membranes modified

with PLL. We have demonstrated that PLL binds LPS, forming aggregates both in solution and on membrane surfaces. Aggregates formed in solution, causing a decrease in solution surface tension and an increase in particle size as measured using DLS, were found to begin at a PLL to LPS ratio of approximately 1:1. Features observed using AFM increased in size with increasing PLL and LPS concentrations, forming stands of aggregates up to 29.3 nm in width and 3.7 nm in height. The interactions of PLL and LPS allowed for LPS adsorption on polymer membranes to varying degrees. Cross-linked PLL bound LPS to greater degrees with increasing concentrations. However, membranes not subjected to cross-linking bound the most LPS using a lower concentration of 1 μg/ml PLL. Higher concentrations of PLL on the membrane presumably bound LPS, forming large aggregates, then dissociated from the membrane. It was also observed that membranes modified using uncross-linked PLL at 1 μg/ml bound similar quantities of LPS as membranes coated with up to 100 μg/ml of cross-linked PLL. The widely used method of cross-linking PLL to membrane surfaces likely compromises large numbers of LPS binding sites, rendering the membrane less adsorbent toward LPS.

REFERENCES

1. Petsch D, Anspach FB. Endotoxin removal from protein solutions. *J Biotechnol* 2000;76:97-119.

2. Magalhães PO, Lopes AM, Mazzola PG, Rangel-Yagui C, Penna TCV, Jr. AP. Methods of endotoxin removal from biological preparations: A review. *J Pharm Pharm Sci* 2007;10:388-404.

3. Henrie M, Ford C, Andersen M, Stroup E, Diaz-Buxo J, Madsen B, et al. In vitro assessment of dialysis membrane as an endotoxin transfer barrier: Geometry, morphology, and permeability. *Artif Organs* 2008;32:701-10.

4. Hayama M, Miyasaka T, Mochizuki S, Asahara H, Yamamoto K-i, Kohori F, et al. Optimum dialysis membrane for endotoxin blocking. *J Membrane Sci* 2003;219:15-25.

5. Gorbet MB, Sefton MV. Endotoxin: The uninvited guest. *Biomaterials* 2005;26:6811-7.

6. Takemoto Y, Nakatani T, Sugimura K, Yoshimura R, Tsuchida K. Endotoxin adsorption of various dialysis membranes: In vitro study. *Artif Organs* 2003;27:1134-7.

7. Anspach FB. Endotoxin removal by affinity sorbents. *J Biochem Bioph Meth* 2001;49:665-81.

8. Linnenweber S, Lonnemann G. Pyrogen retention by the Asahi APS-650 polysulfone dialyzer during in vitro dialysis with whole human donor blood. *ASAIO J* 2000;46:444-7.

9. Bender H, Pflänzel A, Saunders N, Czermak P, Catapano G, Vienken J. Membranes for endotoxin removal from dialysate: Considerations on feasibility of commercial ceramic membranes. *Artif Organs* 2000;24:826-9.

10. Darkow R, Groth T, Albrecht W, Lützow K, Paul D. Functionalized nanoparticles for endotoxin binding in aqueous solutions. *Biomaterials* 1999;20:1277-83.

11. Tetta C, Bellomo R, Inguaaggiato R, Wratten ML, Ronco C. Endotoxin and cytokine removal in sepsis. *Therap Apher Dial* 2002;6:109-15.

12. Sato T, Shoji H, Koga N. Endotoxin adsorption by polymyxin B immobilized fiber column in patients with systemic inflammatory response syndrome. *Therap Apher Dial* 2003;7:252-8.

13. Anspach FB, Hilbeck O. Removal of endotoxins by affinity sorbents. *J Chromatogr A* 1995;711:81-92.

14. Petsch D, Beeskow TC, Anspach FB, Deckwer W-D. Membrane adsorbers for selective removal of bacterial endotoxin. *J Chromatogr B* 1997;693:79-91.

15. Hirayama C, Sakata M, Nakamura M, Ihara H, Kunitake M, Todokoro M. Preparation of poly(ε-lysine) adsorbents and application to selective removal of lipopolysaccharides. *J Chromatogr B* 1999;721:187-95.

16. Bergstrand A, Svanberg C, Langton M, Nyden M. Aggregation behavior and size of lipopolysaccharide from *Escherichia coli* O55:B5. *Colloid Surface B* 2006;40:99-106.

17. Roes S, Seydel U, Gutsmann T. Probing the properties of lipopolysaccharide monolayers and their interaction with the antimicrobial peptide polymyxin B by atomic force microscopy. *Langmuir* 2005;21:6970-8.

18. Aurell CA, Wistrom AO. Critical aggregation concentrations of gram-negative bacterial lipopolysaccharides (LPS). *Biochem Biophys Res Commun* 1998;253:119-23.

19. Santos NC, Silva AC, Castanho MARB, Martins-Silva J, Saldanha C. Evaluation of lipopolysaccharie aggregation by light scattering spectroscopy. *ChemBioChem* 2003;4:96-100.

20. Abraham T, Schooling SR, Beveridge TJ, Katsaras J. Monolayer film behavior of lipopolysaccharide from *Pseudomonas aeruginosa* at the air-water interface. *Biomacromolecules* 2008;9:2799-804.

21. Yu L, Tan M, Ho B, Ding JL, Wohland T. Determination of critical micelle concentrations and aggregation numbers by fluorescence correlation spectroscopy: Aggregation of a lipopolysaccharide. *Anal Chim Acta* 2006;556:216-25.

22. Dhruv H, Pepalla R, Taveras M, Britt DW. Protein insertion and patterning of PEG bearing langmuir monolayers. *Biotechnol Progr* 2006;22:150-5.

23. Levels JHM, Abraham PR, Ende Avd, Deventer SJHv. Distribution and kinetics of lipoprotein-bound endotoxin. *Infect Immun* 2001;69:2821-8.

24. Hayama M, Miyasaka T, Mochizuki S, Asahara H, Tsujioka K, Kohori F, et al. Visualization of distribution of endotoxin trapped in an endotoxin-blocking filtration membrane. *J Membrane Sci* 2002;210:45-53.

25. Yamamoto C, Kim S-T. Endotoxin rejection by ultrafiltration through high-flux hollow fiber filters. *J Biomed Mater Res A* 1996;32:467-71.

26. Zhang L, Dhillon P, Yan H, Farmer S, Hancock REW. Interactions of bacterial cationic peptide antibiotics with outer and cytoplasmic membranes of *Pseudomonas aeruginosa*. *Antimicrob Agents Chemother* 2000;44:3317-21.

27. Bosshart H, Heinzelmann M. Targeting bacterial endotoxin: Two sides of a coin. *Ann NY Acad Sci* 2007;1096:1-17.

28. Petsch D, Rantze E, Anspach FB. Selective adsorption of endotoxin inside a polycationic network of flat-sheet microfiltration membranes. *J Mol Recognit* 1998;11:222-30.

29. II AJD, Brogden KA, Engen R. *Enterobacter agglomerans* lipopolysaccharide-induced changes in pulmonary surfactant as a factor in the pathogenesis of byssinosis. *J Clin Microbiol* 1988;26:778-80.

30. Schram V, Hall SB. Thermodynamic effects of the hydrophobic surfactant proteins on the early adsorption of pulmonary surfactant. *Biophys J* 2001;81:1536-46.

31. Kirkpatrick R, Muhlstein CL. Performance and durability of octadecyltrichlorosilane coated borosilicate glass. *J Non-Cryst Solids* 2007;353:2624-37.

CHAPTER 6

CONCLUSIONS AND FUTURE WORK

KEY FINDINGS

In this work, the modification of polymer hollow fiber membranes was discussed as it related to physicochemical changes incurred during sterilization or reprocessing techniques and the ability of the membranes to remove bacterial endotoxin from solutions. The findings demonstrate dramatic and potentially unintended changes in the physicochemical properties and, subsequently, the filtration abilities of these membranes.

The first investigation focused on physicochemical changes associated with common gas, irradiation, and chemical sterilization processes. It was observed that e-beam sterilization causes a decrease in surface water contact angle, while altering the physical structure of nodule aggregates located at the lumen of the fibers, compared to the ETO sterilized membrane. Also, bleach sterilization did not alter water contact angle from that of the ETO sterilized membrane, but did cause a morphological change similar to the e-beam sterilized fibers. Additionally a new method of characterizing hollow fiber membranes, that of water evaporation rate, was presented as a novel means of deducing sorption characteristics. The results demonstrate that common sterilization methods may inadvertently change membrane properties, which may be detrimental in filtration applications, as well as provide simple post-fabrication methods to tune properties toward specific applications such as cell culture and tissue engineering.

The second and third investigations focused on the removal of bacterial endotoxin from solutions through the use of chemical modifications to the membrane. The second

study focused on polymer chemistry, more specifically PVP content or the addition of PEG, as it related to prevention of back-filtration of LPS during hemodialysis treatment. It was found that hydrophobicity of the membrane plays an important role in membrane adsorption capacity, but that slight changes in PVP content alter the ability of the membrane to prevent back-filtration of LPS. LPS adsorbed strongly to all PS-PVP membranes near the lumen of the fiber, while PS-PEG membranes adsorbed LPS primarily on the outer surface. This observation could play a vital role in preventing LPS transfer to the blood, as well as prevent any possible pyrogenic reaction during hemodialysis treatment.

The third study focused on characterizing interactions of LPS and PLL, while using these interactions to remove LPS from solutions using PS-PVP membranes modified with PLL. It was found that LPS forms large aggregates in solution, independent of solution concentration, that lower the surface tension of solutions. The addition of PLL to a solution caused aggregates to increase in size, with a critical PLL to LPS ratio of 1:1. This binding ratio was found to exist regardless of solution concentration. Polymer hollow fiber membrane modified using PLL were found to effectively remove LPS from solutions. The widely used method of cross-linking PLL to membranes, however, was shown to reduce the ability of PLL to adsorb LPS, as lower concentrations of uncross-linked PLL were found to adsorb similar amounts of LPS.

FUTURE DIRECTIONS

Chemical modifications to filtration membranes in other geometries

It was demonstrated in this dissertation that using PLL-modified polymer hollow fiber membranes was an effective method of increasing the adsorption capacities of these membranes. Numerous other geometries exist and have been tested for LPS removal in the literature including Sepharose beads, ceramic membranes, chloromethyloxirane polymer beads, polyether polymer alloy membranes, and flat sheet nylon microfiltration membranes (1-5).

While these methods have been shown to be effective at removing large percentages of LPS from solutions, much research is being directed at using tangential flow microfiltration systems (6-7). Tangential flow microfiltration systems work by forcing a liquid tangentially across a filtration membrane, whereupon small molecular weight species are forced through the pores of the membrane. The rapid flow of solution across the membrane prevents excess buildup of larger particles, lowering membrane fouling. While the buildup of proteins on a membrane may not be of concern while filtering water used in dialysate, it is paramount in removing LPS from biologically prepared solutions. Modification of tangential flow filtration membranes using PLL may improve the adsorption capacities of these membranes.

Selective removal of LPS from protein solutions

The removal of bacterial endotoxin from biologically prepared solutions, such as those produced using bioprocessing, has been discussed. It was found in this dissertation that membranes modified with PLL were effective at adsorbing LPS in buffered

solutions, however, the selective removal of LPS from solutions containing proteins was not tested. Common proteins tested for clearance with filtration membranes and chromatographic columns include bovine serum albumin, lysozyme, insulin, myoglobin, γ-Globulin, cytochrome c, and immunoglobulin G (1, 3, 8). While a membrane may be very effective at removing LPS through either electrostatic or hydrophobic interactions, these same interactions may cause proteins or cells to bind to the membrane surface. The removal of certain proteins from solution may need to be accompanied by a solution pH change, as may be the case in avoiding the adsorption acidic proteins, such as albumin.

Adsorption of LPS to outer surface of hollow fiber membranes

Perhaps the most intriguing membrane studied in Chapter 4 was the PS-PEG copolymer membrane that exhibited high surface water contact angle, a unique three-layer structure, and adsorbed LPS primarily at the outer wall of the membrane. It is interesting to note that the high water contact angle differs from similar membranes in the literature, where the addition of PS-PEG caused a decrease in surface water contact angle (9). The addition of PS-PEG is used in that study to decrease water contact angle and increase water flux through the membrane. Also, possible restructuring of a polymer network in polydimethylsiloxane-PEG membranes under prolonged exposure to water, causing the PEG chains to swell near the surface, has been investigated (10). While it was theorized in this dissertation that PEG chains were sequestered in the matrix of the membrane, restructuring of the polymer matrix in aqueous conditions can also be investigated.

Limiting LPS adsorption to the outer surface of the PS-PEG hollow fiber in Chapter 4 may be a vital finding for future studies. It has been reported that LPS does not need to be in direct contact with blood to elicit a pyrogenic response (11). Therefore, it would be of interest to the hemodialysis community to attempt to limit LPS adsorption to the outside of the polymer membrane. While PS-PEG was shown to be effective at limiting adsorption of LPS as seen in Fig. 4.11, it did not limit back-filtration of LPS into the blood compartment.

In Chapter 5 it was shown that small quantities of PLL on hollow fiber membranes were effective at adsorbing large quantities of LPS, but adsorption occurred throughout the fiber matrix with large quantities being found near the fiber lumen. The method of preparing hollow fiber membranes is a well-defined process, dependent on the thermodynamics of phase separation techniques (12-13). However, methods to prepare membranes containing small amounts of PLL on the outer surface of the membrane may prove beneficial in removing large quantities of LPS from solution, while encouraging adsorption of LPS far from the lumen of the membrane (Fig 6.1).

Addition of PLL to the outside of the polymer membrane may be achieved during the final testing stage of a hemodialyzer before packaging. Each dialyzer is tested for leaks by pumping water through the dialysate compartment, while air is pumped through the blood compartment. PLL at a low concentration could be mixed with the water to coat the membranes. The amount of PLL deposited on the surface of each dialyzer would need to be monitored to not exceed 0.67 $\mu g/cm^2$ (maximum surface concentration of PLL in the membranes modified using 1 µg/ml PLL in Chapter 5). Because of the porous structure of the membranes, deposition of PLL (70-150 kDa) throughout the membrane

may be considered uniform, except near the lumen where pores become much smaller and PLL would be unable to pass.

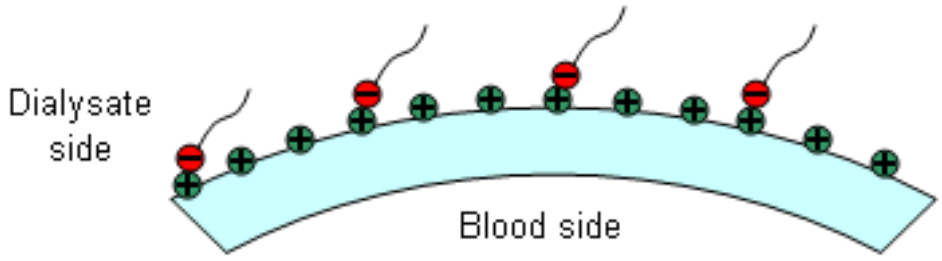

FIG. 6.1. Schematic of cross section of hollow fiber membrane modified using positively-charged PLL as a negatively-charged LPS adsorbent.

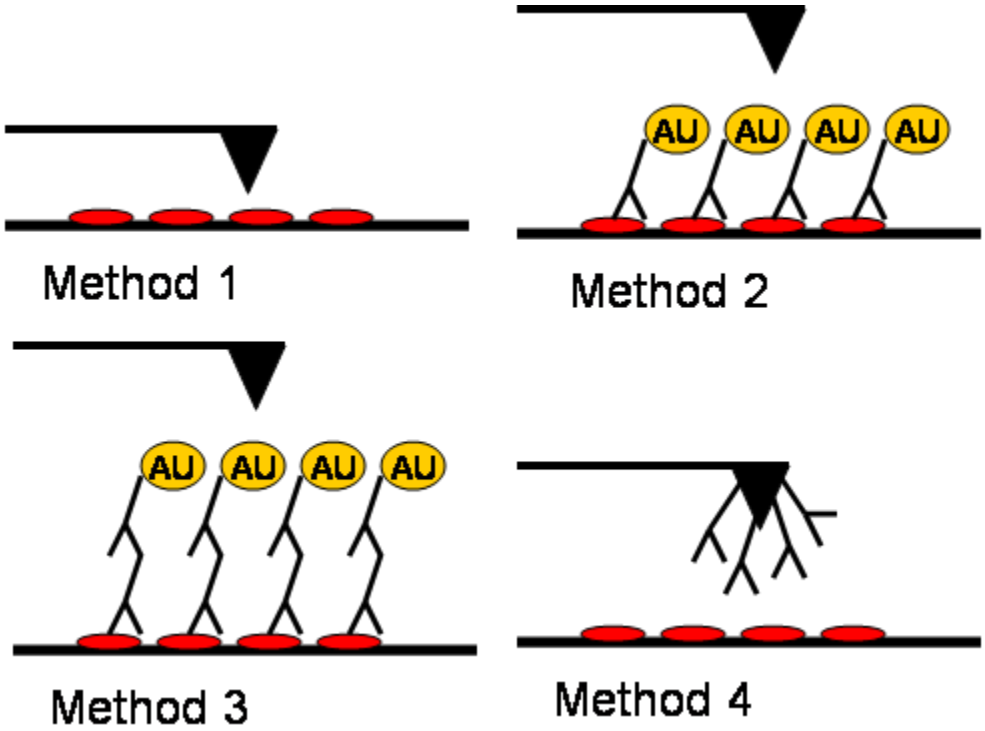

FIG. 6.2. Schematic of methods for imaging LPS with AFM. Method 1 involves tapping mode AFM to view LPS aggregates. Method 2 employs a gold labeled anti-LPS antibody. Method 3 employs an anti-LPS antibody and a labeled anti-antibody antibody. Method 4 involves coating the AFM tip with anti-LPS antibody for use with tapping mode AFM.

Localization of LPS on HFM surfaces

Mapping LPS adsorption to membranes in this dissertation was achieved using cryosectioning of HFMs and imaging with fluorescence microscopy. In this method, HFMs are embedded in a freezing medium and sectioned using a sharp, Teflon-coated blade. There has been concern in the literature that this method of sectioning may cause "smearing" of LPS across the membrane surface (14). Due to the size scale used to image membranes in this dissertation, "smearing" of LPS may be considered to be negligible. However, "smearing" is likely of concern when locating LPS on the nano-scale. To image on this scale, membranes would likely need to be fractured in liquid nitrogen and embedded such that adsorbed LPS is not disturbed.

Localizing LPS on HFMs on the nano-scale may require using new methods beyond that of fluorescence microscopy. TOF-SIMS and AFM have both been utilized to image cross-sections of polymer HFMs, however images produced were unclear (14-16). We found that imaging the cross-section of polymer hollow fiber membranes proved difficult due to the geometry of hollow fiber matrix. However, vague images of HFM cross-sections were produced.

To facilitate the visualization of LPS adsorbed to HFM cross-sections, the use of labeled antibodies may be employed. The use of gold-labeled antibodies may facilitate LPS localization. Gold-labeled antibodies adsorbed directly to the LPS (Method 2, Fig. 6.2), or a method akin to sandwich ELISA (Method 3, Fig. 6.2), would provide a gold signal which may be seen using either TEM or the phase signal of AFM. Anti-LPS antibody may also be adsorbed to an AFM tip itself (17), causing stronger attraction of the AFM tip to areas where LPS is adsorbed (Method 4, Fig. 6.2).

REFERENCES

1. Anspach FB, Hilbeck O. Removal of endotoxins by affinity sorbents. *J Chromatogr A* 1995;711:81-92.

2. Bender H, Pflänzel A, Saunders N, Czermak P, Catapano G, Vienken J. Membranes for endotoxin removal from dialysate: Considerations on feasibility of commercial ceramic membranes. *Artif Organs* 2000;24:826-9.

3. Hirayama C, Sakata M, Nakamura M, Ihara H, Kunitake M, Todokoro M. Preparation of poly(ε-lysine) adsorbents and application to selective removal of lipopolysaccharides. *J Chromatogr B* 1999;721:187-95.

4. Nakatani T, Tsuchida K, Sugimura K, Yoshimura R, Takemoto Y. Investigation of endotoxin adsorption with polyether polymer alloy dialysis membranes. *Int J Mol Med* 2003;11:195-7.

5. Petsch D, Rantze E, Anspach FB. Selective adsorption of endotoxin inside a polycationic network of flat-sheet microfiltration membranes. *J Mol Recognit* 1998;11:222-30.

6. Wickramasinghe SR, Kalbfuss B, Zimmermann A, Thom V, Reichl U. Tangential flow microfiltration and ultrafiltration for human influenza A virus concentration and purification. *Biotechnol Bioeng* 2005;92:199-208.

7. Reis Rv, Zydney A. Membrane separations in biotechnology. *Curr Opin Biotechnol* 2001;12:208-11.

8. Petsch D, Beeskow TC, Anspach FB, Deckwer W-D. Membrane adsorbers for selective removal of bacterial endotoxin. *J Chromatogr B* 1997;693:79-91.

9. Wang Y-Q, Su Y-L, Ma X-L, Sun Q, Jiang Z-Y. Pluronic polymers and polyethersulfone blend membranes with improved fouling-resistant ability and ultrafiltration performance. *J Membrane Sci* 2006;283:440-7.

10. Yamamoto K-i, Matsuda M, Hayama M, Asutagawa J, Tanaka S, Kohori F, et al. Evaluation of the activity of endotoxin trapped by a hollow-fiber dialysis membrane. *J Membrane Sci* 2006;272:211-6.

11. Dhruv, H. Controlling nonspecific adsorption of proteins at bio-interfaces for biosensor and biomedical applications [Dissertation]. Logan, UT: Utah State University; 2009.

12. Heilmann K. Asymmetrical microporous hollow fiber for hemodialysis. United States Patent Nr. Apr. 29, 1988.

13. Mulder M. *Basic Principles of Membrane Technology*. The Netherlands: Kluwer Academic Publishers, 1996.

14. Aoyagi S, Hayama M, Hasegawa U, Sakai K, Hoshi T, Kudo M. TOF-SIMS imaging of protein adsorption on dialysis membrane. *Appl Surf Sci* 2004;231-232:411-5.

15. Aoyagi S, Hayama M, Hasegawa U, Sakai K, Tozu M, Hoshi T, et al. Estimation of protein adsorption on dialysis membrane by means of TOF-SIMS imaging. *J Membrane Sci* 2004;236:91-9.

16. Khulbe KC, Feng C, Matsuura T, Khayet M. AFM images of the cross-section of polyetherimide hollow fibers. *Desalination* 2006;201:130-7.

17. Cai X-E, Yang J. Molecular forces for the binding and condensation of DNA molecules. *Biophys J* 2002;82:357-65.

APPENDICES

APPENDIX A

This appendix presents data collected from flat sheet membranes made from a polymer spin mass containing PS-PVP that were subjected to bleach treatment for various times to determine the effect of bleach on water contact angle. Flat sheet membranes were prepared similar to the casting technique used to prepare hollow fibers. Polymer spin mass of the same content as that used to produce hollow fibers was dispensed on a clean glass cover slip and spun at high revolution per second (3000 rpm) for 10 seconds. While the polymer mixture was spinning, a coagulation fluid was dispensed thereon to initiate phase inversion from wet phase to solid polymer membrane. Upon completion of the spinning process, the membranes were removed from the glass, thoroughly rinsed with water at 70^{o}C, and placed in a drying oven overnight. Membranes were then immersed in a bath containing 0.57% effective sodium hypochlorite content at 70^{o}C for varying amounts of time. Water contact angle was measured similar to the method mentioned in Chapters 3 and 4, however, larger droplets of 1 µL were used (n = 9).

It was seen that longer bleaching times led to an increase in contact angle of both the lumen and backside of the membranes. Water contact angle from 1 minute increased dramatically, contrary to results reported in Chapters 3 and 4. This quicker reaction for flat-sheet membranes may be due to the location and availability of PVP in the flat-sheet geometry versus the hollow fiber geometry. As bleaching time increased to 30 minutes, contact angles of flat-sheet membranes approached approximately 80^{o} for both lumen and backside. This corresponds to the contact angle for PS membranes as seen in Chapter 3. Therefore, it can be inferred that bleaching of PS-PVP membranes removes PVP from the membrane, leaving a membrane composed primarily of hydrophobic PS.

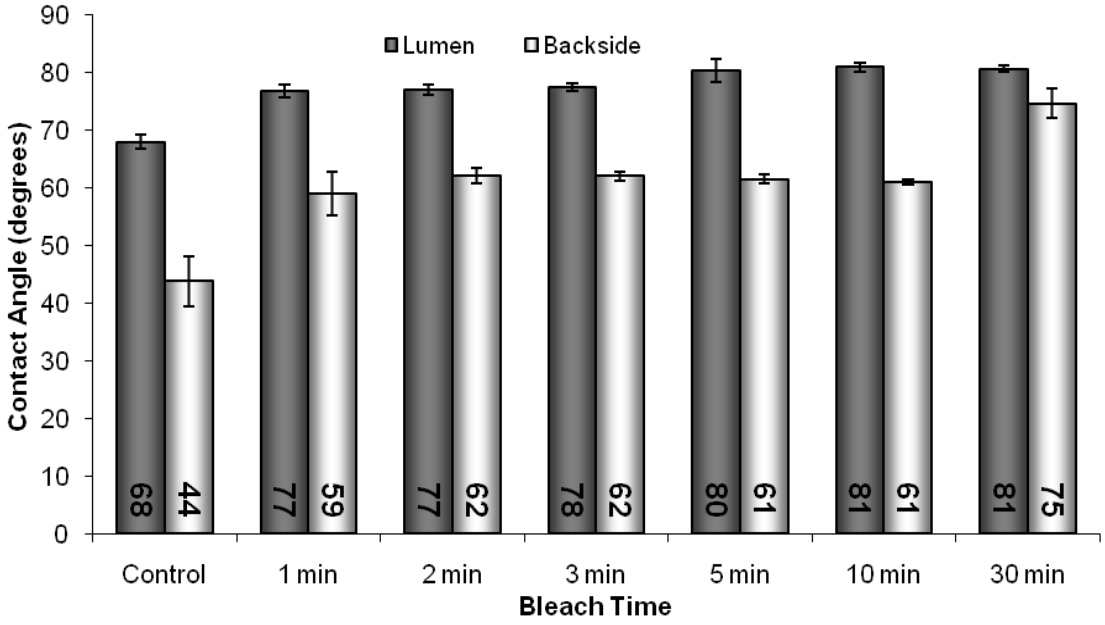

FIG. A.1. Water contact angles of flat-sheet geometry PS-PVP membranes subjected to 0.57% bleach for varying amounts of time. "Lumen" represents the top side of the membrane, equivalent to the lumen side of a hollow fiber membrane. "Backside" represents the bottom side of the membrane, equivalent to the outside surface of a hollow fiber membrane.

APPENDIX B

Here are presented AFM and SEM images of the lumen and outside of hollow fiber membranes examined in Chapter 4 including Optiflux®, bleached, high PVP, low PVP, and copolymer membranes. AFM images were obtained similar to the process described in Chapter 3. Briefly, membranes were sectioned using a stereo microscopy to reveal the lumen surface, and rolled flat to present the outside surface of membrane as a flat surface. A Bioscope AFM was affixed with a silicon nitride cantilever and membrane surfaces were scanned with a 2 x 2 μm^2 scale for lumens and a 10 x 10 μm^2 scale for outside surfaces. Root mean square roughness was performed and is presented as mean ± standard deviation (n = 5). SEM images were obtained according to process outlined in Chapter 4.

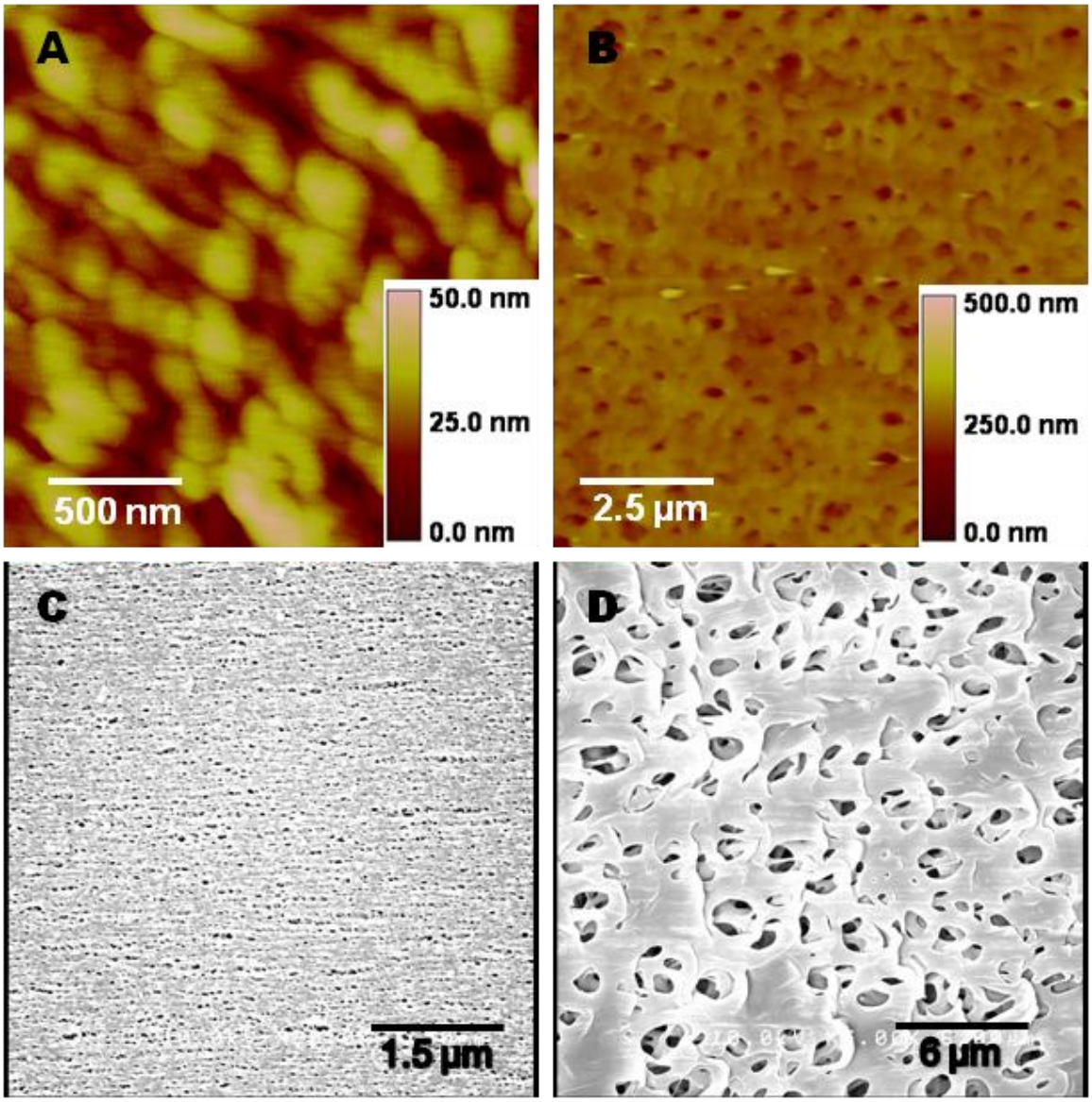

FIG. B.1. AFM and SEM images of control (Optiflux®) membrane. (A) AFM of lumen at 2 x 2 μm^2 x 50 nm. (B) AFM of outside at 10 x 10 μm^2 x 500 nm. (C) SEM of lumen at 20000X. (D) SEM of outside at 5000X. AFM and SEM images reveals nodule aggregates as described in Chapter 3 as well as porous outer membrane.

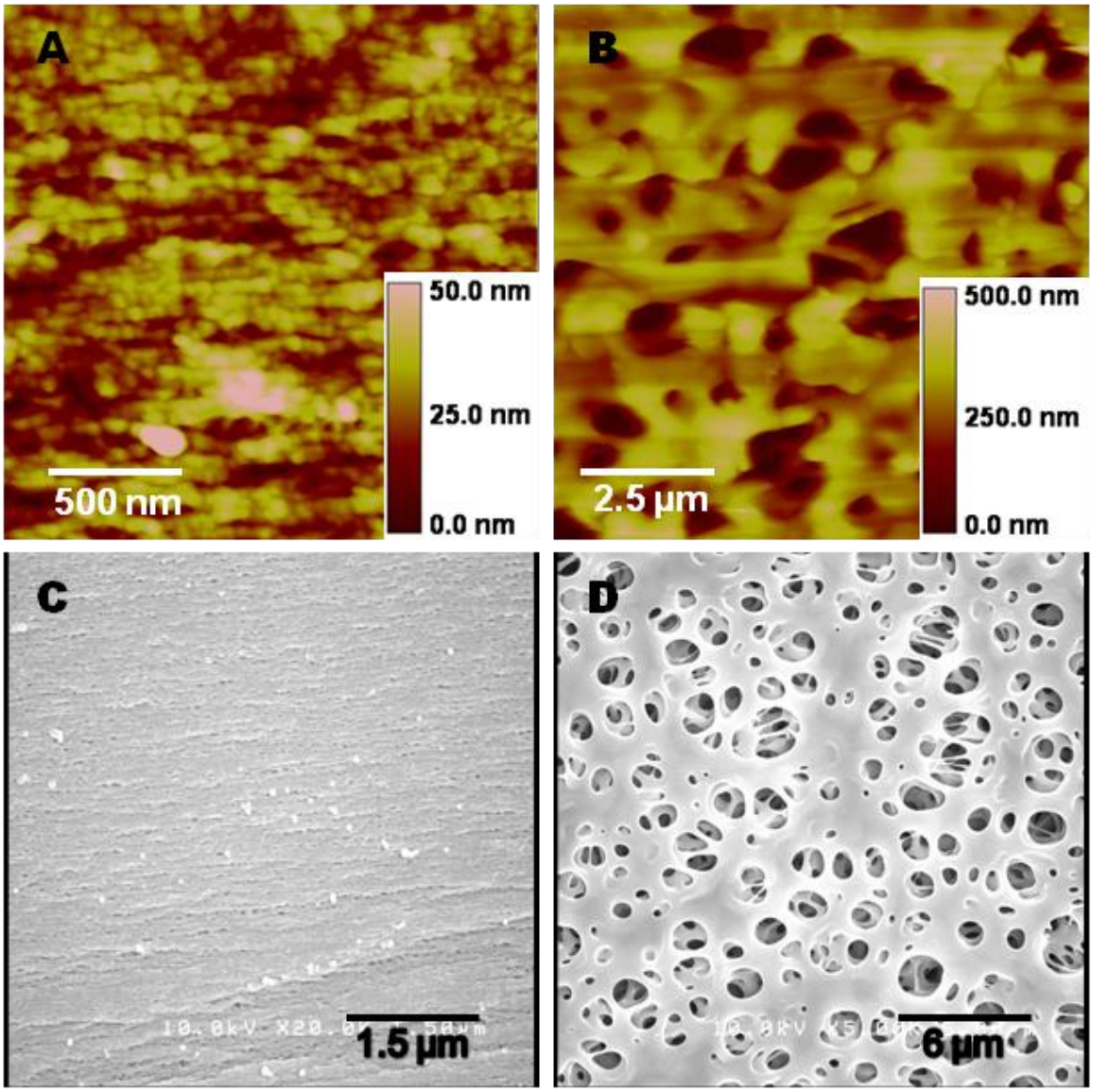

FIG. B.2. AFM images of bleached membrane. (A) AFM of lumen at 2 x 2 μm^2 x 50 nm. (B) AFM of outside at 10 x 10 μm^2 x 500 nm. (C) SEM of lumen at 20000X. (D) SEM of outside at 5000X. Nodule aggregates are smaller than those from the control membrane, while pores on the outside are significantly larger than those of the control membrane.

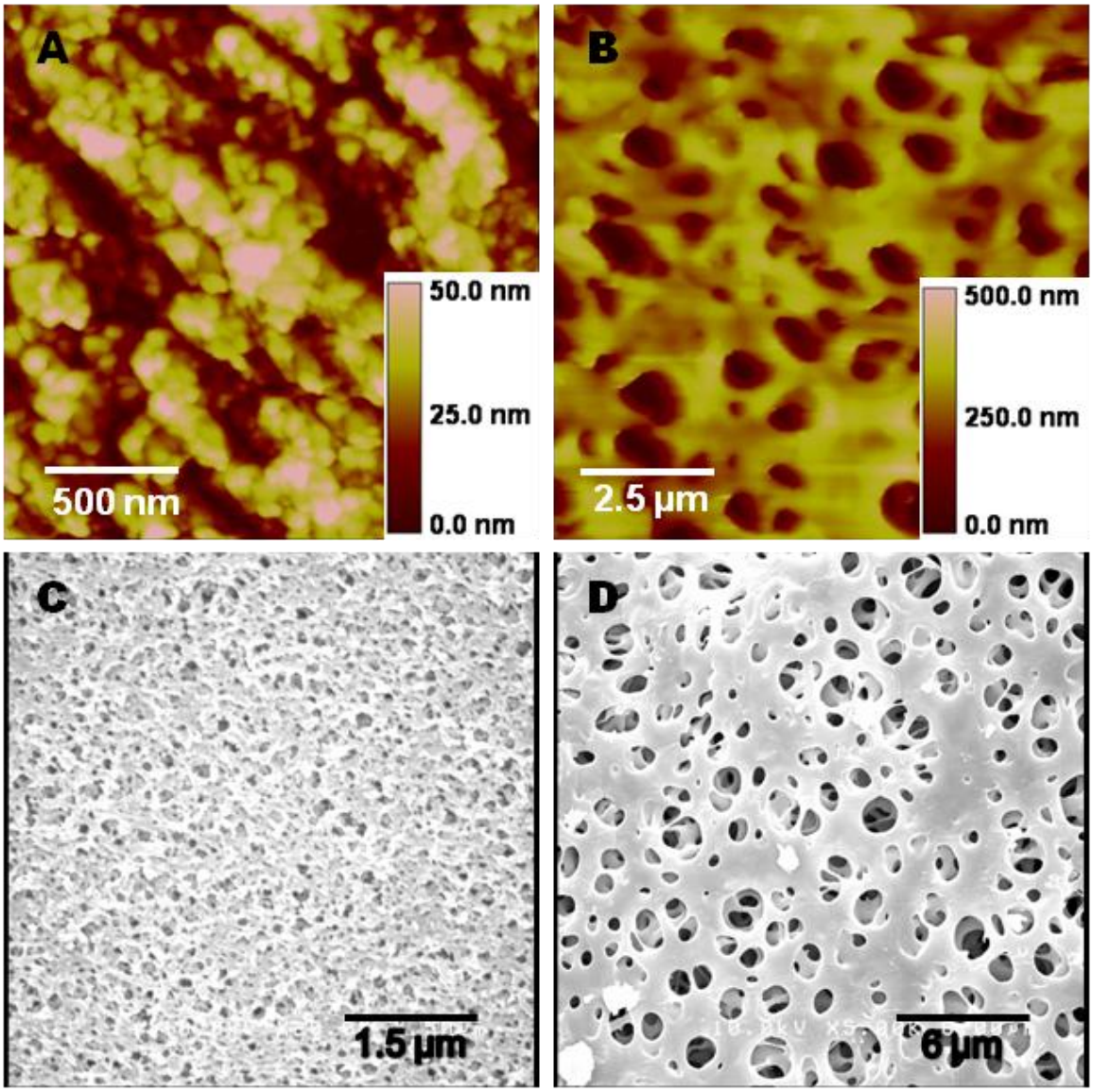

FIG. B.3. AFM images of high PVP membrane. (A) AFM of lumen at 2 x 2 μm^2 x 50 nm. (B) AFM of outside at 10 x 10 μm^2 x 500 nm. (C) SEM of lumen at 20000X. (D) SEM of outside at 5000X. Membrane is very similar to the bleached membrane on the outside, but the lumen exhibits a rougher surface comprised of small nodule aggregates.

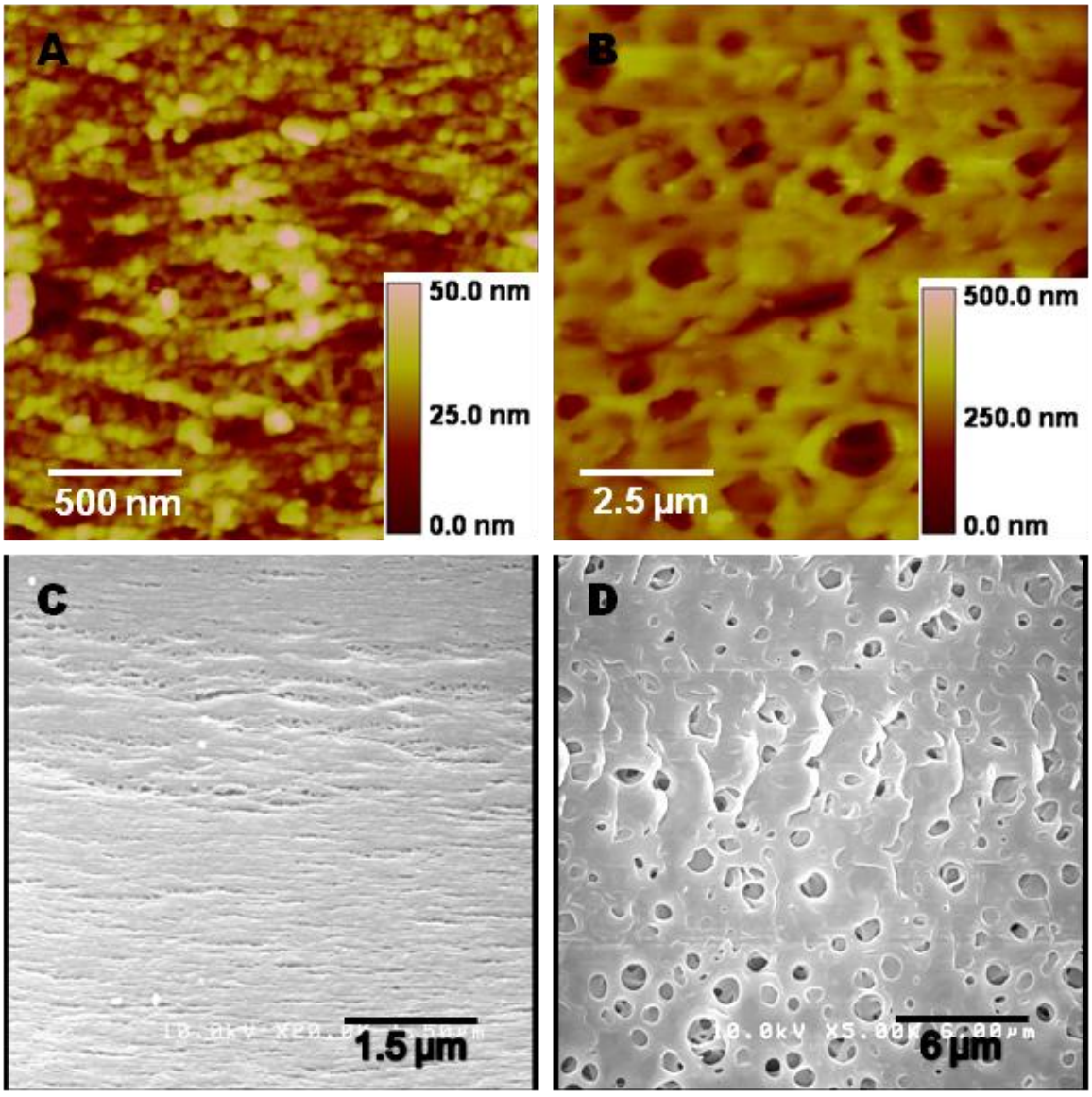

FIG. B.4. AFM images of low PVP membrane. (A) AFM of lumen at 2 x 2 μm^2 x 50 nm. (B) AFM of outside at 10 x 10 μm^2 x 500 nm. (C) SEM of lumen at 20000X. (D) SEM of outside at 5000X. Membrane is similar to bleached and high PVP membrane on both lumen and outside surfaces.

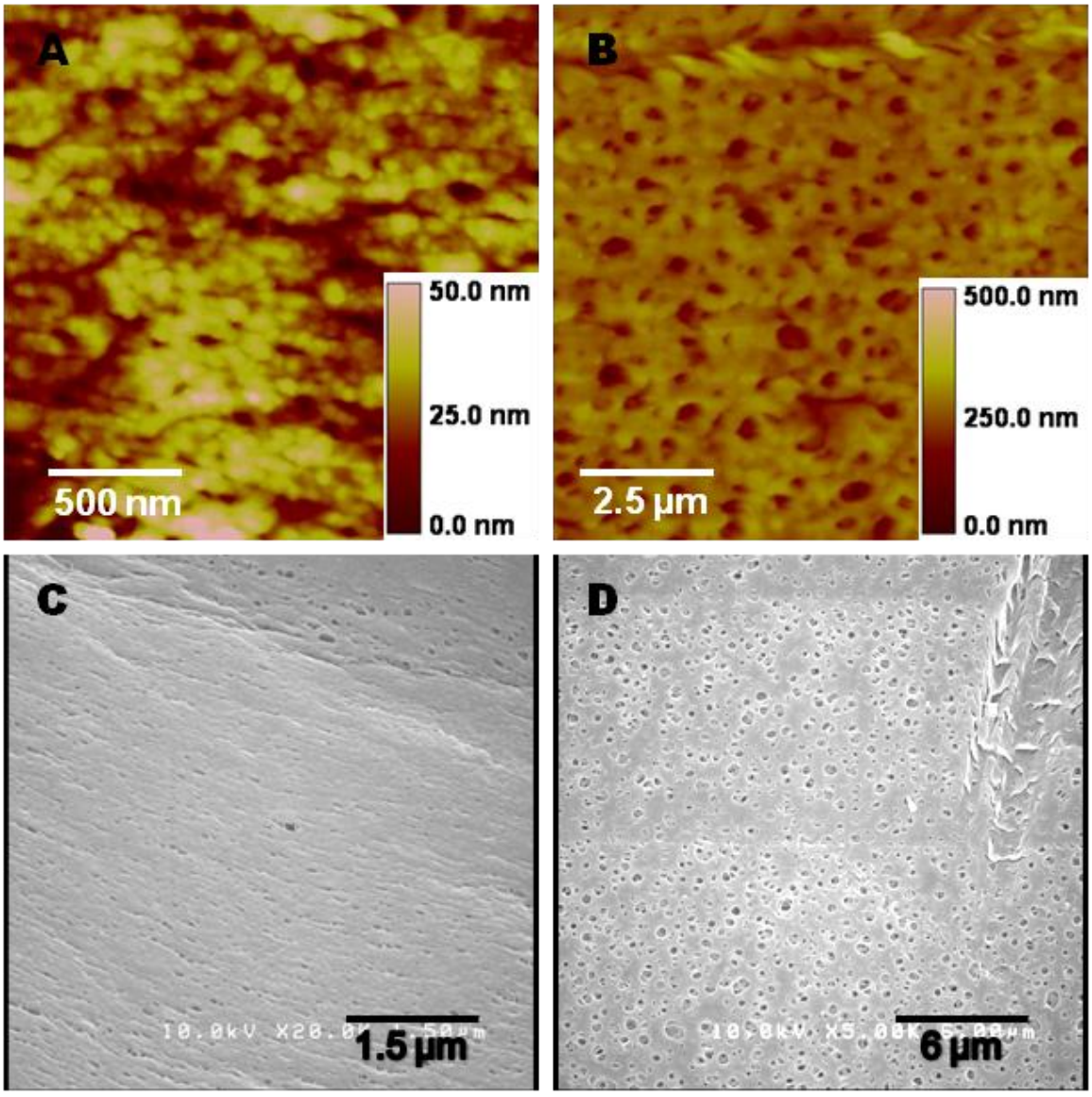

FIG. B.5. AFM images of PS-PEG copolymer membrane. (A) AFM of lumen at 2 x 2 μm^2 x 50 nm. (B) AFM of outside at 10 x 10 μm^2 x 500 nm. (C) SEM of lumen at 20000X. (D) SEM of outside at 5000X. Lumen surface is similar to PS-PVP membranes with small nodule aggregates, but the outside surface is more similar to the control membrane, containing smaller pores.

Table B.1. RMS roughness values for lumen side and outside of membranes (mean ± s.d., n = 5). Lumen side imaged at 2 x 2 μm^2 and outside imaged at 10 x 10 μm^2.

Fiber Type	Lumen Side	Outside
Control	19.7 ± 0.9	38.6 ± 15.2
Bleach	20.8 ± 6.0	105.7 ± 30.1
High-PVP	25.2 ± 7.1	148.5 ± 45.1
Low-PVP	18.6 ± 11.1	85.5 ± 40.9
Copolymer	13.4 ± 3.1	116.1 ± 63.6

Statistical analysis of RMS values showed significant difference between control and copolymer membranes on the lumen side and significantly larger values for bleach, high-PVP, and copolymer membranes compared to the control membrane on the outside. Outside morphologies show smaller pores for the control and copolymer membranes compared to the other membranes. It is interesting to note the differences and similarities of the control and copolymer membranes. While they exhibited similar outside membrane structure, the copolymer membranes had a significantly larger surface roughness. Also, the smaller nodule aggregates lowered overall roughness, but did not cause retention or adsorption of LPS as seen in fluorescence images presented in Chapter 4. The bleached, high PVP, and low PVP membranes all exhibited similar AFM morphologies, yet drastically different adsorptions of LPS indicating that chemical differences may not cause dramatic morphological changes, but do alter adsorption capacities.

SEM images reveal that the high PVP membrane had a much more porous lumen structure compared to all other membranes. Outside morphologies reveal that the copolymer and low PVP membranes were much less porous, with pores on the copolymer membrane being much smaller than those of all other membranes.

APPENDIX C

SEIVING COEFFICIENTS OF POLYMER HOLLOW FIBERS FROM CHAPTER 4

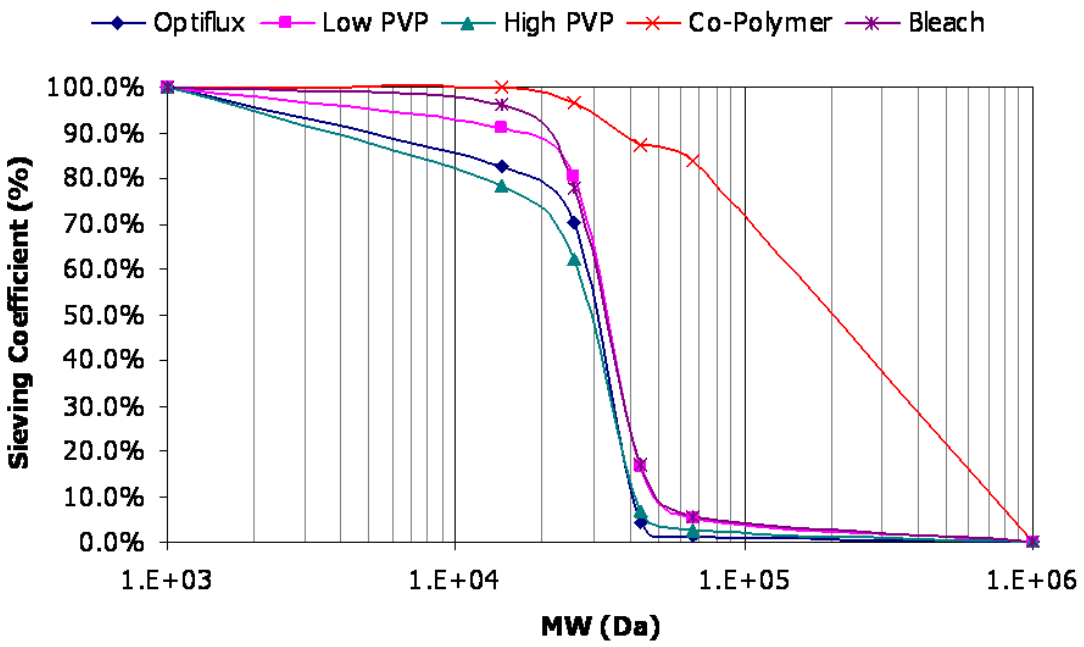

FIG. C.1. Sieving coefficients of polymer hollow fibers. All hollow fibers effectively limit molecular weight transfer below approximately 5% at 60 kDa, except the copolymer membrane. This membrane may have undergone a physical breach allowing transfer of higher molecular weight species.

APPENDIX D

This appendix includes fluorescence images of polymer hollow fibers modified with PLL and challenged with fluorescent-labeled LPS as shown in Chapter 5. Patterns of fluorescence described in Fig. 5.8 are shown in Fig. D.1.

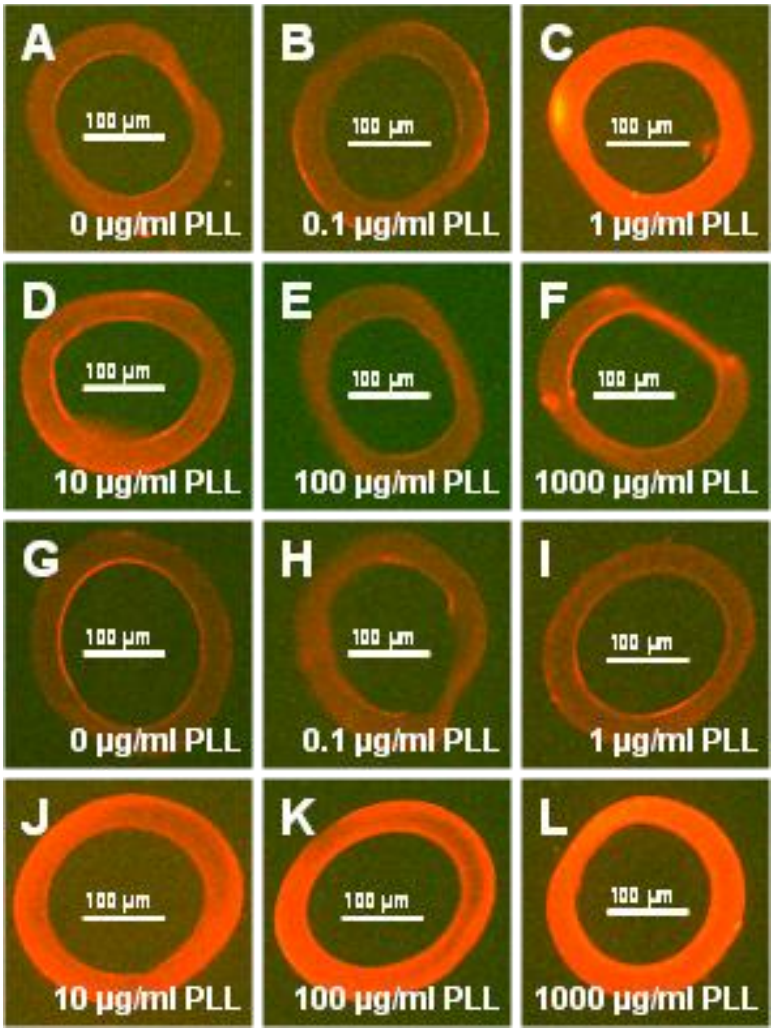

FIG. D.1. Fluorescence images of polymer hollow fiber modified with PLL at various concentrations and challenged with 0.1 µg/ml fluorescent-labeled LPS. Images (A)-(F) represent fibers modified with PLL using no cross-linking agent, whereas images (G)-(L) represent fibers modified with PLL and cross-linked using GA.

APPENDIX E

Included in this appendix are AFM images of LPS and PLL on mica as described in Chapter 5. Also included are line cuts used to measure height and width features of LPS "islands" seen in AFM images of mica touched to the air-water interface of LPS solutions. Images of LPS and PLL on mica show similar trends seen in Chapter 5 with a more organized structure associated with higher concentrations of PLL in LPS. Upon reaching a PLL to LPS ratio of 1:1, a film layer formed on the mica similar in structure to that seen in Panel C of Fig. 5.6.

Line cuts similar to those found in Fig. E.2 were used to calculate height values of features seen in AFM images, as mentioned in Chapter 5. As the concentration of LPS increased in solution, features on the mica surface grew both in height and diameter.

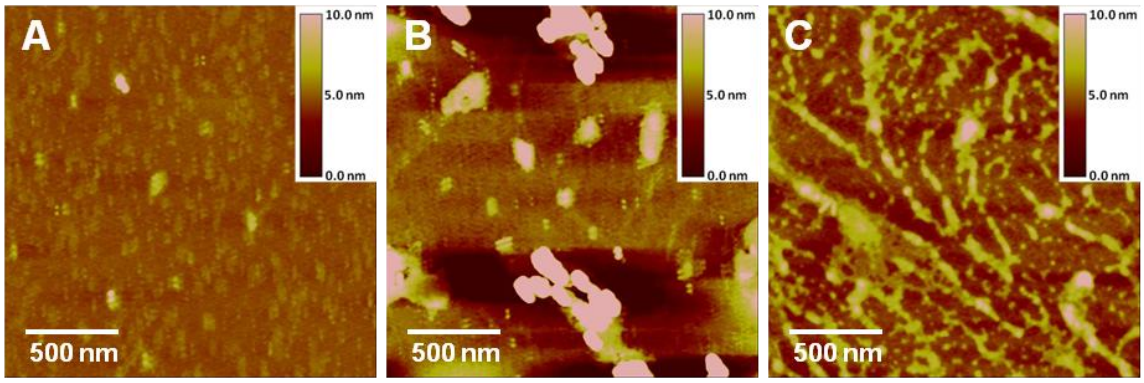

FIG. E.1. AFM images of LPS and PLL on mica from solutions containing 47.5 µg/ml LPS and (A) 0.5 µg/ml PLL, (B) 5 µg/ml PLL, and (C) 50 µg/ml PLL. A film layer of LPS and PLL formed on the mica starting at a concentration of 50 µg/ml PLL.

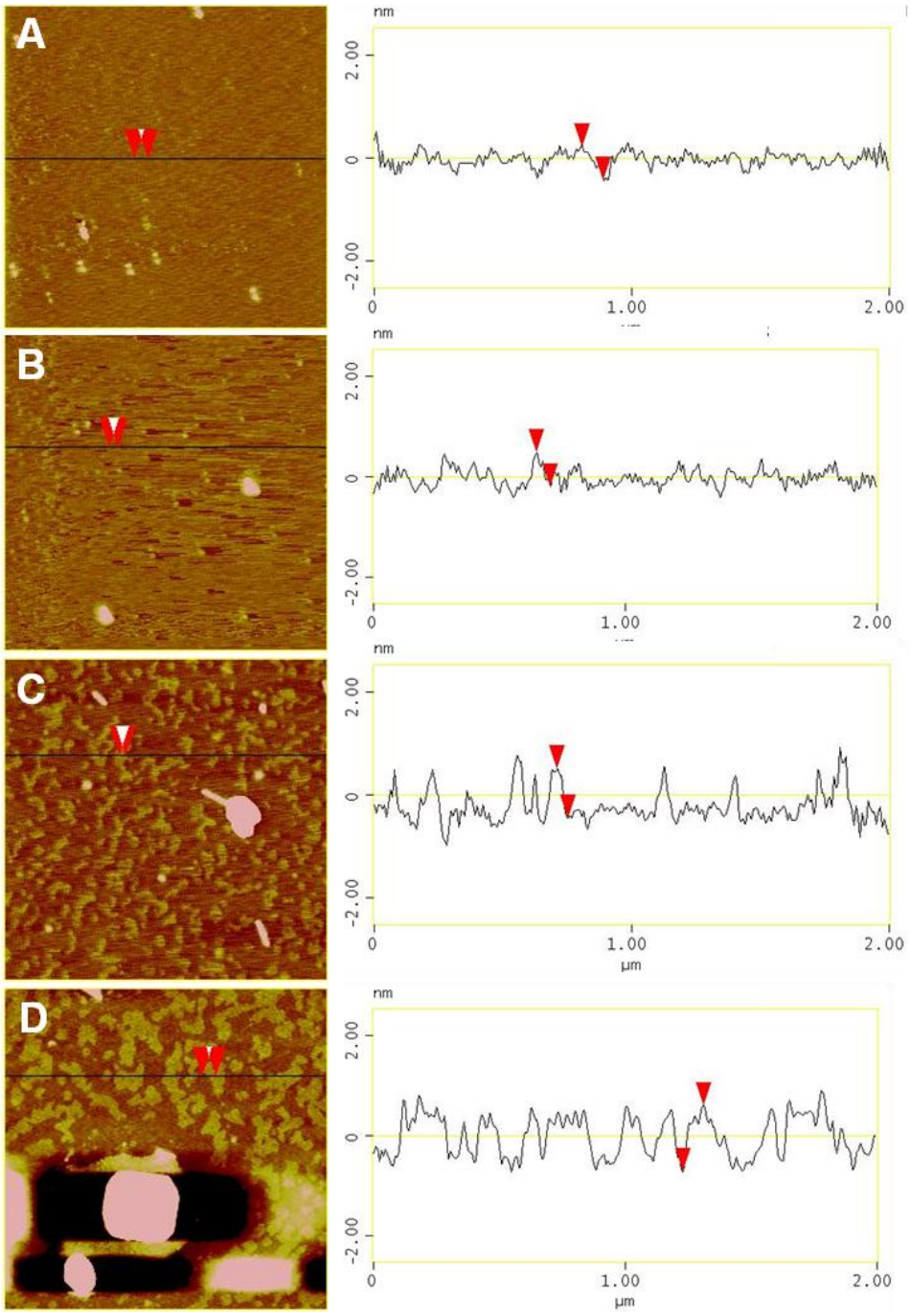

FIG. E.2. AFM images of LPS on mica from solutions containing (A) 1 µg/ml, (B) 10 µg/ml, (C) 50 µg/ml, and (D) 100 µg/ml LPS in PBS, and subsequently profile cuts using Nanoscope III Imaging Software. Solutions containing more than 10 µg/ml LPS led to images containing small "islands", presumably LPS deposits on the mica surface.

APPENDIX F

PERMISSION LETTERS

UtahState University
Department of Biological and Irrigation Engineering
4105 Old Main Hill
Logan, UT 84322-4105
Telephone: (435) 797-2785
Fax: (435) 797-1248

Floyd Griffiths
WesTech Engineering, Inc.
3625 S. West Temple
Salt Lake City, UT 84115

Dear Floyd,

I am in the process of preparing my dissertation in the Department of Biological and Irrigation Engineering at Utah State University. I hope to complete my degree in May of 2010.

I am requesting permission to include the attached paper, of which you are a coauthor, as a chapter in my dissertation. I will include acknowledgements to your contributions as indicated. Please advise me of any changes you require.

Please indicate your approval of this request by signing in the space provided, attaching any other form or instruction necessary to confirm permission. If you have any questions, please contact me.

Thank you,

Benjamin Madsen

I hereby give permission to Benjamin Madsen to use and reprint all of the material that I have contributed to Chapter 3 of his dissertation.

_____

Floyd Griffiths

UtahState University
Department of Biological and Irrigation Engineering
4105 Old Main Hill
Logan, UT 84322-4105
Telephone: (435) 797-2785
Fax: (435) 797-1248

Elise McKenna
New York Medical College
40 Sunshine Cottage Road
Valhalla, NY 10595

Dear Elise,

I am in the process of preparing my dissertation in the Department of Biological and Irrigation Engineering at Utah State University. I hope to complete my degree in May of 2010.

I am requesting permission to include the attached paper, of which you are a coauthor, as a chapter in my dissertation. I will include acknowledgements to your contributions as indicated. Please advise me of any changes you require.

Please indicate your approval of this request by signing in the space provided, attaching any other form or instruction necessary to confirm permission. If you have any questions, please contact me.

Thank you,

Benjamin Madsen

I hereby give permission to Benjamin Madsen to use and reprint all of the material that I have contributed to Chapter 3 of his dissertation.

_____

Elise McKenna

UtahState University
Department of Biological and Irrigation Engineering
4105 Old Main Hill
Logan, UT 84322-4105
Telephone: (435) 797-2785
Fax: (435) 797-1248

Michael Henrie
Fresenius Medical Care North America
475 West 13th Street
Ogden, UT 84404-5554

Dear Michael,

I am in the process of preparing my dissertation in the Department of Biological and Irrigation Engineering at Utah State University. I hope to complete my degree in May of 2010.

I am requesting permission to include the attached paper, of which you are a coauthor, as a chapter in my dissertation. I will include acknowledgements to your contributions as indicated. Please advise me of any changes you require.

Please indicate your approval of this request by signing in the space provided, attaching any other form or instruction necessary to confirm permission. If you have any questions, please contact me.

Thank you,

Benjamin Madsen

I hereby give permission to Benjamin Madsen to use and reprint all of the material that I have contributed to Chapter 4 of his dissertation.

_____

Michael Henrie

UtahState University
Department of Biological and Irrigation Engineering
4105 Old Main Hill
Logan, UT 84322-4105
Telephone: (435) 797-2785
Fax: (435) 797-1248

Cheryl Ford
Fresenius Medical Care North America
475 West 13th Street
Ogden, UT 84404-5554

Dear Cheryl,

I am in the process of preparing my dissertation in the Department of Biological and Irrigation Engineering at Utah State University. I hope to complete my degree in May of 2010.

I am requesting permission to include the attached paper, of which you are a coauthor, as a chapter in my dissertation. I will include acknowledgements to your contributions as indicated. Please advise me of any changes you require.

Please indicate your approval of this request by signing in the space provided, attaching any other form or instruction necessary to confirm permission. If you have any questions, please contact me.

Thank you,

Benjamin Madsen

I hereby give permission to Benjamin Madsen to use and reprint all of the material that I have contributed to Chapter 4 of his dissertation.

_____

Cheryl Ford

UtahState University
Department of Biological and Irrigation Engineering
4105 Old Main Hill
Logan, UT 84322-4105
Telephone: (435) 797-2785
Fax: (435) 797-1248

Eric Stroup
Fresenius Medical Care North America
475 West 13th Street
Ogden, UT 84404-5554

Dear Eric,

I am in the process of preparing my dissertation in the Department of Biological and Irrigation Engineering at Utah State University. I hope to complete my degree in May of 2010.

I am requesting permission to include the attached paper, of which you are a coauthor, as a chapter in my dissertation. I will include acknowledgements to your contributions as indicated. Please advise me of any changes you require.

Please indicate your approval of this request by signing in the space provided, attaching any other form or instruction necessary to confirm permission. If you have any questions, please contact me.

Thank you,

Benjamin Madsen

I hereby give permission to Benjamin Madsen to use and reprint all of the material that I have contributed to Chapter 4 of his dissertation.

_____

Eric Stroup

UtahState University
Department of Biological and Irrigation Engineering
4105 Old Main Hill
Logan, UT 84322-4105
Telephone: (435) 797-2785
Fax: (435) 797-1248

Brent Maltby
Fresenius Medical Care North America
475 West 13th Street
Ogden, UT 84404-5554

Dear Brent,

I am in the process of preparing my dissertation in the Department of Biological and Irrigation Engineering at Utah State University. I hope to complete my degree in May of 2010.

I am requesting permission to include the attached paper, of which you are a coauthor, as a chapter in my dissertation. I will include acknowledgements to your contributions as indicated. Please advise me of any changes you require.

Please indicate your approval of this request by signing in the space provided, attaching any other form or instruction necessary to confirm permission. If you have any questions, please contact me.

Thank you,

Benjamin Madsen

I hereby give permission to Benjamin Madsen to use and reprint all of the material that I have contributed to Chapter 4 of his dissertation.

_____

Brent Maltby

UtahState University
Department of Biological and Irrigation Engineering
4105 Old Main Hill
Logan, UT 84322-4105
Telephone: (435) 797-2785
Fax: (435) 797-1248

Doug Olmstead
Fresenius Medical Care North America
475 West 13th Street
Ogden, UT 84404-5554

Dear Doug,

I am in the process of preparing my dissertation in the Department of Biological and Irrigation Engineering at Utah State University. I hope to complete my degree in May of 2010.

I am requesting permission to include the attached paper, of which you are a coauthor, as a chapter in my dissertation. I will include acknowledgements to your contributions as indicated. Please advise me of any changes you require.

Please indicate your approval of this request by signing in the space provided, attaching any other form or instruction necessary to confirm permission. If you have any questions, please contact me.

Thank you,

Benjamin Madsen

I hereby give permission to Benjamin Madsen to use and reprint all of the material that I have contributed to Chapter 4 of his dissertation.

_____

Doug Olmstead

UtahState University
Department of Biological and Irrigation Engineering
4105 Old Main Hill
Logan, UT 84322-4105
Telephone: (435) 797-2785
Fax: (435) 797-1248

Marion Andersen
Fresenius Medical Care North America
475 West 13th Street
Ogden, UT 84404-5554

Dear Marion,

I am in the process of preparing my dissertation in the Department of Biological and Irrigation Engineering at Utah State University. I hope to complete my degree in May of 2010.

I am requesting permission to include the attached paper, of which you are a coauthor, as a chapter in my dissertation. I will include acknowledgements to your contributions as indicated. Please advise me of any changes you require.

Please indicate your approval of this request by signing in the space provided, attaching any other form or instruction necessary to confirm permission. If you have any questions, please contact me.

Thank you,

Benjamin Madsen

I hereby give permission to Benjamin Madsen to use and reprint all of the material that I have contributed to Chapter 4 of his dissertation.

_____

Marion Andersen

CURRICULUM VITAE

Benjamin Reese Madsen

139 N 875 E #3, Logan, UT 84321
(435) 760-4004
madsen.ben@gmail.com

Education

Ph.D. Biological Engineering — Utah State University — Logan, UT
Expected Graduation: December 2009

B.S. Biological Engineering — Utah State University — Logan, UT
Graduated: May 2004

Relevant Course Work

Engineering
- Biochemical Engineering – Important biochemical pathways of organisms
- Bioengineering Unit Operations – Biochemical operations in cells and systems
- Biological Engineering Design – Design included constructing and running a fermentor using immobilized yeast cells
- Numerical Methods – Numerical method techniques using Fortran
- Tissue Engineering – Culturing of mammalian cells with scaffolds and specific signals

Science
- Microbiology/Microbial Physiology – Biology of microorganisms including bacteria, fungi, viruses
- Modeling Biological Systems – Modeled biological systems using C
- Cell Culture – Basics of culturing mammalian cells

Mathematics
- Multivariable Calculus – Calculus using several variables and coordinate systems
- Differential Equations/Linear Algebra – Solving linear systems and simple differential equations
- Design of Experiments – Statistical models optimizing experiments using SAS

Professional Experience

Research Assistant, Utah State University, Department of Biological Engineering
- Jan 2004-Present
- Lab work under the supervision of Dr. David Britt and Fresenius Medical Care
- Experience with several microscopy methods including AFM, SEM, light, fluorescence; several experimental procedures including spectrophotometry, LAL assay, contact angle measurement, tensiometery, flow systems using dialyzers; designing and running novel experiments relevant to the requirements of several projects.

Academic Honors and Awards

2nd place Oral Presentation, IBE Regional Conference (2008)
Young Innovator Fellowship, ASAIO (2007)
Presidential Fellowship, Utah State University (2006-2007)
Presidential Scholarship, Utah State University (1997-2003)

Refereed Journal Articles, Scientific Presentations, Conference Proceedings

1st Annual IBE Regional Conference, Utah State University, Session Chair, Oct. 18, 2008.

Henrie, M., C. Ford, M. Andersen, E. Stroup, J. Diaz-Buxo, B. Madsen, D.W. Britt, C.-H. Ho, *In Vitro Assessment of Dialysis Membrane as an Endotoxin Transfer Barrier: Geometry,Morphology, and Permeability*. Artificial Organs **32**(9) 701-710, **2008**.

Beck, J. R. Angus, B. Madsen, D.W. Britt, B. Vernon, K.T. Nguyen, *Islet Encapsulation – Strategies to enhance islet cell functions*. Tissue Engineering **13**(3) 589-599, **2007**

Madsen, B., D. Britt, C.-H. Ho, M. Henrie, C. Ford, E. Stroup, B. Maltby, D. Olmstead, M. Andersen, *Hemodialysis membrane surface chemistry as a barrier to endotoxin transfer*. ASAIO's 53rd Annual Conference. Chicago, IL. June 7-9, 2007.

Henrie, M., C. Ho, E. Stroup, B. Maltby, D. Olmstead, M. Andersen, C. Ford, D. Britt, B. Madsen. *Hemodialysis membrane as a barrier to endotoxin transfer*. UM-CME 27th Annual Dialysis Conference. Denver, CO. Feb. 18-20, 2007.

Ho, C., M. Henrie, C. Ford, E. W. Stroup, B. Maltby, D. Olmstead, M. Andersen, D. Britt, B. Madsen. *Hemodialysis membrane geometry as a barrier to endotoxin transfer*. ASN's 39th Annual Renal Week Meeting. San Diego, CA. Nov. 14-19, 2006

Madsen, B., D. Britt, F. Griffiths, C. Ford, D. Thomas. *Validation of a flat-sheet model of hydrophilic semipermeable membranes*. First Annual Mountain West Biomedical Engineering Conference. Snowbird, UT. Sept. 16-17, 2005.

Other Relevant Information

Experience in several labs including general, organic, biochemistry, and microbiology labs, material science, and instrumentations. Background in mechanical and biological engineering. Knowledgeable in several software programs including Word, Excel, PowerPoint, Origin. Programming experience in C, Fortran, SAS. Proficient in German.